Cover Page

The handle http://hdl.handle.net/1887/37038 holds various files of this Leiden University dissertation

Author: Ninaber, Maarten
Title: Pulmonary structure and function analysis in systemic sclerosis : clinical assessment of complicating interstitial lung disease and pulmonary vasculopathy
Issue Date: 2015-12-15

Pulmonary structure and function analysis in systemic sclerosis

Clinical assessment of complicating interstitial lung disease and pulmonary vasculopathy

Maarten Ninaber

Cover	Gijs Ninaber
Layout	Renate Siebes	Proefschrift.nu
Printed by	Ridderprint, Ridderkerk
ISBN	978-94-90791-41-4

Pulmonary structure and function analysis in systemic sclerosis

Clinical assessment of complicating interstitial lung disease and pulmonary vasculopathy

Proefschrift

ter verkrijging van
de graad van Doctor aan de Universiteit Leiden,
op gezag van Rector Magnificus prof. mr. C.J.J.M. Stolker,
volgens besluit van het College voor Promoties
te verdedigen op dinsdag 15 december 2015
klokke 15.00 uur

door

Maarten Ninaber

geboren te Capelle a/d IJssel
in 1979

Voor Wilma, Gijs en mijn ouders

Contents

Chapter 1

Introduction

Introduction to systemic sclerosis

Systemic sclerosis (SSc) is a systemic autoimmune disease that is characterised by endothelial dysfunction resulting in a small-vessel vasculopathy, fibroblast dysfunction with resultant excessive collagen production and fibrosis. The classification of SSc is based on the extent of skin involvement into diffuse cutaneous sclerosis (dcSSc) and limited cutaneous sclerosis (lcSSc) (1). Mortality in SSc is high; in a systematic review and a meta-analysis of the literature (2) including 2,691 SSc patients in 9 cohort studies, the pooled Standardized Mortality Ratio was (SMR) was 3.53. Among 732 deaths, heart involvement was the most frequent cause of death (29%), followed by lung involvement (2). In the EULAR Scleroderma Trials and Research group (EUSTAR) database (3), 55% of deaths were due to SSc, whereas 45% of deaths were thought to be unrelated to SSc. Of the SSc-related deaths, 26% were cardiac (predominantly heart failure and arrhythmias), whereas 29% of non-SSc related deaths were due to cardiac causes.

Pulmonary involvement in systemic sclerosis

While virtually any organ system may be involved in the disease process, fibrotic and vascular pulmonary manifestations of SSc, including interstitial lung disease (ILD) and pulmonary hypertension (PH), are the leading cause of death (4).

In SSc, the two most common types of direct pulmonary involvement are ILD and PH, which together account for 60% of SSc-related deaths (5). While certain pulmonary manifestations may occur more commonly in a subset of SSc (i.e. ILD is more common in dcSSc while PH is more common in lcSSc) (6), all of the known pulmonary manifestations reported have been described in each of the subsets of disease. In the following text, these two complications are further discussed.

Interstitial lung disease

Interstitial lung disease is very common in SSc. In early autopsy studies, up to 100% of patients were found to have parenchymal involvement (7;8). As many as 90% of patients will have interstitial abnormalities on high-resolution computed tomography (HRCT) (9;10) and 40–75% will have changes in pulmonary function tests (PFTs) (11-13). Parenchymal lung involvement often appears early after the diagnosis of SSc, with 25% of patients developing clinically significant lung disease within 3–5 years (11). Symptoms and complaints include dyspnea (at rest and at exertion), chest tightness and non-productive cough. Risk factors for

its development include African–American ethnicity, skin score, hypothyroidism and cardiac involvement (14;15). Genetic factors, specific serological findings (anti-topoisomerase and anti-endothelial cell antibodies predict the presence of lung involvement) and the pattern of skin disease (patients with dcSSc have a higher incidence of interstitial disease) all contribute (16;17). Predictors of severe restrictive lung disease (defined by a forced vital capacity (FVC) less than 50% predicted) include African–American ethnicity (18), male sex, the degree of physiological abnormalities at diagnosis (FVC and diffusing capacity of the lung for carbon monoxide (DLCO)) and younger age (18;19).

Role of pulmonary function tests in ILD

Screening pulmonary physiology shows a reduction in FVC in 40–75% of patients, with 15% having a severe reduction (12;18;20). DLCO is reduced in almost all patients with other PFT abnormalities (21;22) and correlates with the extent of lung disease on HRCT(22). DLCO is lower in patients with UIP on biopsy (21) and, although FVC and DLCO are both identified as adverse prognostic markers (18;19), a declining DLCO is the single most significant marker of poor outcome (21).

Pulmonary hypertension

PH can occur in all forms of SSc and is associated with early mortality. First symptoms and complaints include dyspnea at exertion, palpitations and chest discomfort. Patients with SSc have the highest prevalence of PH among patients with a collagen vascular disease (CVD) (23). The updated clinical classification of PH divides patients into five groups based on the aetiology of their PH (24). SSc patients may fall into group 1 (isolated PAH, defined as a resting mean pulmonary artery pressure (mPAP) ≥25 mmHg with a pulmonary capillary wedge pressure ≤15 mmHg (25), group 2 (PH resulting from left ventricular involvement or diastolic dysfunction) and group 3 (PH resulting from ILD/hypoxaemia). Furthermore, patients can have combinations of these forms of PH. The prevalence of PH in SSc (SSc-PH) is variable and depends on the method of detection and the population studied. Using transthoracic Doppler echocardiography to screen SSc patients, the prevalence of PAH has been reported to range from 13% to 35% (26). However, when right heart catheterisation (RHC) is performed on "high-risk" SSc patients (defined as a combination of abnormal echocardiography findings, reduced DLCO in the absence of pulmonary fibrosis, a fall in DLCO and/or unexplained dyspnoea), a prevalence of 7–13% is found (27). PH can develop anytime during the course of SSc (28) and is more common in lcSSc when compared to

diffuse disease (29). In the European League against Rheumatism (EULAR) Scleroderma Trials and Research database, a multinational open scleroderma cohort with over 3,000 patients, isolated PH was seen in 9.2% of lcSSc and 5.8% of dcSSc patients. Multiple risk factors have been identified including increased age at diagnosis (30), more severe Raynaud's phenomena (31), the presence of digital tip ulcers (32), a diagnosis of lcSSc, decreased nailfold capillary density (33) and increased numbers of teleangiectasias on examination (33). Specific autoantibodies, including the presence of anti-U3 ribonucleoprotein antibodies (34), anti-topoisomerase IIa antibodies and anti-centromere antibodies (35), appear to be associated with a higher risk of PH. The presence of anti-Scl70 antibodies is associated with progressive ILD and appears to be less associated with PH (31). Patients with SSc-PH are older, more severely ill and more likely to be female when compared to idiopathic PH (36).

Role of echocardiography in PH

Transthoracic echocardiography is the most widely used tool to screen for PH in SSc. The performance characteristics of echocardiography depend on the population evaluated and the cut-off used. Studies show that 55–86% of patients with an echocardiography suggestive of PH (right ventricular systolic pressure (RVSP) 30–40 mmHg or higher with or without symptoms) will have PH on RHC (37). Higher cut-off points for RVSP as well as other characteristics of increased pulmonary pressures, such as increased right atrial or right ventricular size, decreased right ventricular function, increases the specificity of echocardiography for the diagnosis of PH. False positive and false negative results regularly occur in patients with mild disease. False negative results have been reported in patients earlier in the course of disease (38).

Role of pulmonary function tests in PH

Reductions in DLCO are very common in SSc. In 19% of all SSc patients isolated reductions in DLCO were found (39), but only a minority developed PH. However, a moderate reduction (DLCO <55% predicted) in association with an FVC/ DLCO ratio >1.4% (40) or a DLCO that is low or declining in the absence of parenchymal lung disease predicts the development of PH in SSc (31). Hachulla et al. (41) found that a DLCO <60% predicted in the absence of parenchymal lung disease was significantly associated with PH (OR 9.23, 95% CI 2.73–31.15). Steen and Medsger (31) found a significantly lower DLCO in patients with PH at an average of 4.5 years before the diagnosis of PH (52% versus 81%, p<0.001). In addition, they found that a declining DLCO over 15 years strongly predicts the development of PH.

Importance of management of SSc patients at risk for PH and ILD

The prevalence of PH in SSc exceeds 10% (8–13%), its presence increases morbidity and mortality. Since effective treatments are available (42), screening for PH is appropriate. However, despite echocardiography is currently widely used as a first screening tool, it lacks sufficient sensitivity and specificity in mildly increased pulmonary arterial pressures (43). Therefore, it cannot be used to screen for developing PH, which is now recognized of increasing importance in SSc (44).

As SSc patients who develop significant and progressive interstitial lung disease lung function tests and HRCT chest imaging should be considered. In patients with measurable disease, the extent of the abnormalities identified is important as patients with mild physiological or imaging abnormalities are likely to remain clinically stable. In contrast, those with more severe disease are at increased risk for disease progression (45).

Changes in FVC or DLCO should indicate HRCT chest imaging; evidence of disease progression should start a discussion regarding the treatment. Treatment of significant interstitial lung disease may include Cyclophosphamide (46), autologous stem cell transplantation (47) and/or Mycophenolate Mofetil (for maintenance therapy) in patients requiring treatment. A simple stratification scheme developed by Goh et al. (45) utilises HRCT extent of disease and lung function tests and provides discriminatory prognostic information. Surgical lung biopsy in these patients is not routinely necessary as the clinical course and outcome is similar between the major histopathological subsets in SSc-ILD (i.e. NSIP and UIP) (21). However, despite its feasibility, the Goh' score remains qualitative and is subjective to limited reproducibility.

This thesis focuses on the early recognition of complicating pulmonary hypertension and interstitial lung disease. In addition it studies the relation between structure and function using different imaging and lung function techniques. By doing so, an improved characterisation of the individual SSc patient may be achieved facilitating personalized care.

Cardiopulmonary exercise testing in the evaluation of pulmonary arterial hypertension in systemic sclerosis

Dyspnea on exertion, fatigue and reduced exercise tolerance are common symptoms in patients with systemic sclerosis. PH may develop in the course of the disease resulting from developing pulmonary vasculopathy (PV). PV impairs dilatation of pulmonary blood

vessels in rest and during exercise, giving rise to impaired blood flow. The impedance of the respiratory system is thereby affected and results from primarily the reduced compliance of the pulmonary vasculature (48). Pulmonary arterial hypertension related to SSc (PAH-SSc) is associated with high morbidity and mortality as well as poorer response to therapy and worse outcomes compared with the idiopathic form of PAH (iPAH) (49). After three years of follow-up, less than 50% of PAH-SSc patients were still alive versus 83% of iPAH patients.

There is a need to identify variables that predict disease progression early in the course of PAH-SSc. These variables must be associated with clinical outcomes and responsive to therapeutic intervention (50). Among these new variables, exercise pulmonary hemodynamics may promise major determinants of heart failure in PAH-SSc. Exercise stress in PAH-SSc as well as in patients with developing PV tests the ability of the diseased heart to increase its output and the pulmonary vasculature to respond to an increased blood flow. Failure of these adaptations will result in impaired stroke volume increase or even decrease (51). During exercise, the increase in mean pulmonary artery pressure (mPAP) in relation to oxygen uptake ($V'O_2$) may show either a "takeoff" or "plateau" pattern.

Patients with severe exercise induced PAH (EIPAH) and resting PAH will show a "plateau" physiology. In these patients mPAP will increase as well as the pulmonary vascular resistance (PVR) during exercise until the cardiac output is compromised and starts to fall. Eventually, with a decline in cardiac output as a result of right ventricular dysfunction, mPAP will not further increase or even fall resulting in a compensatory tachycardia. In contrast, patients with mild to moderate EIPAH showed a "take-off" physiology, suggesting pulmonary vasoconstriction during incremental exercise. In these patients, mPAP further increases in which the cardiac output does not decrease. Therefore, it seems plausible that patients with PAH of varying duration and severity will exhibit different mPAP responses to exercise (51).

Several studies have been performed to assess the occurrence and or presence of EIPAH in SSc (43;44;48;52). Combination of echocardiography and cardiopulmonary exercise testing (CPET) in these patients revealed an elevated systolic pulmonary artery pressure (SPAP) during right-sided heart catheterization and a low peak oxygen uptake. By discriminating patients during CPET using peak oxygen uptake (peak $V'O_2$), low oxygen pulse ($V'O_2/HR$), a low oxygen uptake to work rate ratio ($\Delta V'O_2/\Delta WR$) and an elevated ventilatory equivalent for CO_2 ($V'E/V'CO_2$) pulmonary vasculopathy could be distinguish from left ventricular disease and a normal response (48). Interestingly, several patients showed a marked decrease in their oxygen uptake to heart rate increase ratio ($\Delta V'O_2/\Delta HR$) resulting in a breakpoint

(48). Furthermore, peak oxygen uptake was significantly lower than in patients not showing this response. This breakpoint represents a change in cardiovascular response to exercise by an abrupt increase in heart rate since cardiac output cannot effectively increase by stroke volume alone. This indicates that the rise in HR is disproportionally faster than $V'O_2$ as work rate increases and may be related to increasing pulmonary arterial pressures. However, whether this breakpoint analysis relates to impaired aerobic capacity or impaired stroke volumes i.e. pulmonary arterial pressures is not known.

The aim of chapter 2 is to analyse the $V'O_2$/HR slope breakpoint method in the detection of pulmonary vasculopathy by using an automated breakpoint detection algorithm. Furthermore, the relation between this novel analysis of $V'O_2$/HR slopes, pulmonary arterial pressures and peak oxygen uptake in SSc is discussed.

Novel assessment of myocardial involvement in systemic sclerosis

Myocardial involvement in SSc may include pericarditis, microvascular coronary artery disease, conduction abnormalities and in particular, impaired myocardial contractility or relaxation of right or left ventricle with or without heart failure (53). Myocardial dysfunction is presumably caused by myocardial fibrosis and inflammation giving rise to microangiopathy, vasospasms and poor vasodilator reserve (54). In a post-mortem study, myocardial fibrosis was detected in up to 70% of patients with SSc (54). Early diagnosis of myocardial involvement therefore plays an important role in the management of these patients.

Conventional echocardiographic assessment of left (LV) and right ventricular (RV) function is based on the LV ejection fraction (LVEF) and tricuspid annular plain systolic excursion (TAPSE) (55). However, these measurements have shown limited sensitivity for assessment of myocardial abnormalities in patients with SSc (53). Tissue Doppler imaging (TDI) assesses myocardial tissue velocities and is able to provide information on longitudinal function at the mitral valve annular level (56). Results of initial studies using tissue Doppler imaging suggested that myocardial velocity and deformation (strain) might be more sensitive than conventional measures in identifying subtle cardiac dysfunction in asymptomatic patients with SSc (57-59). Furthermore, myocardial analysis by TDI is significantly limited by angle dependency and does not allow for the evaluation of all LV segments and of different directions of myocardial deformation.

Recently, 2-dimensional speckle-tracking strain analysis has been proposed as a sensitive, non-invasive and accurate method for the evaluation of subclinical myocardial dysfunction (60). It provides measures of LV regional and global strain in three orthogonal directions (longitudinal, circumferential and radial).

The aim of chapter 3 is to assess LV dysfunction and its relation with functional capacity using this novel technique in patients with SSc and controls. Chapter 4 focuses on RV free wall strain and its association with pulmonary fibrosis and elevated pulmonary arterial pressures in patients with SSc and controls.

Dyspnea assessment and control of breathing in systemic sclerosis

Humans can sense a wide range of respiratory sensations such as respiratory motion, lung position, irritation, urge to cough, chest tightness and sense of effort. Among these respiratory sensations, specific aspects such as chest tightness and sense of effort are the most important contributors to the sensation of dyspnea (61). In systemic sclerosis, complicating interstitial lung disease and pulmonary hypertension may result into dyspnea (46). In SSc, an increased impedance of the respiratory system is recognized as the most frequent cause of dyspnea (62). The impedance of the respiratory system is influenced by the lung and chest wall compliance and the respiratory flow resistance (62). In progressive SSc, reduced chest wall and lung compliance may result from limited chest wall excursions and a thickened thoracic skin (63;64). Lung volumes and gas transfer studies are related to disease severity in systemic sclerosis (46). However, whether the magnitude of dyspnea relates to these function tests is not known.

To assess the respiratory drive as a function of the impedance of the respiratory system, resting ventilation (V'E) can be evaluated. However, ventilation, is an imperfect output parameter since it is affected by alterations in the impedance of the respiratory system (62). Mouth occlusion pressures (MOP) provide an excellent reproducibility and reported normal values are independent of age and sex (62). In a study of normal subjects and patients with ILD, MOP were able to distinguish between these groups (65). Furthermore, in combination with CO_2 rebreathing, the respiratory drive to hypercapnia provides insight into the central chemoreflex (66). These determinants of the respiratory drive may assess the dyspnea sensation more precisely than lung volumes and gas transfer studies do.

Dyspnea in SSc may also arise from an altered control of breathing (67). Specifically, an inappropriate response upon the chemoreflex drive at rest and during exercise to carbon dioxide (CO_2) may influence their control of breathing (68). The peripheral chemoreflex plays in important role in the control of breathing and therefore in the sensation of dyspnea (69). It not only ensures oxygen homeostasis, but also helps maintain CO_2 levels at rest and during exercise (68). The carotid bodies, the site of the peripheral chemoreflex to oxygen, CO_2 and pH, contain a complex microvascular anatomy in a macrovascular environment. Systemic sclerosis related inflammatory and fibrotic responses may cause a diminished peripheral chemoreflex response (70). This response may result into an increased susceptibility to exercise intolerance and consequently reported dyspnea during exercise (71).

The aim of chapter 5 was to evaluate the respiratory drive at rest and during CO_2 rebreathing by mouth occlusion pressures (MOP) and their correlation with reported dyspnea. Furthermore, the aim of chapter 6 was to assess the peripheral chemoreflex drive at rest and during exercise in healthy subjects and SSc patients.

Quantitative analysis of interstitial lung disease in systemic sclerosis

Clinical risk assessment of organ manifestations in systemic sclerosis (SSc) has revealed that interstitial lung disease (ILD) is present in 53% of cases with diffuse cutaneous SSc (dcSSC) and in 35% of cases with limited cutaneous SSc (lcSSc) (72). The most common pathological finding in lung biopsies of ILD in patients with SSc is nonspecific interstitial pneumonia (NSIP), although usual interstitial pneumonitis (UIP) is also occasionally found (73). However, discrimination between NSIP or UIP pathology does not improve outcome (21). Hence, the discrimination between these subtypes of ILD is limited to computed tomography (CT) scanning.

Currently, chest high-resolution computed tomography (HRCT) is the most reliable means of detecting SSc-ILD (74;75). The chest radiograph, although a valuable initial screening tool, is

notoriously insensitive in the detection of SSc-ILD (76). The HRCT profile in SSc-ILD is typical of that seen in idiopathic NSIP and most commonly consists of a variable mixture of ground-glass attenuation and reticulation, without honeycomb change. However, in a minority of patients, honeycomb change is more prominent and is likely to be indicative of a histological pattern of UIP (74). Although the relative proportions of ground-glass attenuation, reticulation, and honeycombing have been quantified in several clinical studies,

this exercise does not, in general, provide clinically useful information. The exception to this rule is the occasional patient with prominent ground-glass attenuation which, in the absence of traction bronchiectasis, identifies a high likelihood of reversible inflammatory disease.

Both the severity and the extent of ILD are usually estimated by semi-quantitative scoring of a limited number of cross-sectional slices through the lungs (77;78). Clear survival discrimination was demonstrated by an easy to perform staging algorithm in combination with pulmonary function test data (45). However, despite this benefit visual scoring has limited reproducibility because of its subjective nature. In contrast, formal quantification of the extent of disease on HRCT is currently widely used in clinical studies but is insufficient for routine clinical evaluation due to its complexity and its performance with a lack of volume correction (74;79;80).

HRCT data provide a means to quantitatively analyze the structure of the whole lung, since inflammation, ground glass opacities, and fibrosis can be quantified by lung densitometry. Therefore, objective quantitative techniques by CT densitometry may provide a more sensitive measurement, similar to what has been proven in assessing progression of pulmonary emphysema by the percentile density method (81). Since these quantitative techniques are automated, it is feasible to quantify the entire lungs instead of only a limited number of slices, with a smaller chance of missing pathological changes.

Previously, Camiciotolli et al. (79) reported that lung density histogram parameters are more reproducible than visual assessment of HRCT and are more closely related to functional, exercise, and quality-of-life impairment in SSc. In their evaluation of each patient, they calculated the average global density of the lung and included kurtosis and skewness of the density histogram of the whole lung. However, this analysis did not provide a single overall score for the structure of the lungs, and lung density values were not corrected for lung volume. In a recent report, the same investigators clearly demonstrated the need for volume correction of density parameters (80). Volume-corrected lung density parameters calculated by specific software may be useful outcome measures in evaluating the progression of ILD and the response to treatment.

The aim of chapter 7 focuses is to identify the optimal percentile density threshold by using novel quantitative CT densitometry. In addition, we compared the change in percentile density score over time with changes in FVC and DLCO.

References

(1)   LeRoy EC, Black C, Fleischmajer R, Jablonska S, Krieg T, Medsger TA, Jr. et al. Scleroderma (systemic sclerosis): classification, subsets and pathogenesis. J Rheumatol 1988;15(2): 202-5.

(2)   Elhai M, Meune C, Avouac J, Kahan A, Allanore Y. Trends in mortality in patients with systemic sclerosis over 40 years: a systematic review and meta-analysis of cohort studies. Rheumatology (Oxford) 2012;51(6):1017-26.

(3)   Tyndall AJ, Bannert B, Vonk M, Airo P, Cozzi F, Carreira PE et al. Causes and risk factors for death in systemic sclerosis: a study from the EULAR Scleroderma Trials and Research (EUSTAR) database. Ann Rheum Dis 2010;69(10):1809-15.

(4)   Steen VD, Conte C, Owens GR, Medsger TA, Jr. Severe restrictive lung disease in systemic sclerosis. Arthritis Rheum 1994;37(9):1283-9.

(5)   Steen VD, Medsger TA. Changes in causes of death in systemic sclerosis, 1972-2002. Ann Rheum Dis 2007;66(7):940-4.

(6)   Morelli S, Barbieri C, Sgreccia A, Ferrante L, Pittoni V, Conti F et al. Relationship between cutaneous and pulmonary involvement in systemic sclerosis. J Rheumatol 1997;24(1): 81-5.

(7)   D'Angelo WA, Fries JF, Masi AT, Shulman LE. Pathologic observations in systemic sclerosis (scleroderma). A study of fifty-eight autopsy cases and fifty-eight matched controls. Am J Med 1969;46(3):428-40.

(8)   Fischer A, Pfalzgraf FJ, Feghali-Bostwick CA, Wright TM, Curran-Everett D, West SG et al. Anti-th/to-positivity in a cohort of patients with idiopathic pulmonary fibrosis. J Rheumatol 2006;33(8):1600-5.

(9)   Weaver AL, Divertie MB, Titus JL. The lung scleroderma. Mayo Clin Proc 1967; 42(11):754-66.

(10)   Weaver AL, Divertie MB, Titus JL. Pulmonary scleroderma. Dis Chest 1968;54(6):490-8.

(11)   Steen VD. The lung in systemic sclerosis. J Clin Rheumatol 2005;11(1):40-6.

(12)   Steen VD, Medsger TA, Jr. Severe organ involvement in systemic sclerosis with diffuse scleroderma. Arthritis Rheum 2000;43(11):2437-44.

(13)   Steen VD, Graham G, Conte C, Owens G, Medsger TA, Jr. Isolated diffusing capacity reduction in systemic sclerosis. Arthritis Rheum 1992;35(7):765-70.

(14)   Greidinger EL, Flaherty KT, White B, Rosen A, Wigley FM, Wise RA. African-American race and antibodies to topoisomerase I are associated with increased severity of scleroderma lung disease. Chest 1998;114(3):801-7.

(15)   McNearney TA, Reveille JD, Fischbach M, Friedman AW, Lisse JR, Goel N et al. Pulmonary involvement in systemic sclerosis: associations with genetic, serologic, sociodemographic, and behavioral factors. Arthritis Rheum 2007;57(2):318-26.

(16)   Steele R, Hudson M, Lo E, Baron M. Clinical decision rule to predict the presence of interstitial lung disease in systemic sclerosis. Arthritis Care Res (Hoboken) 2012;64(4):519-24.

(17)   Briggs DC, Vaughan RW, Welsh KI, Myers A, duBois RM, Black CM. Immunogenetic prediction of pulmonary fibrosis in systemic sclerosis. Lancet 1991;338(8768):661-2.

(18)   Steen VD, Conte C, Owens GR, Medsger TA, Jr. Severe restrictive lung disease in systemic sclerosis. Arthritis Rheum 1994;37(9):1283-9.

(19)   Morgan C, Knight C, Lunt M, Black CM, Silman AJ. Predictors of end stage lung disease in a cohort of patients with scleroderma. Ann Rheum Dis 2003;62(2):146-50.

(20)   Steen VD, Owens GR, Fino GJ, Rodnan GP, Medsger TA, Jr. Pulmonary involvement in systemic sclerosis (scleroderma). Arthritis Rheum 1985;28(7):759-67.

(21)   Bouros D, Wells AU, Nicholson AG, Colby TV, Polychronopoulos V, Pantelidis P et al. Histopathologic subsets of fibrosing alveolitis in patients with systemic sclerosis and their relationship to outcome. Am J Respir Crit Care Med 2002;165(12):1581-6.

(22)   Wells AU, Hansell DM, Rubens MB, King AD, Cramer D, Black CM et al. Fibrosing alveolitis in systemic sclerosis: indices of lung function in relation to extent of disease on computed tomography. Arthritis Rheum 1997;40(7):1229-36.

(23)   Hoeper MM. Pulmonary hypertension in collagen vascular disease. Eur Respir J 2002;19(3):571-6.

(24)   Simonneau G, Gatzoulis MA, Adatia I, Celermajer D, Denton C, Ghofrani A et al. Updated clinical classification of pulmonary hypertension. J Am Coll Cardiol 2013;62(25 Suppl):D34-D41.

(25)   Badesch DB, Champion HC, Sanchez MA, Hoeper MM, Loyd JE, Manes A et al. Diagnosis and assessment of pulmonary arterial hypertension. J Am Coll Cardiol 2009;54(1 Suppl):S55-S66.

(26)   Battle RW, Davitt MA, Cooper SM, Buckley LM, Leib ES, Beglin PA et al. Prevalence of pulmonary hypertension in limited and diffuse scleroderma. Chest 1996;110(6):1515-9.

(27)   Avouac J, Airo P, Meune C, Beretta L, Dieude P, Caramaschi P et al. Prevalence of pulmonary hypertension in systemic sclerosis in European Caucasians and metaanalysis of 5 studies. J Rheumatol 2010;37(11):2290-8.

(28)   Hachulla E, Launay D, Mouthon L, Sitbon O, Berezne A, Guillevin L et al. Is pulmonary arterial hypertension really a late complication of systemic sclerosis? Chest 2009;136(5):1211-9.

(29)   Stupi AM, Steen VD, Owens GR, Barnes EL, Rodnan GP, Medsger TA, Jr. Pulmonary hypertension in the CREST syndrome variant of systemic sclerosis. Arthritis Rheum 1986;29(4):515-24.

(30)   Schachna L, Wigley FM, Chang B, White B, Wise RA, Gelber AC. Age and risk of pulmonary arterial hypertension in scleroderma. Chest 2003;124(6):2098-104.

(31)   Steen V, Medsger TA, Jr. Predictors of isolated pulmonary hypertension in patients with systemic sclerosis and limited cutaneous involvement. Arthritis Rheum 2003;48(2):516-22.

(32)   Yamane K, Ihn H, Asano Y, Yazawa N, Kubo M, Kikuchi K et al. Clinical and laboratory features of scleroderma patients with pulmonary hypertension. Rheumatology (Oxford) 2000;39(11):1269-71.

(33) Ong YY, Nikoloutsopoulos T, Bond CP, Smith MD, Ahern MJ, Roberts-Thomson PJ. Decreased nailfold capillary density in limited scleroderma with pulmonary hypertension. Asian Pac J Allergy Immunol 1998;16(2-3):81-6.

(34) Okano Y, Steen VD, Medsger TA, Jr. Autoantibody to U3 nucleolar ribonucleoprotein (fibrillarin) in patients with systemic sclerosis. Arthritis Rheum 1992;35(1):95-100.

(35) Walker UA, Tyndall A, Czirjak L, Denton C, Farge-Bancel D, Kowal-Bielecka O et al. Clinical risk assessment of organ manifestations in systemic sclerosis: a report from the EULAR Scleroderma Trials And Research group database. Ann Rheum Dis 2007;66(6):754-63.

(36) Clements PJ, Tan M, McLaughlin VV, Oudiz RJ, Tapson VF, Channick RN et al. The pulmonary arterial hypertension quality enhancement research initiative: comparison of patients with idiopathic PAH to patients with systemic sclerosis-associated PAH. Ann Rheum Dis 2012;71(2):249-52.

(37) Denton CP, Cailes JB, Phillips GD, Wells AU, Black CM, Bois RM. Comparison of Doppler echocardiography and right heart catheterization to assess pulmonary hypertension in systemic sclerosis. Br J Rheumatol 1997;36(2):239-43.

(38) Phung S, Strange G, Chung LP, Leong J, Dalton B, Roddy J et al. Prevalence of pulmonary arterial hypertension in an Australian scleroderma population: screening allows for earlier diagnosis. Intern Med J 2009;39(10):682-91.

(39) Steen VD, Graham G, Conte C, Owens G, Medsger TA, Jr. Isolated diffusing capacity reduction in systemic sclerosis. Arthritis Rheum 1992;35(7):765-70.

(40) Steen VD, Graham G, Conte C, Owens G, Medsger TA, Jr. Isolated diffusing capacity reduction in systemic sclerosis. Arthritis Rheum 1992;35(7):765-70.

(41) Hachulla E, Gressin V, Guillevin L, Carpentier P, Diot E, Sibilia J et al. Early detection of pulmonary arterial hypertension in systemic sclerosis: a French nationwide prospective multicenter study. Arthritis Rheum 2005;52(12):3792-800.

(42) Vachiery JL, Coghlan G. Screening for pulmonary arterial hypertension in systemic sclerosis. Eur Respir Rev 2009;18(113):162-9.

(43) Mukerjee D, St GD, Knight C, Davar J, Wells AU, du Bois RM et al. Echocardiography and pulmonary function as screening tests for pulmonary arterial hypertension in systemic sclerosis. Rheumatology (Oxford) 2004;43(4):461-6.

(44) Kovacs G, Maier R, Aberer E, Brodmann M, Scheidl S, Hesse C et al. Assessment of pulmonary arterial pressure during exercise in collagen vascular disease: echocardiography vs right-sided heart catheterization. Chest 2010;138(2):270-8.

(45) Goh NS, Desai SR, Veeraraghavan S, Hansell DM, Copley SJ, Maher TM et al. Interstitial lung disease in systemic sclerosis: a simple staging system. Am J Respir Crit Care Med 2008;177(11):1248-54.

(46) Tashkin DP, Elashoff R, Clements PJ, Goldin J, Roth MD, Furst DE et al. Cyclophosphamide versus placebo in scleroderma lung disease. N Engl J Med 2006;354(25):2655-66.

(47) van Laar JM, Farge D, Sont JK, Naraghi K, Marjanovic Z, Larghero J et al. Autologous hematopoietic stem cell transplantation vs intravenous pulse cyclophosphamide in diffuse cutaneous systemic sclerosis: a randomized clinical trial. JAMA 2014;311(24):2490-8.

(48) Dumitrescu D, Oudiz RJ, Karpouzas G, Hovanesyan A, Jayasinghe A, Hansen JE et al. Developing pulmonary vasculopathy in systemic sclerosis, detected with non-invasive cardiopulmonary exercise testing. PLoS One 2010;5(12):e14293.

(49) Fisher MR, Mathai SC, Champion HC, Girgis RE, Housten-Harris T, Hummers L et al. Clinical differences between idiopathic and scleroderma-related pulmonary hypertension. Arthritis Rheum 2006;54(9):3043-50.

(50) Chaouat A, Sitbon O, Mercy M, Poncot-Mongars R, Provencher S, Guillaumot A et al. Prognostic value of exercise pulmonary haemodynamics in pulmonary arterial hypertension. Eur Respir J 2014;44(3):704-13.

(51) Tolle JJ, Waxman AB, Van Horn TL, Pappagianopoulos PP, Systrom DM. Exercise-induced pulmonary arterial hypertension. Circulation 2008;118(21):2183-9.

(52) Kovacs G, Maier R, Aberer E, Brodmann M, Scheidl S, Troster N et al. Borderline pulmonary arterial pressure is associated with decreased exercise capacity in scleroderma. Am J Respir Crit Care Med 2009;180(9):881-6.

(53) Allanore Y, Meune C, Vonk MC, Airo P, Hachulla E, Caramaschi P et al. Prevalence and factors associated with left ventricular dysfunction in the EULAR Scleroderma Trial and Research group (EUSTAR) database of patients with systemic sclerosis. Ann Rheum Dis 2010;69(1):218-21.

(54) Follansbee WP, Miller TR, Curtiss EI, Orie JE, Bernstein RL, Kiernan JM et al. A controlled clinicopathologic study of myocardial fibrosis in systemic sclerosis (scleroderma). J Rheumatol 1990;17(5):656-62.

(55) Rudski LG, Lai WW, Afilalo J, Hua L, Handschumacher MD, Chandrasekaran K et al. Guidelines for the echocardiographic assessment of the right heart in adults: a report from the American Society of Echocardiography endorsed by the European Association of Echocardiography, a registered branch of the European Society of Cardiology, and the Canadian Society of Echocardiography. J Am Soc Echocardiogr 2010;23(7):685-713.

(56) Meune C, Avouac J, Wahbi K, Cabanes L, Wipff J, Mouthon L et al. Cardiac involvement in systemic sclerosis assessed by tissue-doppler echocardiography during routine care: A controlled study of 100 consecutive patients. Arthritis Rheum 2008;58(6):1803-9.

(57) Mele D, Censi S, La CR, Merli E, Lo MA, Locaputo A et al. Abnormalities of left ventricular function in asymptomatic patients with systemic sclerosis using Doppler measures of myocardial strain. J Am Soc Echocardiogr 2008;21(11):1257-64.

(58) Kepez A, Akdogan A, Sade LE, Deniz A, Kalyoncu U, Karadag O et al. Detection of subclinical cardiac involvement in systemic sclerosis by echocardiographic strain imaging. Echocardiography 2008;25(2):191-7.

(59) D'Andrea A, Stisi S, Bellissimo S, Vigorito F, Scotto di UF, Tozzi N et al. Early impairment of myocardial function in systemic sclerosis: non-invasive assessment by Doppler myocardial and strain rate imaging. Eur J Echocardiogr 2005;6(6):407-18.

(60) Blessberger H, Binder T. NON-invasive imaging: Two dimensional speckle tracking echocardiography: basic principles. Heart 2010;96(9):716-22.

(61) Nishino T. Dyspnoea: underlying mechanisms and treatment. Br J Anaesth 2011;106(4): 463-74.

(62) Whitelaw WA, Derenne JP, Milic-Emili J. Occlusion pressure as a measure of respiratory center output in conscious man. Respir Physiol 1975;23(2):181-99.

(63) Nageh TT, du Bois RM. Non-invasive ventilation in hypercapnic respiratory failure secondary to sclerodermic chest wall restriction. Respir Med 1998;92(9):1170-2.

(64) Pugazhenthi M, Cooper D, Ratnakant BS, Postlethwaite A, Carbone L. Hypercapnic respiratory failure in systemic sclerosis. J Clin Rheumatol 2003;9(1):43-6.

(65) Scott GC, Burki NK. The relationship of resting ventilation to mouth occlusion pressure. An index of resting respiratory function. Chest 1990;98(4):900-6.

(66) Jordan C. Automatic method for measuring mouth occlusion pressure response to carbon dioxide inhalation. Med Biol Eng Comput 1981;19(3):279-86.

(67) Cherniack RM, SNIDAL DP. The effect of obstruction to breathing on the ventilatory response to CO2. J Clin Invest 1956;35(11):1286-90.

(68) Wasserman K. Breathing during exercise. N Engl J Med 1978;298(14):780-5.

(69) Prabhakar NR, Peng YJ. Peripheral chemoreceptors in health and disease. J Appl Physiol (1985) 2004;96(1):359-66.

(70) Matucci-Cerinic M, Kahaleh B, Wigley FM. Review: evidence that systemic sclerosis is a vascular disease. Arthritis Rheum 2013;65(8):1953-62.

(71) Lugliani R, Whipp BJ, Seard C, Wasserman K. Effect of bilateral carotid-body resection on ventilatory control at rest and during exercise in man. N Engl J Med 1971;285(20):1105-11.

(72) Walker UA, Tyndall A, Czirjak L, Denton C, Farge-Bancel D, Kowal-Bielecka O et al. Clinical risk assessment of organ manifestations in systemic sclerosis: a report from the EULAR Scleroderma Trials And Research group database. Ann Rheum Dis 2007;66(6):754-63.

(73) Bouros D, Wells AU, Nicholson AG, Colby TV, Polychronopoulos V, Pantelidis P et al. Histopathologic subsets of fibrosing alveolitis in patients with systemic sclerosis and their relationship to outcome. Am J Respir Crit Care Med 2002;165(12):1581-6.

(74) Wells AU, Margaritopoulos GA, Antoniou KM, Denton C. Interstitial lung disease in systemic sclerosis. Semin Respir Crit Care Med 2014;35(2):213-21.

(75) Wells AU. High-resolution computed tomography and scleroderma lung disease. Rheumatology (Oxford) 2008;47 Suppl 5:v59-v61.

(76)   Schurawitzki H, Stiglbauer R, Graninger W, Herold C, Polzleitner D, Burghuber OC et al. Interstitial lung disease in progressive systemic sclerosis: high-resolution CT versus radiography. Radiology 1990;176(3):755-9.

(77)   Goh NS, Desai SR, Veeraraghavan S, Hansell DM, Copley SJ, Maher TM et al. Interstitial lung disease in systemic sclerosis: a simple staging system. Am J Respir Crit Care Med 2008;177(11):1248-54.

(78)   Kazerooni EA, Martinez FJ, Flint A, Jamadar DA, Gross BH, Spizarny DL et al. Thin-section CT obtained at 10-mm increments versus limited three-level thin-section CT for idiopathic pulmonary fibrosis: correlation with pathologic scoring. AJR Am J Roentgenol 1997;169(4):977-83.

(79)   Camiciottoli G, Orlandi I, Bartolucci M, Meoni E, Nacci F, Diciotti S et al. Lung CT densitometry in systemic sclerosis: correlation with lung function, exercise testing, and quality of life. Chest 2007;131(3):672-81.

(80)   Camiciottoli G, Diciotti S, Bartolucci M, Orlandi I, Bigazzi F, Matucci-Cerinic M et al. Whole-lung volume and density in spirometrically-gated inspiratory and expiratory CT in systemic sclerosis: correlation with static volumes at pulmonary function tests. Sarcoidosis Vasc Diffuse Lung Dis 2013;30(1):17-27.

(81)   Stolk J, Versteegh MI, Montenij LJ, Bakker ME, Grebski E, Tutic M et al. Densitometry for assessment of effect of lung volume reduction surgery for emphysema. Eur Respir J 2007;29(6):1138-43.

Chapter 2

Detection of pulmonary vasculopathy by novel analysis of oxygen uptake in patients with systemic sclerosis: association with pulmonary arterial pressures

Maarten K. Ninaber, Willem B.G.J. Hamersma, Anne A. Schouffoer, Gabor Kovacs, Horst Olschewski, Eduard R. Holman, Nina Ajmone Marsan and Jan Stolk

Abstract

Objective: During cardiopulmonary exercise testing (CPET) compromised pulmonary vasculature in patients with systemic sclerosis (SSc) may lead to increases in pulmonary arterial pressures (PAP) and decreased oxygen uptake. We hypothesized that this may lead into a disproportional heart rate (HR) increase with a corresponding $V'O_2/HR$ breakpoint and relates to systolic PAP at rest.

Methods: In a prospective design we evaluated $V'O_2/HR$ slopes for breakpoints. To understand its physiological meaning, we evaluated $V'O_2/HR$ and $V'O_2/mPAP$ slopes for breakpoints in a historic data set of SSc patients, in which CPET and right heart catheterization was performed simultaneously. $V'O_2/HR$ slopes with a peak oxygen uptake outside the normal range were defined as pathologic.

Results: A breakpoint occurred in *both* $V'O_2/mPAP$ and $V'O_2/HR$ slope in 16/34 patients in the historic dataset and occurred in the $V'O_2/mPAP$ slope at a lower $V'O_2$ in 15 patients. In the prospective dataset, 73/121 patients showed a $V'O_2/HR$ breakpoint and achieved a significantly lower peak oxygen uptake compared to 48/121 patients without a $V'O_2/HR$ breakpoint (p=0.036). Mean systolic PAP in 41/121 patients with a pathologic $V'O_2/HR$ slope differed significantly from patients without a pathologic $V'O_2/HR$ slope (p=0.027). In 27/121 patients with a systolic PAP <35 mmHg a pathologic $V'O_2/HR$ slope was observed.

Conclusion: SSc patients with a $V'O_2/HR$ breakpoint are characterized by a decreased oxygen uptake, likely caused by sudden PAP increases during exercise. Importantly, in patients with normal resting SPAP pathologic $V'O_2/HR$ slopes were observed. This suggests that these patients are at risk for developing pulmonary hypertension.

Introduction

Patients with SSc are at risk for developing pulmonary hypertension (PH) with an estimated prevalence of 8–12% (1-3;3;4). In SSc, Doppler echocardiography (DE) is used for screening of PH and a SPAP threshold of 35 mmHg is used to define elevated pulmonary pressures which may suggest the presence of PH (3;4). CPET is another important tool in the evaluation of patients with suspected PH which reveals impaired gas exchange and might therefore be useful as an early detection tool (2;5;6). The oxygen pulse, which normalizes oxygen consumption for heart rate, is widely used as an indirect measurement for cardiac stroke volume (SV) (7) and is correlated with invasively measured SV (8). Usually reported against load or time during exercise (6), it may also be described as the oxygen uptake against heart rate ($V'O_2$/HR) (9). Peak oxygen uptake serves as a marker for cardiac performance during exercise in patients with PH (10-12). In SSc, elevated systolic pulmonary arterial pressures, SPAP ≥35 mmHg, are inversely correlated with peak oxygen uptake (13). However, the relation between the $V'O_2$/HR slope and the occurrence of cardiovascular dysfunction due to SSc related pulmonary vasculopathy (PV) is unknown. Therefore, this slope may contain additional information on the cardiovascular response to exercise in SSc.

In our clinical experience, a significant number of SSc patients show a $V'O_2$/HR slope with a breakpoint during exercise testing while pulmonary pressures measured by DE at rest are normal (9). In these patients, the heart rate suddenly increases disproportionally to an increase in $V'O_2$ before reaching the predicted peak oxygen uptake. This response may reflect acute increased pulmonary arterial pressures to indicate a change in cardiac response (7;12). We therefore hypothesized that the onset of a breakpoint in the $V'O_2$/HR slope is a result of a sudden increase in pulmonary arterial pressures. In these patients the exercise capacity and oxygen uptake may be decreased and may be related to SPAP at rest.

Methods

Ethics statement

The local Medical Ethical Committee of the Leiden University Medical Center approved the protocol. A written informed consent was obtained from each patient prior to enrollment.

The V'O$_2$/HR breakpoint principle and analysis

Both oxygen uptake (on a breath-by-breath basis) as well as heart rate are recorded continuously during CPET. Both variables are related to each other and therefore may be presented in a single graph, resulting into a V'O$_2$/HR slope. In general, several hypothetical V'O$_2$/HR slopes (tracks) during CPET may be obtained (Figure 2.1). Patients may either show a monophasic or a biphasic V'O$_2$/HR slope (9) characterized by one or two angles, respectively. In patients
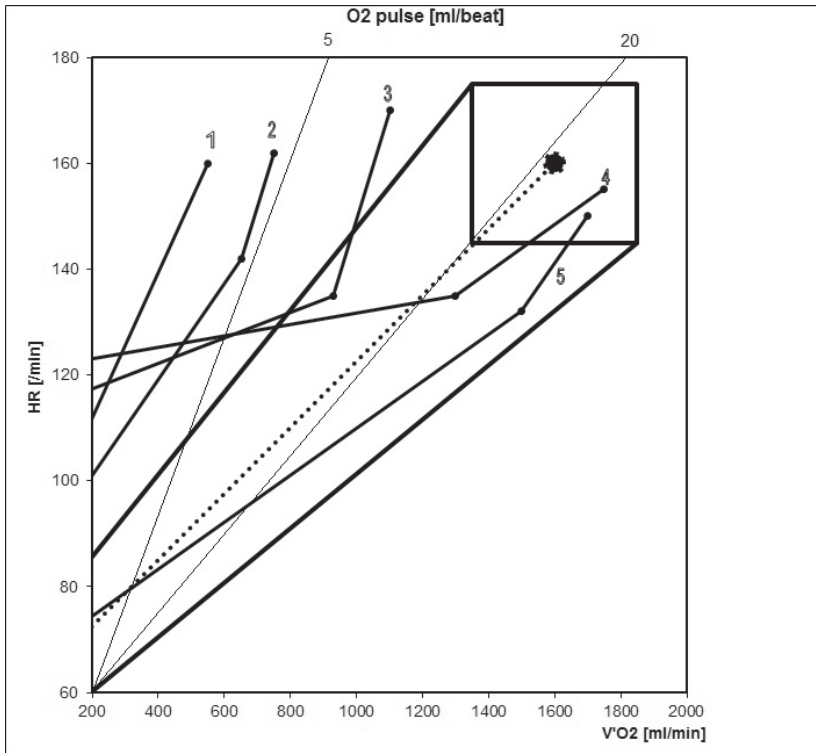
Figure 2.1   Hypothetical V'O$_2$/HR slopes, in which corrected HR values are used.
Normal V'O$_2$/HR slopes are located in the area defined by highly weighted black tracks: the heart rate has an upper and lower limit of 220-age (yr) ± 15 beats/minute, whereas the peak V'O$_2$ has and upper and lower limit of predicted V'O$_2$ ± 15% (9). The oxygen pulse isopleths are provided at 5 and 20 ml per beat.
The dotted track in the middle of this area represents the ideal V'O$_2$/HR, whereas the black dot in the square box represents the predicted peak oxygen pulse.
Track 1 represents a steep V'O$_2$/HR slope reflecting low stroke volumes from the start of exercise.
Track 2 represents a V'O$_2$/HR with a breakpoint and a peak oxygen pulse located outside the normal range (i.e. pathological oxygen pulse slope).
Track 3 represents an abnormal V'O$_2$/HR from the start, including a breakpoint and a peak oxygen pulse outside the normal range.
Track 4 represents initially an abnormal V'O$_2$/HR, including a breakpoint, which normalizes as exercise progresses (i.e. "nervous anticipation").
Track 5 represents a V'O$_2$/HR with a breakpoint and a normal peak oxygen pulse (i.e. V'O$_2$peak = V'O$_2$max)

showing a biphasic V'O$_2$/HR slope, the heart rate is increasing disproportionally against an increase in oxygen uptake when exercise is in progress, and is reflected by a breakpoint. This breakpoint represents a change in cardiovascular response to exercise by an abrupt increase in heart rate since cardiac output cannot effectively increase by stroke volume alone.

Patients may show a biphasic V'O$_2$/HR slope and a peak V'O$_2$/HR located outside the normal range as indicated in Figure 2.1, track 2 and 3. On the other hand, patients may show no breakpoint but only a steep V'O$_2$/HR slope completely located outside the normal range (Figure 2.1, track 1). Both responses are defined by us as pathologic.

The analytical problem was to mathematically identify the breakpoint in a biphasic V'O$_2$/HR slope. Regression lines were calculated between subsequent increases in V'O$_2$ and HR to define a breakpoint by applying freely available software for these calculations (example Figure 2.2) (14). In this program, a joinpoint (i.e. breakpoint) regression model is applied to describe such continuous changes. We used the grid-search method to fit the regression function with a predefined number of jointpoints and assumed constant variance and uncorrelated errors. As a result, this predefined joinpoint is found by performing several permutation tests. Other possible approaches, such as a polynomial fit to the data, could
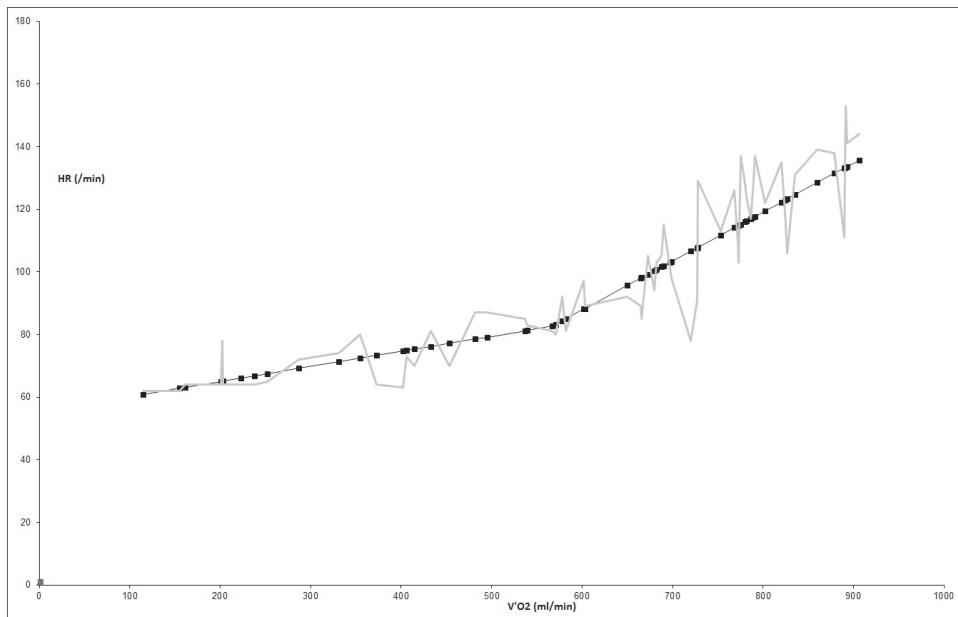

Figure 2.2   Example of a mathematically defined breakpoint in a V'O$_2$/HR slope in a single patient (track with square dots).
Grey track represents the actual derived heart rate and V'O$_2$.

be considered, however, these do not produce a single value for a breakpoint. Therefore we adopted the joinpoint method in our analysis.

Patients

First, we explored the kinetics of V'O$_2$/HR slopes in a historic Austrian dataset of SSc patients. Data of some of these patients were described previously (5) and contained SSc patients in whom pulmonary artery pressures measured by right heart catheterization (RHC) were obtained during CPET. An increase in the pulmonary pressures reflects a decreased pulmonary vessel wall compliance resulting in a sudden increase in heart rate or right ventricular stroke volume. Therefore, we were not only able to evaluate whether a breakpoint in the V'O$_2$/HR slope was present but also if it was related to a change in mPAP (i.e. a V'O$_2$/mPAP breakpoint). In these patients, 40 out of 45 patients completed both CPET and RHC tests which proved eligible for our analysis. We applied our software for regression analysis to calculate a V'O$_2$/HR and V'O$_2$/mPAP breakpoint, respectively (14). Figure 2.3 shows the disposition of patients.

Secondly, in the Leiden University Medical Center (LUMC) we screened 131 SSc patients consecutively referred to an outpatient targeted health care program in a prospective design. Patients were classified as limited cutaneous systemic sclerosis (lcSSc) or diffuse cutaneous systemic sclerosis (dcSSc) according to the LeRoy criteria (15). All SSc patients underwent Doppler echocardiography using a commercially available system (Vingmed Vivid 7 and E9, General Electric Vingmed Ultrasound, Horten, Norway). Images were obtained using a 3.5-Mhz transducer and digitally stored in cine-loop format. Subsequent offline analysis was performed using EchoPAC version 110.0.0 (General Electric-Vingmed Ultrasound, Horten, Norway). In all patients Doppler envelopes were well developed. SPAP could therefore be estimated from the tricuspid regurgitation peak gradient using the Bernoulli equation, adding the right atrial pressure estimated by the dimension and the degree of the inferior vena cava respiratory collapse (16;17). Patients were considered to have elevated pulmonary systolic pressures if SPAP was ≥35 mmHg (17). Furthermore, all patients had laboratory testing, pulmonary function testing (PFTs) (18;19), symptom limiting non-invasive CPET (6;10;20), six minute walk test (6MWT) and high-resolution CT scan (HRCT). CT scans were scored as less or more than 20% involvement of interstitial lung disease (ILD) (21). All tests were done in one or two consecutive days.

Statistical analysis

Statistical analysis was performed with the SPSS 20.0 package (SPSS, Inc., Chicago, IL, USA). All data were checked for normal distribution. Continuous variables are expressed as mean value ± standard deviations. Two-sided p-values <0.05 were considered significant. Categorical data are presented as frequencies and percentages. Statistical comparisons were performed by using Student's T-test for continuous variables, and chi square test for binary variables.

Results

Evaluation of the V'O$_2$/HR breakpoint principle in a historic dataset

In 40 out of 45 patients of the historic dataset CPET and RHC data were available and suitable for analysis (Figure 2.3). Six patients showed a mixed response in the occurrence of breakpoints. In total, 16 out of 34 of these SSc patients (47%) had a breakpoint in *both* V'O$_2$/HR and V'O$_2$/mPAP slopes. The remaining 18 patients had no breakpoint in either slope. As an example, Figure 2.4 shows the breakpoint in a V'O$_2$/HR slope and in a V'O$_2$/mPAP slope during exercise. For each patient we calculated the difference in V'O$_2$ between these two breakpoints. Mean difference in V'O$_2$ was 127 ml ± 63 ml. In 15/16 (94%) of these patients, the breakpoint in the V'O$_2$/mPAP slope preceded the breakpoint in the V'O$_2$/HR slope (i.e. earlier during exercise) (Figure 2.4). Taken together, these data suggest that a sudden increase in pulmonary arterial pressures results into a disproportional heart rate response to exercise.

Patient characteristics

Patient characteristics of the prospectively collected data are shown in Table 2.1. Patients with left ventricular dysfunction or heart valve disease (n=4), use of beta-receptor blocking agents (n=3) or endothelin receptor antagonists (n=3) were excluded from analysis.

Based on the SPAP measured by DE, SSc patients were stratified into a SPAP below and above 35 mmHg (98 and 23 patients respectively, Table 2.1). Both groups did not differ in terms of gender, age or BMI. However patients with a SPAP ≥35 mmHg had significantly higher NT-proBNP, FVC and transfer factor for carbon monoxide were lower (Table 2.1).
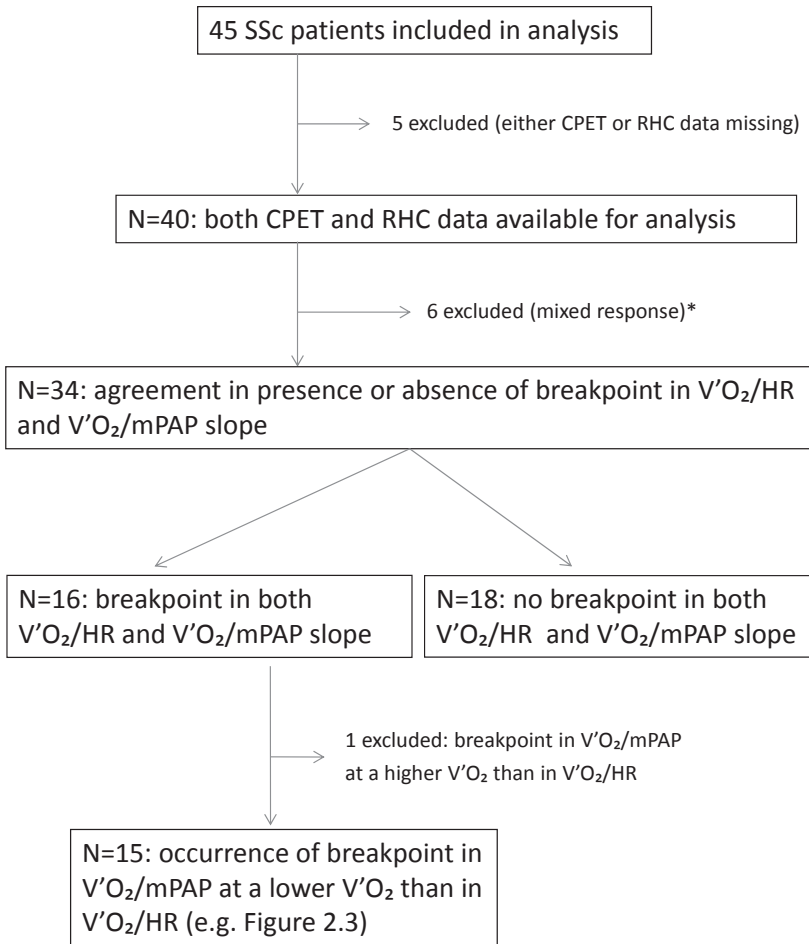
Figure 2.3   Flowchart of SSc patient selection from Graz, Austria.
* either V'O$_2$HR or V'O$_2$mPAP breakpoint.

Also, more ILD was present in patients with a SPAP ≥35 mmHg (p=0.04). During exercise testing, patients with SPAP ≥35 mmHg showed a significant decrease in peak V'O$_2$ and peak V'O$_2$/HR, an increase in V'E/V'CO$_2$ and a significant difference in Δ P$_{et}$CO$_2$*AT*- P$_{et}$CO$_2$start (Table 2.2).
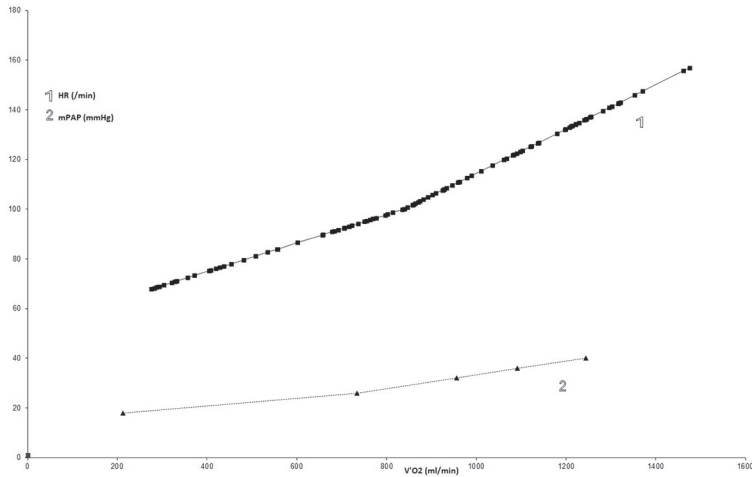
Figure 2.4   Example of a breakpoint in the V'O$_2$/HR slope (track 1) and in the V'O$_2$/mPAP slope (track 2) during exercise from an SSc patient.
Breakpoint in the V'O$_2$/HR slope occurred at a V'O$_2$ of 840 ml. In the V'O$_2$/mPAP slope the breakpoint occurred at a V'O$_2$ of 734 ml.

Table 2.1   Demographic characteristics of 121 SSc patients prospectively screened at LUMC

	SPAP <35 mmHg (n=98)	SPAP ≥35 mmHg (n=23)	P-value
Gender (female) n (%)	78 (79)	18 (78)	0.89
Age, years	55 ± 14.2	60 ± 15.4	0.097
BMI (kg/m^2)	22.8 ± 3.4	21.4 ± 3.1	0.68
lcSSc, n (%)	52 (53)	11 (48)	0.79
Laboratory results			
Hb, mmol L^{-1}	8.1 ± 0.7	7.8 ± 0.6	0.09
Pro-BNP	186 ± 345	944 ± 961	<0.001
Doppler echocardiography			
SPAP	26.8 ± 4.4	42.4 ± 7.7	<0.001
Pulmonary function test			
FVC % pred	96.8 ± 20.9	78.0 ± 21.8	<0.001
DLCOc SB % pred	66.5 ± 16.5	49.3 ± 10.4	<0.001
FVC / DLCO	1.49 ± 0.39	1.59 ± 0.37	0.26
TLC-He % pred	88.9 ± 17.1	73.9 ± 17.5	<0.001
HRCT thorax			
>20% extent of disease, n (%)	24 (24)	9 (39)	0.04

BMI, Body mass index; lcSSc, limited systemic sclerosis; Hb, Hemoglobin; pro-BNP, pro-brain natriuretic peptide; SPAP, systolic pulmonary arterial pressure; FVC, forced vital capacity; DLCOc SB, diffusion capacity for carbon monoxide single breath; TLC-He, total lung capacity, Helium dilution method; HRCT, high-resolution computed tomography.

Table 2.2   CPET variables of 121 SSc patients prospectively studied

	SPAP <35 mmHg (n=98)	SPAP >35 mmHg (n=23)	P-value
Aerobic capacity			
Peak V'O$_2$ (% pred)	88 ± 22	70 ± 19	0.001
AT (% peak V'O$_2$)	43 ± 14	38 ± 7	0.14
RER	1.18 ± 0.12	1.18 ± 0.11	0.95
Cardiac function			
Peak O$_2$-pulse (% pred)	97 ± 25	72 ± 21	0.006
ΔV'O$_2$/ΔWR (ml/min/W)	9.1 ± 1.9	8.6 ± 2.0	0.56
HRR	14.6 ± 20.6	10.7 ± 14.6	0.29
Ventilatory efficiency			
V'E/V'CO$_2$AT	31.5 ± 4.4	35.7 ± 4.5	<0.001
P$_{et}$CO$_2$AT (mmHg)	35.9 ± 3.79	33.7 ± 5.0	0.025
ΔP$_{et}$CO$_2$AT- P$_{et}$CO$_2$start (mmHg)	4.17 ± 2.2	1.4 ± 1.9	0.002

Peak V'O$_2$, peak oxygen uptake; AT, anaerobic threshold; RER, respiratory exchange ratio; peak O$_2$-pulse, peak oxygen pulse; ΔV'O$_2$/ΔWR, oxygen uptake against work rate; HRR, heart rate reserve; V'E/V'CO$_2$AT, ventilatory equivalent for carbon dioxide at anaerobic threshold; P$_{et}$CO$_2$AT, end-tidal carbon dioxide tension.

The V'O$_2$/HR breakpoint principle and analysis

In the prospectively designed study in LUMC SSc patients with a breakpoint in the V'O$_2$/HR slope had a significant lower peak V'O$_2$% predicted compared to patients without a breakpoint (Table 2.3, p=0.036). Disease duration did not differ between these groups. Pathologic slopes classified 41/121 patients (34%, Table 2.3). Classified by a V'O$_2$/HR breakpoint, patients with and without a pathologic V'O$_2$/HR slope differed significantly in 6MWD (p=0.015 and p=0.005).

Of 23 LUMC patients with a SPAP ≥35 mmHg, 14 had a pathologic V'O$_2$/HR slope (61%). Furthermore, mean SPAP differed significantly between patients with and without a pathologic V'O$_2$/HR (31.8 vs. 28.2 mmHg, respectively, p=0.027). Importantly, of 98 LUMC SSc patients 27 (28%) had a pathologic V'O$_2$/HR slope not expected by SPAP at rest (resting SPAP <35 mmHg).

Table 2.3   V'O$_2$/HR breakpoint and pathologic slope of LUMC SSc patients

LUMC population N=121	Breakpoint in V'O$_2$/HR N=73	No breakpoint in V'O$_2$/HR N=48	P-value
Peak V'O$_2$ (% pred)	81	90	0.036
SPAP (mmHg)	30	29	0.52
6MWD (m)	482	527	0.074

	Pathologic V'O$_2$/HR N=23	No pathologic V'O$_2$/HR N=50	P-value	Pathologic V'O$_2$/HR N=18	No pathologic V'O$_2$/HR N=30	P-value
Peak V'O$_2$ (% pred)	57	92	<0.001	79	108	<0.001
SPAP (mmHg)	32	28	0.10	31	28	0.12
6MWD (m)	413	515	0.015	489	587	0.005

Peak V'O$_2$, peak oxygen uptake (ml/min); SPAP, systolic pulmonary artery pressure; 6MWD, 6 minute walking distance.

Discussion

We report a novel analysis of the V'O$_2$/HR slope to exercise in the clinical evaluation of systemic sclerosis patients which showed that a breakpoint in the V'O$_2$/HR slope is preceded by a breakpoint in the slope of pulmonary arterial pressures against oxygen uptake. This suggests that the increase in pulmonary pressures results in a change in heart rate response to maintain sufficient cardiac output. In patients with a breakpoint in the V'O$_2$/HR slope, peak oxygen uptake was limited and differed significantly compared to patients without a breakpoint. Importantly, in patients with normal SPAP at rest, non-invasive CPET identified patients with a V'O$_2$/HR slope not fitting in the normal range (i.e. pathologic V'O$_2$/HR slope). In the evaluation of SSc patients, analysis of the V'O$_2$/HR slope may therefore reveal important information extending that of resting Doppler echocardiography. Taken together, these patients may be at risk for developing pulmonary vasculopathy and ultimately pulmonary hypertension.

Since SSc patients may develop PH in their course of the disease, early detection and careful monitoring are warranted (22). Previously, Doppler echocardiography and right heart catheterization have been evaluated to estimate or measure elevated pulmonary arterial pressures at rest (3;8;17;23). Stress Doppler echocardiography has been recently studied longitudinally and an increase of 18 mmHg during exercise was found to correspond with a

sensitivity of 50% and a specificity of 90% of developing PH during follow-up (24). However, disadvantages of this technique include patient and operator dependent issues, such as evaluating exercise echocardiography images. Non-invasive CPET is another important tool in the evaluation of PH. Analysis of various gas exchange and cardiocirculatory parameters such as oxygen uptake is feasible and can be easily interpreted. Therefore we focused on additional analysis of these cardiocirculatory parameters during exercise.

In our clinical experience, SSc patients may display a breakpoint in the V'O$_2$/HR slope during exercise. In these patients, cardiac output cannot effectively increase by stroke volume alone. In general, in patients with increasing pulmonary pressures during exercise, heart rate increase is the main mechanism for increasing cardiac output. This results in a significantly steeper slope of V'O$_2$/HR (25-27), which may contain a breakpoint at which the heart rate "takes off" (e.g. Figure 2.1, track 2) (6;9;10). To confirm that these responses are also present in SSc patients, we applied our slope analysis to a historic dataset in which exercise testing and right heart catheterization were done simultaneously. We found that a sudden increase in the pulmonary pressures results in a disproportional sudden increase in HR during exercise.

Since the occurrence of a breakpoint in a V'O$_2$/HR slope may vary during exercise and reflects a sudden change in the pulmonary vasculature, it may be the result of a reduced compliance of the pulmonary vasculature. Indeed, the pulmonary vasculature in SSc may be affected by progressive obliteration of microvascular structures resulting into a reduced compliance (1;4). When the pulmonary vascular resistance (PVR) is abnormally increased during exercise, or does not decrease appropriately, right ventricular function can become compromised (28). In patients with exercise induced pulmonary hypertension (EIPAH), two different groups were defined by the nature of their mPAP response to exercise (2;28). Data during exercise were analyzed using best-fit two-segment plots of mPAP versus oxygen uptake. Patients with severe EIPAH and resting PAH showed a "plateau" physiology (2). In these patients mPAP will increase as well as PVR during exercise until the cardiac output is compromised and starts to fall. Eventually, with a decline in cardiac output as a result of right ventricular dysfunction, PAP will not further increase or even fall resulting in a compensatory tachycardia. In contrast, patients with mild to moderate EIPAH showed a "take-off" physiology, suggesting pulmonary vasoconstriction during incremental exercise (2;28). In these patients, mPAP further increases in which the cardiac output does not decrease. Therefore, it seems plausible that patients with PAH of varying duration and severity will exhibit different mPAP responses to exercise. Likewise, different comparable V'O$_2$/HR slopes may be expected in these patients.

In SSc pulmonary vascular remodeling occurs and may progress into pulmonary vasculopathy and pulmonary hypertension (29). Intimal proliferation, decreased compliance and increased elastance of the pulmonary vasculature may cause a "take-off" physiology. Indeed, 15 Austrian patients showed a "take-off" pattern and none a "plateau" pattern. Mean PAP in these patients measured at 50 Watts and at maximum exercise corresponded well to reported values in other patients with a "take-off" physiology (2;28). Therefore, these pressures may represent an intermediate stage between a physiologic response and manifest PAH (29). Furthermore, in these patients sudden increases in pulmonary pressures during exercise were followed by sudden increases in heart rate against oxygen uptake. Since different mPAP responses in patients with varying PAH or EIPAH are present, different $V'O_2/HR$ responses are likely to occur. In other words, pulmonary vasculopathy, as reflected by a sudden increase in pulmonary pressures, may result into a breakpoint in the $V'O_2/HR$ slope during non-invasive CPET. Consequently, the pulmonary vasculature may be more affected in patients showing a pathologic $V'O_2/HR$ slope compared to patients without a pathologic $V'O_2/HR$ slope. Mean SPAP was significantly different between these groups (Table 2.3). Likewise, in patients showing a breakpoint in the $V'O_2/HR$ slope, predicted peak oxygen uptake ($V'O_2\%$ predicted) was significantly lower than in patients without a $V'O_2/HR$ breakpoint (Table 2.3) indicating the importance of the $V'O_2/HR$ slope analysis.

Concerning the occurrence of a breakpoint in the $V'O_2/HR$ slope, some clarifications are important. First, in the absence of anemia, carboxyhemoglobinemia, poor blood oxygenation in the lung, right-to-left shunt or low peripheral oxygen extraction, a breakpoint in the $V'O_2/HR$ slope may reflect an impaired cardiovascular response (7;9). However, in all these responses, a normal peak $V'O_2$ may still be achieved. Furthermore, in some subjects, a breakpoint due to "nervous anticipation" to exercise is observed (Figure 2.1, track 4) or when $V'O_2$ is approaching $V'O_2$max (Figure 2.1, track 5). These latter responses to exercise are considered by us the only physiological exceptions when a $V'O_2/HR$ slope contains a breakpoint (9). Secondly, in patients displaying a pathologic $V'O_2/HR$ slope, a $V'O_2/HR$ breakpoint may not always be present. Moreover, their $V'O_2$ slope may be steep from start of exercise (e.g. Figure 2.1, track 1). Nevertheless, pulmonary hypertension at rest may develop in the course of their disease. In contrast, patients may display a pathologic $V'O_2/HR$ slope *with* a breakpoint (e.g. Figure 2.1, track 2). The latter response, however, is considered by us less pathologic since the slope starts less steep and peak $V'O_2$ approaches the predicted value more closely. Thirdly, in the LUMC dataset a decrease or a less than normal increase in end-tidal pCO_2 ($\Delta P_{et}CO_2 AT$-$P_{et}CO_2$start, Table 2.2) was present in some of these patients,

which may reflect hypoperfusion in well-ventilated acini (6). Fourthly, none of our patients showed an oxygen desaturation during CPET as measured by pulse oximetry. Therefore, reduced peripheral oxygen extraction as a cause of the pathological $V'O_2/HR$ slope was not likely in the LUMC patients. Finally, in the present study, 9 patients with a SPAP ≥35 mmHg and 24 patients with a SPAP <35 mmHg had ≥20% involvement of ILD on their HRCT according to the classification of Goh et al (21). However, in both groups breakpoints in the $V'O_2/HR$ slopes did not influence peak oxygen uptake nor pathologic $V'O_2/HR$ slopes were observed (data not shown). Therefore, the reduced peak oxygen uptake and pathologic $V'O_2/HR$ slopes were considered to reflect changes in the pulmonary vasculature during exercise.

We conclude that our novel analysis of the $V'O_2/HR$ slope showed that SSc patients with a breakpoint in this slope are characterized by a decreased oxygen uptake and exercise capacity. This breakpoint is preceded by a sudden increase in pulmonary arterial pressures and may therefore reflect an inadequate increase or even decrease in stroke volumes. Importantly, non-invasive CPET identified patients with a pathologic $V'O_2/HR$ slope despite normal echocardiographic pulmonary pressures at rest. These patients may have a compromised pulmonary vasculature and are at risk for developing pulmonary vasculopathy and ultimately pulmonary hypertension. To assess the predictive value of the $V'O_2/HR$ breakpoint analysis, we currently perform serial CPET and echocardiography in patients with normal SPAP and a pathologic $V'O_2/HR$ slope or with a $V'O_2/HR$ breakpoint. Our results imply that analysis of the $V'O_2/HR$ slope is warranted in every newly diagnosed SSc patient. In addition, since a compromised pulmonary vasculature is not restricted to systemic sclerosis, our novel analysis may also be applicable to other types of lung disease coinciding with cardiovascular malfunction.

Acknowledgements

References

(1)   Black CM. Scleroderma. Br J Hosp Med 1979;22(1):28, 30, 32-28, 30, 33.

(2)   Tolle JJ, Waxman AB, Van Horn TL, Pappagianopoulos PP, Systrom DM. Exercise-induced pulmonary arterial hypertension. Circulation 2008;118(21):2183-9.

(3)   Mukerjee D, St GD, Knight C, Davar J, Wells AU, Du Bois RM et al. Echocardiography and pulmonary function as screening tests for pulmonary arterial hypertension in systemic sclerosis. Rheumatology (Oxford) 2004;43(4):461-6.

(4)   Stupi AM, Steen VD, Owens GR, Barnes EL, Rodnan GP, Medsger TA, Jr. Pulmonary hypertension in the CREST syndrome variant of systemic sclerosis. Arthritis Rheum 1986;29(4):515-24.

(5)   Kovacs G, Maier R, Aberer E, Brodmann M, Scheidl S, Troster N et al. Borderline pulmonary arterial pressure is associated with decreased exercise capacity in scleroderma. Am J Respir Crit Care Med 2009;180(9):881-6.

(6)   Dumitrescu D, Oudiz RJ, Karpouzas G, Hovanesyan A, Jayasinghe A, Hansen JE et al. Developing pulmonary vasculopathy in systemic sclerosis, detected with non-invasive cardiopulmonary exercise testing. PLoS One 2010;5(12):e14293.

(7)   Whipp BJ, Higgenbotham MB, Cobb FC. Estimating exercise stroke volume from asymptotic oxygen pulse in humans. J Appl Physiol (1985) 1996;81(6):2674-9.

(8)   Walkey AJ, Ieong M, Alikhan M, Farber HW. Cardiopulmonary exercise testing with right-heart catheterization in patients with systemic sclerosis. J Rheumatol 2010;37(9):1871-7.

(9)   Hansen JE, Sue DY, Wasserman K. Predicted values for clinical exercise testing. Am Rev Respir Dis 1984;129(2 Pt 2):S49-S55.

(10)   Wasserman K, Beaver WL, Whipp BJ. Gas exchange theory and the lactic acidosis (anaerobic) threshold. Circulation 1990;81(1 Suppl):II14-II30.

(11)   Astrand PO. Measurement of maximal aerobic capacity. Can Med Assoc J 1967;96(12):732-5.

(12)   Hermansen L, Saltin B. Oxygen uptake during maximal treadmill and bicycle exercise. J Appl Physiol 1969;26(1):31-7.

(13)   Morelli S, Ferrante L, Sgreccia A, Eleuteri ML, Perrone C, De MP et al. Pulmonary hypertension is associated with impaired exercise performance in patients with systemic sclerosis. Scand J Rheumatol 2000;29(4):236-42.

(14)   Kim HJ, Fay MP, Feuer EJ, Midthune DN. Permutation tests for joinpoint regression with applications to cancer rates. Stat Med 2000;19(3):335-51.

(15)   Leroy EC, Black C, Fleischmajer R, Jablonska S, Krieg T, Medsger TA, Jr. et al. Scleroderma (systemic sclerosis): classification, subsets and pathogenesis. J Rheumatol 1988;15(2):202-5.

(16)   Kircher BJ, Himelman RB, Schiller NB. Noninvasive estimation of right atrial pressure from the inspiratory collapse of the inferior vena cava. Am J Cardiol 1990;66(4):493-6.

(17) Rudski LG, Lai WW, Afilalo J, Hua L, Handschumacher MD, Chandrasekaran K et al. Guidelines for the echocardiographic assessment of the right heart in adults: a report from the American Society of Echocardiography endorsed by the European Association of Echocardiography, a registered branch of the European Society of Cardiology, and the Canadian Society of Echocardiography. J Am Soc Echocardiogr 2010;23(7):685-713.

(18) MacIntyre N, Crapo RO, Viegi G, Johnson DC, van der Grinten CP, Brusasco V et al. Standardisation of the single-breath determination of carbon monoxide uptake in the lung. Eur Respir J 2005;26(4):720-35.

(19) Miller MR, Hankinson J, Brusasco V, Burgos F, Casaburi R, Coates A et al. Standardisation of spirometry. Eur Respir J 2005;26(2):319-38.

(20) Buchfuhrer MJ, Hansen JE, Robinson TE, Sue DY, Wasserman K, Whipp BJ. Optimizing the exercise protocol for cardiopulmonary assessment. J Appl Physiol Respir Environ Exerc Physiol 1983;55(5):1558-64.

(21) Goh NS, Desai SR, Veeraraghavan S, Hansell DM, Copley SJ, Maher TM et al. Interstitial lung disease in systemic sclerosis: a simple staging system. Am J Respir Crit Care Med 2008;177(11):1248-54.

(22) Iudici M, Codullo V, Giuggioli D, Riccieri V, Cuomo G, Breda S et al. Pulmonary hypertension in systemic sclerosis: prevalence, incidence and predictive factors in a large multicentric Italian cohort. Clin Exp Rheumatol 2013;31(2 Suppl 76):31-6.

(23) Currie PJ, Seward JB, Chan KL, Fyfe DA, Hagler DJ, Mair DD et al. Continuous wave Doppler determination of right ventricular pressure: a simultaneous Doppler-catheterization study in 127 patients. J Am Coll Cardiol 1985;6(4):750-6.

(24) Codullo V, Caporali R, Cuomo G, Ghio S, D'Alto M, Fusetti C et al. Stress Doppler echocardiography in systemic sclerosis: evidence for a role in the prediction of pulmonary hypertension. Arthritis Rheum 2013;65(9):2403-11.

(25) Schwaiblmair M, Behr J, Fruhmann G. Cardiorespiratory responses to incremental exercise in patients with systemic sclerosis. Chest 1996;110(6):1520-5.

(26) Sun XG, Hansen JE, Oudiz RJ, Wasserman K. Exercise pathophysiology in patients with primary pulmonary hypertension. Circulation 2001;104(4):429-35.

(27) Markowitz DH, Systrom DM. Diagnosis of pulmonary vascular limit to exercise by cardiopulmonary exercise testing. J Heart Lung Transplant 2004;23(1):88-95.

(28) Waxman AB. Exercise physiology and pulmonary arterial hypertension. Prog Cardiovasc Dis 2012;55(2):172-9.

(29) Kovacs G, Maier R, Aberer E, Brodmann M, Scheidl S, Hesse C et al. Assessment of pulmonary arterial pressure during exercise in collagen vascular disease: echocardiography vs right-sided heart catheterization. Chest 2010;138(2):270-8.

Chapter 3

Left ventricular dysfunction assessed by speckle tracking strain analysis in systemic sclerosis patients: relationship with functional capacity and ventricular arrhythmias

Kai Hang Yiu, Anne A. Schouffoer, Nina Ajmone Marsan, Maarten K. Ninaber, Jan Stolk, Thea Vliet-Vlieland, Roderick W. Scherptong, Victoria Delgado, Eduard R. Holman, Hung Fat Tse, Tom W.J. Huizinga, Jeroen J. Bax and Annemie J.M. Schuerwegh

Abstract

Background: Systemic sclerosis is a connective tissue disease characterized by vascular inflammation and fibrosis. Visceral involvement, including cardiac manifestations can lead to severe clinical complications, such as congestive heart failure, arrhythmias and sudden death. Conventional echocardiography parameters have limited sensitivity to detect subtle myocardial dysfunction in patients with systemic sclerosis (SSc). The aim of the study was to assess, using novel speckle tracking strain analysis, the presence of myocardial dysfunction in SSc patients and to investigate its relationship with functional capacity and ventricular arrhythmias.

Methods: A total of 104 SSc patients (age 54±11 yrs, 77% female) were included and underwent cardiopulmonary exercise testing, 24-hour electrocardiography Holter, and transthoracic echocardiography. For comparison purposes, 37 matched healthy controls were included.

Results: The total population consisted of 51 patients with limited SSc and 53 patients with diffuse SSc. Peak VO_2% predicted was 91±20% and 28 patients had abnormal Holter findings (ventricular tachycardia or ventricular ectopics >100/day). Patients with SSc have impaired global longitudinal (-18.2±1.8%) and circumferential strains (-18.2±2.3%) as compared to controls (21.3±1.7%, p<0.01, p<0.01 respectively), but not left ventricular ejection fraction (63.5±7.2% vs 64.6±4.4%, p=0.20). In patients with SSc, global longitudinal (r=-0.46, p<0.01) and circumferential strains (r=-0.41, p<0.01) correlated with peak VO_2% predicted. Multivariate analysis showed that global longitudinal and circumferential strains were independently associated with peak VO_2% predicted. Patients with abnormal Holter findings showed impaired global longitudinal (-18.5±1.5 vs -17.1±2.1%, p<0.01) and circumferential (-18.7±2.0 vs -17.3±2.5%, p=0.01) strains as compared to controls, and were independently associated with abnormal Holter findings.

Conclusion: Speckle tracking strain analysis detected subtle myocardial dysfunction in SSc patients. Importantly, decreased global longitudinal and circumferential strains are associated with lower functional capacity and rhythm disturbances.

Introduction

Systemic sclerosis (SSc) is an autoimmune disease characterized by deposition of collagen in multiple organs and associated with significant disability and reduced life expectancy (1). Cardiovascular involvement has been shown to be one of the leading causes of mortality in SSc (2) and to occur in up to 70% of patients as autoptic finding (3). Early diagnosis and accurate staging of myocardial involvement are therefore crucial for the management of these patients and for therapeutic strategies.

Conventional echocardiographic assessment of left ventricular (LV) systolic function is based on the measure of LV ejection fraction (EF). This approach however showed limited sensitivity for the assessment of myocardial abnormalities in SSc patients, being able to identify only 5% of patients with cardiac involvement (4). More sophisticated and sensitive techniques for the assessment of LV function are therefore needed to improve the detection of subclinical myocardial dysfunction in SSc patients. Initial studies using tissue Doppler imaging suggested that myocardial velocity and deformation (strain) might be more sensitive than conventional measures in identifying subtle cardiac dysfunction in asymptomatic SSc patients (5-7). However, the clinical implications of this alternative approach for LV function assessment have not been evaluated.

Recently, two-dimensional (2D) speckle tracking analysis has been proposed as a sensitive and accurate method for the evaluation of subclinical myocardial dysfunction, providing measures of LV regional and global strain in three orthogonal directions (longitudinal, circumferential and radial) (8). The aim of this study was therefore to apply this novel technique to assess the presence of LV systolic dysfunction in a large cohort of SSc patients. Furthermore, the clinical value of the measure of LV global strain by 2D speckle tracking analysis was evaluated in relation with functional capacity and ventricular arrhythmias.

Methods

Patient population and protocol

The current study included 113 consecutive patients with SSc referred to the department of Rheumatology, Leiden University Medical Center. The patients were recruited from two studies; a randomized controlled trial evaluating the effectiveness of a multidisciplinary team care program (9) and a study evaluating the outcomes of a two-days diagnostic

multidisciplinary daycare program (10). All patients underwent an extensive screening, including detailed physical examination, a Modified Rodnan Skin Score assessment (11), laboratory testing (including erythrocyte sedimentation rate, anti-nuclear, anti-topoisomerase I, anti-RNP and anti-centromere antibodies assessments), chest X-ray and lung function test. Interstitial lung disease was diagnosed by chest X-ray and by lung function test, and with computed tomography scan when indicated. Patients were classified as limited systemic sclerosis (lSSc) or diffuse systemic sclerosis (dSSc), according to the classification system described by LeRoy et al. (12) In addition, cardiopulmonary exercise (CPET) and 24-hour electrocardiography (ECG) Holter monitoring were performed to assess patient functional capacity and potential ventricular arrhythmias, respectively. All patients had no angina pectoris or symptoms attributable to cardiovascular disease and therefore specific tests for microvascular and macrovascular ischemia were not performed. Transthoracic echocardiography was performed to evaluate conventional parameters of cardiac function and to assess subclinical LV systolic dysfunction using novel speckle tracking analysis. The relationship of LV function with functional capacity and ventricular arrhythmias was evaluated.

Seven patients were not able to perform CPET (because of severe pulmonary hypertension in 4 patients, severe aortic valve stenosis in 1 patient and severe SSc disease status in 2 patients) and therefore excluded from the analysis. In addition, 2 patients were excluded because of an incomplete clinical assessment. The final study population consisted of 104 patients.

For comparison purposes, 37 normal individuals (1:3 ratio with SSc patients) matched for age and gender were included as a control group. These subjects were referred for atypical chest pain, palpitations, or syncope without murmur and showed normal structural heart on echocardiography.

The study protocol was approved by the Ethics Committee of the Leiden University Medical Center. All participants provided written informed consent for the studies in which they participated

Lung function test

Lung function test was performed in all SSc patients and included spirometry and single breath diffusion lung capacity for carbon monoxide (DLCO). Spirometry measurements included forced vital capacity (FVC) and total lung capacity (TLC) measured according to

the American Thoracic Society/European Respiratory Society recommendations (13-15) and expressed as percentage predicted.

Conventional echocardiography

All SSc patients and controls were imaged in the left lateral decubitus position using a commercially available system (Vingmed Vivid 7, General Electric Vingmed Ultrasound, Milwaukee, USA). Images were obtained using a 3.5-MHz transducer and digitally stored in cine-loop format; offline analysis was performed using EchoPAC version 108.1.5 (General Electric – Vingmed, Horten, Norway). LV dimensions, volumes and EF were measured according to the current recommendations (16). Evaluation of LV diastolic function was based on the pulsed-wave Doppler of mitral valve inflow as recommended by the American Society of Echocardiography (17), measuring peak early diastolic velocity (E), peak late (A) diastolic velocity, their ratio (E/A) and the E wave deceleration. Pulmonary venous flow velocities during systole (S) and diastole (D) were also recorded. Using tissue Doppler imaging, the early diastolic velocity (E`) and systolic velocity (S`) was measured at the level of the LV basal lateral segment. In addition, E/E` ratio was calculated as an estimation of LV filling pressure (18). LV diastolic dysfunction was therefore categorized as previously described: normal; mild, defined as LV impaired relaxation without evidence of increased filling pressure; moderate, defined as LV impaired relaxation associated with moderate elevation of filling pressures or pseudo-normal filling; and severe, defined as restrictive LV filling (17). Pulmonary arterial systolic pressure (PASP) was estimated by right ventricular systolic pressure, which was calculated from the tricuspid regurgitation peak gradient using Bernoulli equation, and adding right atrial pressure estimated by the dimension and the degree of inferior vena cava respiratory collapse (19).

Two-dimensional speckle tracking strain analysis

Two-dimensional speckle tracking analysis is a novel imaging technique which allows the assessment of LV myocardial deformation by tracking natural acoustic markers (speckles) in a frame-to-frame basis within the cardiac cycle. The speckles are visible in the standard gray-scale 2D images and are equally distributed within the myocardium. As represented in Figure 3.1, LV deformation can be assessed in three orthogonal directions as longitudinal, circumferential and radial strain (20).
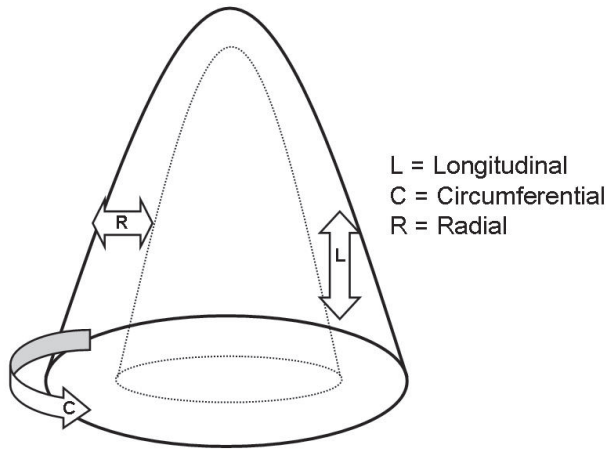
Figure 3.1   Schematic representations of the three orthogonal directions of strain measured with two-dimensional speckle tracking analysis.
Global longitudinal strain evaluates the shortening/lengthening of the myocardial wall. Radial strain evaluates the thickening and thinning of the myocardial wall and circumferential strain asses the shortening/lengthening along the curvature of the LV.

Longitudinal strain, evaluating the shortening/lengthening of the myocardial wall, was measured from the 3 apical views: 2-chamber view (including anterior and inferior walls), 4-chamber view (posteroseptal and lateral walls) and long axis view (anteroseptal and posterior walls). Each wall was divided into 3 levels (basal, mid and apical) and subsequently 18 segmental strain curves were obtained. Global longitudinal strain was calculated as the average of peak systolic strain values of the 18 segments (Figure 3.2a).

From LV mid-ventricular short-axis view, circumferential strain (evaluating myocardial shortening/lengthening along LV curvature) and radial strain (evaluating myocardial thickening/thinning) were measured. The global values of circumferential and radial strains were derived from the average of peak systolic strain values of 6 segments, as illustrated in Figure 3.2b and 3.2c, respectively. Global longitudinal and circumferential strains are expressed as negative values, and a lower strain is represented by less negative values. Global radial strain is expressed as positive values, and lower values indicate lower strain.

The intra- and inter-observer agreement for the measurements of longitudinal, circumferential and radial strains have been reported previously (20).

3
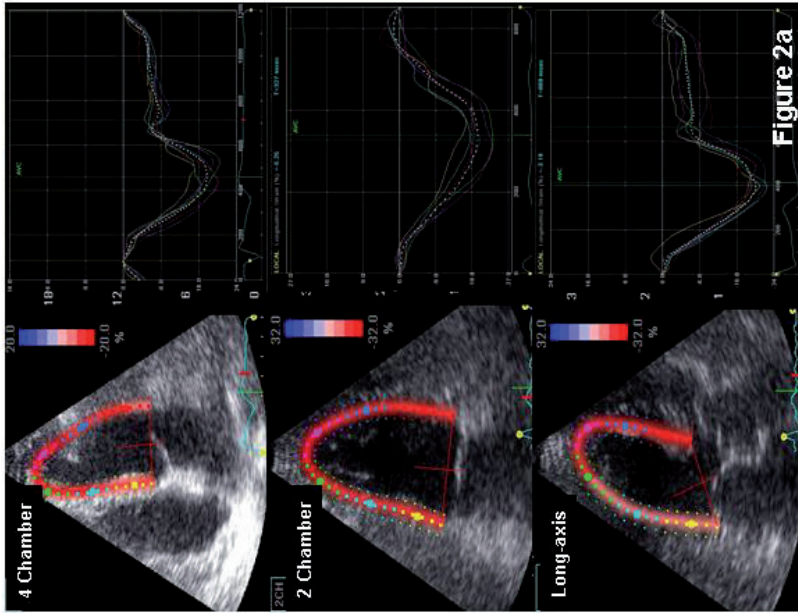
Figure 3.2   Left ventricular strain assessment in 3 orthogonal directions by two-dimensional speckle tracking analysis.
Figure 3.2a illustrates the calculation of global longitudinal strain from the apical 4-chamber, 2-chamber and the long-axis views. Each color line denotes regional segmental strain (6 segments per views, for a total of 18 segments) and the white dotted line represents the average strain value of each view. The global longitudinal strain is calculated by the average of peak strain in the three apical views. From the mid-ventricular short-axis view of the LV, global circumferential (Figure 3.2b) and radial (Figure 3.2c) strains are calculated by averaging the peak strain of six LV segments.
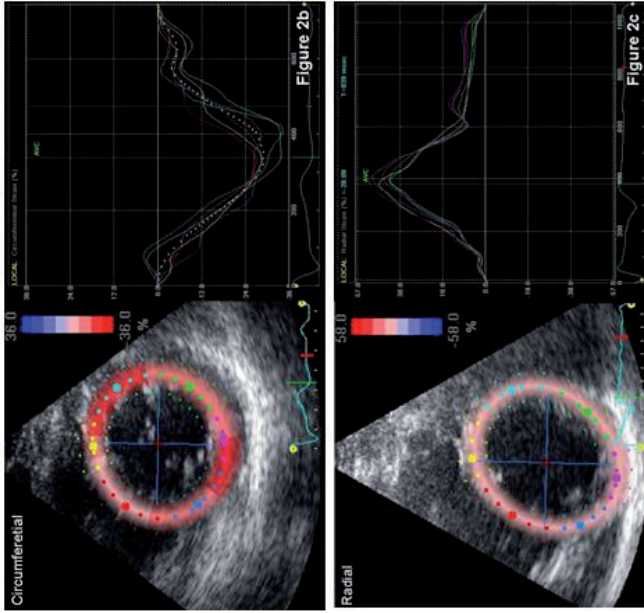
Cardiopulmonary exercise testing

All SSc patients performed a maximal exercise stress test on an electrically braked stationary cycle ergometer using a ramp protocol according to the American Thoracic Society/ American College of Chest Physician statement on cardiopulmonary testing (21). Briefly, a tight fitting facemask was worn by the patients and allowed ventilation and metabolic gas exchange measurements (Oxycon Pro, Jaeger-Viasys Healthcare, Hoechberg, Germany). The initial work load was 30W, with further increment of 5W every 30 seconds. Patients were encouraged to exercise until exhaustion or until supervising physician stopped the test because of significant symptoms, such as chest pain, dizziness, ST-segment deviations, or marked systolic hypotension or hypertension. Peak VO_2 was defined as the highest oxygen consumption during any stage of maximal exercise. Furthermore, peak VO_2 was adjusted to age, gender and weight and expressed as percentage predicted.

24-hour electrocardiography Holter monitoring

A 24-hour ECG Holter monitoring was performed in 100 out of 104 patients to detect potential ventricular arrhythmias. Abnormal Holter results were defined as the presence of intermittent bundle branch block, ventricular arrhythmias including frequent monomorphic and/or polymorphic premature ventricular contractions >100 per day, or non-sustained or sustained ventricular tachycardia (22).

Statistical analysis

Continuous variables are presented as mean ± standard deviation. Categorical data are presented as frequencies and percentages. Continuous variables were tested for normal distribution with the Kolmogorov-Smirnov test. Statistical comparisons were performed by using Student's t test for continuous variables, and chi square test for binary variables. Univariate linear regression analysis was used to identify potential determinants of peak VO_2% predicted. Correlations were expressed in terms of Pearson's correlation coefficient. Moreover, univariate binary logistic regression was used to determine the factors associated (using odd ratios (OR) and confidence intervals (CI)) with abnormal Holter results. The final multivariate models for peak VO_2% predicted and abnormal Holter results were obtained using the enter method by including parameters that were statistically significant in univariate analysis. To avoid bias from multicollinearity, multi-directional global strains

were entered to the step-wise model individually. ANCOVA tests with covariates to correct for significant different variables of subpopulation characteristics were performed. All statistical analysis were performed using the statistical package SPSS for windows (Version 15.0, SPSS, Chicago, USA). A p-value <0.05 was considered to be statistically significant.

Results

Clinical characteristics of the patient population

A total of 51 (49%) patients were classified as having lSSc and 53 (51%) patients as having dSSc. Clinical characteristics of the total population and of the 2 subtypes of SSc (limited and diffuse) are shown in Table 3.1. According to the matching criteria, age (54±10 vs. 54±12, p=0.82) and gender (female 77% vs. 73%, p=0.66) were similar between SSc patients and controls. Most of SSc patients were positive for antinuclear antibodies and approximately 50% had underlying interstitial lung disease. In addition, 24 patients (20 dSSc patients and 4 lSSc patients) received a treatment with cyclophosphamide, and 13 patients (all dSSC) stem cell transplantation. A total of 4 patients had mild pulmonary hypertension (2 due to underlying interstitial lung disease and 2 due to pulmonary arterial hypertension), 1 patient had a previous myocardial infarction and 2 patients were known for epicardial coronary artery disease.

Patients with dSSc were associated with a younger age, shorter time since diagnosis and time since onset of Raynaud's phenomenon and skin manifestation. Moreover, patients with dSSc were more likely to have underlying interstitial lung disease, lower TLC% predicted and to receive angiotensin-converting enzyme inhibitors (mainly to prevent renal crisis) as compared to patients with lSSc. Patients with lSSc had a significantly lower prevalence of anti-topoisomerase antibodies and a lower modified Rodnan skin score.

Echocardiographic characteristics of the patient population

Conventional echocardiographic parameters of LV systolic and diastolic function of SSc patients and controls are shown in Table 3.2. No significant differences were noted in LV volumes and EF between SSc patients and controls (Table 3.2). Moreover, S` velocity derived from tissue Doppler imaging was similar to controls. However, estimated PASP was significantly higher in SSc patients as compared to controls and E/E` ratio and LV diastolic

dysfunction grade were significantly worse. When comparing the 2 different subtypes of SSc, both groups showed similar values of conventional echocardiographic parameters.

In order to detect subtle LV dysfunction, myocardial strain values in three orthogonal directions were measured by speckle tracking analysis (Table 3.2). Both global longitudinal and circumferential strains were significantly impaired in SSc patients as compared to controls. However, no difference was noted in global radial strain between SSc patients

Table 3.1 Clinical characteristics of the 104 patients with systemic sclerosis (SSc) and comparison between patients with limited systemic sclerosis (lSSc) and diffuse systemic sclerosis (dSSc)

	SSc (n=104)	lSSc (n=51)	dSSc (n=53)	p-value
Age (yrs)	54±12	58±12	50±12	**<0.01**
Female gender, n (%)	80 (77)	43 (84)	37 (70)	0.08
Time since diagnosis, yrs	5.1±2.3	7.1±3.5	4.1±2.5	**<0.01**
Time since onset of Raynaud's, yrs	8.6±6.3	15.0±5.8	5.8±4.2	**<0.01**
Time since onset of skin manifestation, yrs	5.6 ±3.5	7.1 ±6.2	4.7 ±2.8	**0.02**
Modified Rodnan Skin Score	5.6±6.1	2.8±2.2	8.3±7.4	**<0.01**
Systolic blood pressure, mmHg	122±18	125±18	119±18	0.08
Diastolic blood pressure, mmHg	71±9	70±8	72±11	0.23
Systemic hypertension	11 (11)	2 (18)	9 (82)	**0.03**
ESR, mm/hr	20.5±17.6	20.7±19.8	20.3±15.4	0.91
Immune markers				
Anti-nuclear, n (%)	94 (90)	46 (90)	48 (91)	0.61
Anti-topoisomerase, n (%)	36 (35)	7 (14)	29 (58)	**<0.01**
Anti-centromere, n (%)	25 (24)	21 (41)	4 (7)	**<0.01**
Anti-RNP, n (%)	7 (7)	5 (10)	2 (4)	0.38
Interstitial lung disease, n (%)	49 (47)	15 (28)	34 (64)	**<0.01**
Pulmonary hypertension	4 (4)	1 (2)	3 (6)	0.62
*Chronic kidney disease	10 (10)	6 (12)	4 (8)	0.52
Lung function				
FVC% predicted	94.4±14.4	94.9±12.4	93.9±15.9	0.73
TLC% predicted	86.9±18.1	92.7±17.2	82.1±17.5	**<0.01**
DLCO% predicted	63.3±16.8	65.4±17.5	61.2±16.1	0.22
Current immunosuppressive medication (%)				
Corticosteroids, n (%)	15 (14)	6 (12)	9 (17)	0.45
Methotrexate, n (%)	4 (8)	3 (6)	4 (8)	0.52
Azathioprine, n (%)	2 (4)	4 (8)	2 (4)	0.32
Current cardiovascular medications (%)				
Calcium antagonists, n (%)	46 (44)	17 (33)	29 (55)	**0.03**
ACE inhibitors, n (%)	42 (40)	12 (24)	30 (57)	**<0.01**

ACE, Angiotensin converting-enzyme; dSSc, Diffuse systemic sclerosis; DLCO, Diffusion lung capacity for carbon monoxide; ESR, Erythrocyte sedimentation rate; FVC, Forced vital capacity; TLC, Total lung capacity.
* Chronic kidney disease defined as an estimated glomerular filtration clearance rate <60 ml/min/1.73m^2 for more than 3 months.

and normal subjects. Of note, dSSc patients showed worse values of global longitudinal and circumferential strain as compared to lSSc patients.

Table 3.2 Conventional echocardiographic parameters and two-dimensional speckle tracking strain measurements in patients with systemic sclerosis (SSc) versus controls and in patients with limited (lSSc) versus diffuse (dSSc) systemic sclerosis

	Controls (n=37)	SSc (n=104)	p-value	lSSc (n=51)	dSSc (n=53)	p-value
Conventional echocardiographic parameters						
LV end diastolic volume (ml)	70.6±20.6	76.0±25.4	0.21	72.9±22.4	78.9±23.0	0.24
LV end systolic volume (ml)	26.6±5.7	29.1±13.1	0.13	28.8±13.9	29.4±12.5	0.82
LV ejection fraction (%)	64.6±4.4	63.5±7.2	0.20	64.6±7.9	63.4±6.4	0.19
PASP (mmHg)	21.7±6.3	28.9±8.7	**<0.01**	29.5±8.3	28.3±9.1	0.48
LV diastolic function, n (%)						
Normal	21 (62)	35 (34)	**<0.01**	18 (35)	17 (32)	0.62
Mild	9 (24)	24 (23)		12 (24)	12 (23)	
Moderate	5 (14)	30 (29)		16 (31)	14 (26)	
Severe	0 (0)	15 (14)		5 (10)	10 (19)	
E` velocity (cm/s)	9.8±2.0	8.5±2.8	**0.03**	8.8±2.7	8.1±3.0	0.22
E/E` ratio	7.7±1.9	10.1±3.8	**<0.01**	10.2±3.8	10.0±3.7	0.73
S` velocity (cm/s)	6.4±1.4	6.3±2.1	0.81	6.8±2.0	5.7±2.0	**<0.01**
Speckle tracking analysis						
Global longitudinal strain (%)	-21.3±1.7	-18.2±1.8	**<0.01**	-18.6±1.6	-17.9±1.9	**0.02**
Global circumferential strain (%)	-21.3±2.1	-18.2±2.3	**<0.01**	-19.0±2.0	-17.5±2.3	**<0.01**
Global radial strain (%)	40.3±12.4	37.0±13.9	0.18	37.6±13.1	36.3±14.7	0.65

LV, Left ventricular; PASP, Pulmonary arterial systolic pressure; E, Early; A, Late; E`, Early diastolic velocity at basal mitral annulus; for other abbreviations, see Table 3.1.

Cardiopulmonary exercise testing

All SSc patients completed the CPET with at least 50W exercise level and reached anaerobic threshold, the heart rate recovery (HRR) was >12 beats/minute and a respiratory exchange ratio >1.00, suggesting a satisfactory exercise capacity in the study population. The mean peak VO_2% predicted was 90.6±20.4% and the maximum exercise time was 9.9±3.6 min suggesting a relatively preserved functional capacity in the population. Patients with dSSc had a significantly lower peak VO_2% predicted compared to those with lSSc (83.2±21.1 vs. 99.7±24.7%, p<0.01).

According to Pearson's correlation analysis, peak VO_2% predicted was not related to conventional echocardiographic parameters including LV dimensions, LVEF and LV

diastolic function (p>0.05). However, peak VO_2% predicted was significantly related to global longitudinal (r=-0.46, p<0.01), circumferential (r=-0.41, p<0.01) and radial (r=0.20, p=0.05) strains (Figure 3.3).

Univariate analysis revealed that among all the clinical and echocardiographic characteristics, age (β=0.24, Confidence interval [CI] = 0.09–0.83, p=0.02), subtype dSSc (β=0.40, CI=0.30–0.79, p<0.01), underlying interstitial lung disease (β=0.24, CI=2.23–20.6, p=0.02), TLC% predicted (β=0.40, CI=0.30–0.79, p<0.01) and DLCO% predicted (β=0.49, CI=0.46–0.96, p<0.01) were significantly associated with peak VO_2% predicted. Strain measurements were adjusted with the aforementioned parameters in a multivariate analysis, which demonstrated that global longitudinal (β=-0.36, CI=-2.72–-7.25, p<0.01) and circumferential (β=-0.34, CI=-1.77–-5.47, p<0.01) strains were independently associated with peak VO_2% predicted, together with age and DLCO%.

24-hour ECG Holter monitoring

Among the 100 SSc patients who underwent 24-hour ECG Holter monitoring, 28 (28%) patients had abnormal results. In particular, 9 patients presented with non-sustained ventricular tachycardia and 19 patients had ventricular ectopic >100 per day.

Clinical and echocardiographic parameters differences between patients with or without abnormal Holter results are shown in Table 3.3. Patients with abnormal Holter results were more likely to be male and with underlying interstitial lung disease. Conventional LV systolic function, LV diastolic dysfunction grade, and S` velocity were similar between patients with or without abnormal Holter results. However, E/E` ratio was significantly higher in patients with abnormal Holter results. Moreover, global longitudinal and circumferential strains, but not global radial strain, were significantly impaired in patients with abnormal Holter results.

Univariate analysis demonstrated that the presence of abnormal Holter results was associated with male gender (OR=2.94, CI=1.12–7.69, p<0.01), interstitial lung disease (OR=3.32, CI=1.32–8.36, p<0.01), higher E/E` ratio (OR=1.15, CI=1.02–1.32, p=0.04), and lower values of global longitudinal (OR=1.71, CI=1.24–2.38, p<0.01) and circumferential strains (OR=1.55, CI=1.18–2.03, p<0.01). After multivariate adjustment, both global longitudinal (OR=1.47, CI=1.05–2.07, p=0.03) and circumferential (OR=1.35, CI=1.01–1.82, p=0.04) strains remained the only independent predictors of abnormal Holter results in SSc patients.
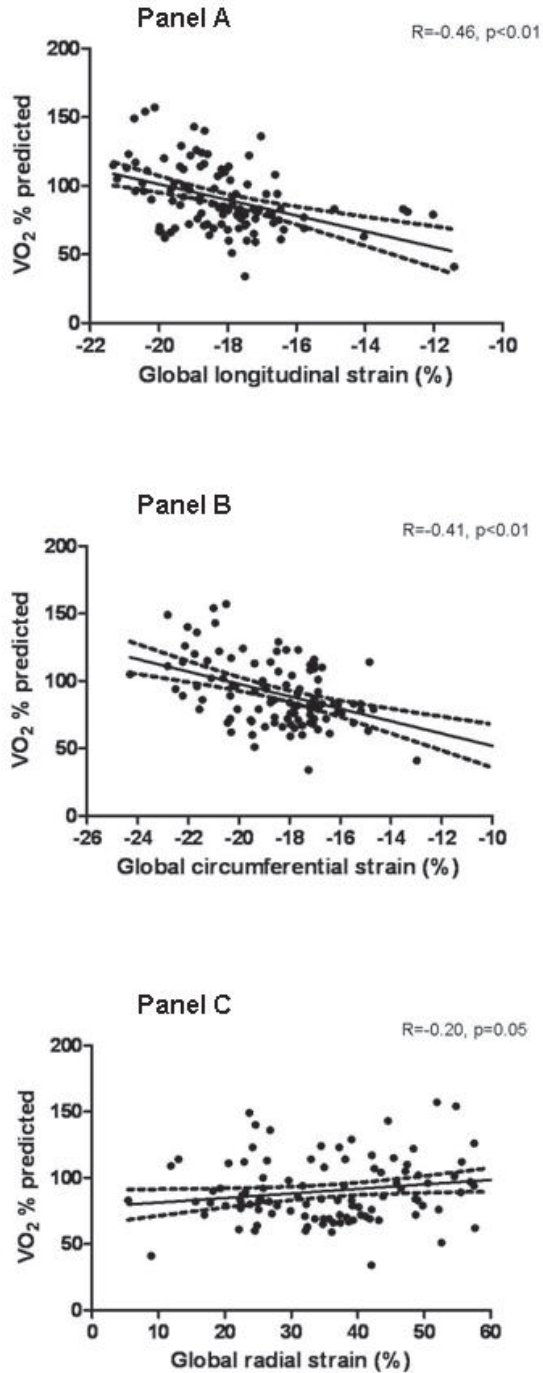
Figure 3.3   Correlation between peak VO$_2$% predicted and global longitudinal (Panel A), circumferential (Panel B) and radial (Panel C) strain measured by two-dimensional speckle tracking analysis.
Dashed lines correspond to 95% confidence interval.

Table 3.3 Clinical and echocardiographic characteristics of systemic sclerosis patients with and without abnormal 24 hour ECG Holter monitoring results

	Normal Holter (n=72)	Abnormal Holter (n=28)	p-value
Clinical characteristics			
Age, yrs	54±13	56±12	0.45
Female gender, n (%)	59 (81.9)	17 (60.7)	**0.04**
Interstitial lung disease, n (%)	9 (32.1)	19 (67.9)	**0.01**
Diffuse systemic sclerosis, n (%)	35 (48.6)	19 (67.9)	0.12
Modified Rodnan Skin Score	5.1±5.8	7.2±7.1	0.16
Immune markers			
Anti-nuclear, n (%)	65 (90.3)	26 (92.9)	1.00
Anti-topoisomerase, n (%)	22 (31.4)	13 (46.4)	0.17
Anti-centromere, n (%)	17 (26.2)	7 (25)	1.00
Anti-RNP, n (%)	6 (8.6)	1 (3.6)	0.67
Lung function			
FVC% predicted	89.0±17.8	83.2±18.5	0.17
TLC% predicted	64.6±17.2	60.4±16.1	0.25
DLCO% predicted	95.4±13.7	93.6±15.0	0.58
Conventional echocardiographic parameters			
LV end diastolic volume, ml	73.5±22.4	79.4±28.7	0.34
LV end systolic volume, ml	27.5±9.9	32.1±18.8	0.23
LV ejection fraction, %	63.9±6.6	62.8±9.1	0.57
PASP, mmHg	28.0±7.5	30.1±10.2	0.36
LV diastolic function, n (%)			
Normal	26 (36)	8 (29)	0.36
Mild	17 (24)	5 (18)	
Moderate	21 (29)	8 (29)	
Severe	8 (11)	7 (25)	
E` velocity, cm/s	8.6±2.9	8.1±2.6	0.35
E/E` ratio	9.4±3.8	11.7±4.0	**0.04**
S` velocity, cm/s	6.3±2.0	6.2±2.2	0.79
Speckle tracking analysis			
Global longitudinal strain, %	-18.5±1.5	-17.1±2.1	**<0.01**
Global circumferential strain, %	-18.7±2.0	-17.3±2.5	**0.01**
Global radial strain, %	37.8±14.0	33.7±13.1	0.17

Abbreviations: see Table 3.1 and 3.2.

Discussion

The results of the current study demonstrated that patients with SSc present subtle LV systolic dysfunction, as assessed by 2D speckle tracking strain analysis, despite normal LVEF and dimensions. More importantly, LV global longitudinal and circumferential strains, but not

conventional echocardiographic parameters, were independently associated with functional capacity assessed by CPET, and ventricular arrhythmias detected by 24-hour ECG Holter monitoring.

Cardiac involvement in patients with SSc has been mainly described by the presence of elevated PASP and LV diastolic dysfunction (5;6). Recent studies (5-7) using tissue Doppler imaging in relatively small groups of SSc patients, have also suggested an impairment in myocardial systolic deformation (strain), despite preserved LVEF and dimensions (4;23). However, strain analysis by tissue Doppler imaging is significantly limited by angle dependency (the measure changes with the insonation angle) and does not allow for the evaluation of all LV segments and of different directions of myocardial deformation. The advent of 2D speckle tracking analysis overcomes these limitations and allows angle-independent, direct evaluation of LV global strain in all three orthogonal directions, providing more accurate assessment of LV function (8).

The current study applied this novel analysis in a large cohort of SSc patients and found that both LV global longitudinal and circumferential strains were modestly but significantly impaired in SSc patients as compared to controls. The relatively small difference of strain values noted between the 2 groups could be explained by the fact that SSc patients in the present cohort were asymptomatic and had a relatively preserved functional capacity, suggestive of mild and subclinical cardiovascular involvement. Furthermore, dSSc patients showed worse values of global longitudinal and circumferential strains as compared to lSSc patients, confirming a more common and severe cardiac involvement in the diffuse form of the disease (5;24). Therefore, the use of more sensitive echocardiographic parameters may enable the detection of subtle LV systolic dysfunction before clinical manifestation, not identified by conventional approaches. Of note, both the present result and the studies from Mele and Kepez et al. (5;6) failed to show a significant difference in myocardial function by using tissue Doppler imaging derived S` velocity between SSc patients and controls. These findings therefore suggest that 2D speckle tracking derived strain analysis, which allows angle-independent and global LV functional assessment, is superior to tissue Doppler imaging derived S` velocity to detect subtle myocardial dysfunction in SSc patients.

Although the mechanism underlying LV systolic dysfunction is unknown, previous studies have demonstrated the presence of significant myocardial fibrosis in SSc patients, using delayed gadolinium enhanced magnetic resonance imaging (25;26). These structural alterations, mainly caused by repeated focal ischemia due to abnormal vasoreactivity, may be

responsible for myocardial dysfunction. Interestingly in the current study, multi-directional strain analysis demonstrated significant impairment of longitudinal and circumferential strains (shortening), but not of radial strain (thickening). This finding may suggest that myocardial involvement of the subendocardial layer (responsible for longitudinal and circumferential shortening) occurs earlier as compared to the subepicardial layer (responsible for radial deformation), since the subendocardium is more susceptible to ischemia and fibrosis phenomena. Nevertheless, the exact mechanism of myocardial dysfunction requires further studies.

Patients with SSc were shown to have reduced cardiopulmonary exercise capacity measured by VO_2% predicted, which could be caused by multiple factors (27-30). Previous studies have suggested that lung pathology is one of the main determinants of impaired functional capacity in these patients (28;31). Similarly, the present study also showed the important role of lung function assessed by DLCO% predicted, which was independently associated with VO_2% predicted (31). In addition, a recent study by Walkey and colleagues has also suggested that exercise induced LV diastolic dysfunction, undetected by resting echocardiography, was a cause of impaired exercise capacity (29). However, the potential role of LV systolic dysfunction as an important contributing factor to functional capacity, has not been demonstrated before. Importantly, the present study demonstrated that LV global longitudinal and circumferential strains were significantly related with VO_2% predicted, independently of age, SSc subtype and lung function. This observation thus provided direct evidence that LV systolic dysfunction significantly contributes to impaired functional capacity in patients with SSc. Therefore, novel 2D speckle tracking strain analysis may be used in conjunction with lung function testing in order to provide a global assessment and monitoring of the cardiopulmonary status in SSc patients.

Ventricular arrhythmias commonly occur in patients with SSc (32) and, are responsible for up to 6% of the deaths, as demonstrated by a recent study (2). In particular, the presence of non-sustained ventricular tachycardias has been reported in 6–10% of patients with SSc and showed to be significantly associated with total mortality and sudden death (31;32). In the current study, 24-hour ECG Holter monitoring was systematically performed in a large group of SSc patients and identified non-sustained ventricular tachycardias in 9% of the cases. Importantly at the multivariate analysis, LV systolic dysfunction, assessed by LV global longitudinal and circumferential strains, was the only independent predictor of ventricular arrhythmias (ventricular ectopics and non-sustained ventricular tachycardia). These results suggest that subtle LV systolic dysfunction is *per se* an important factor associated with

ventricular arrhythmias and may also reflect the extent of myocardial fibrosis, which is a well-known arrhythmogenic substrate (25). These novel echocardiographic parameters therefore represent a valuable tool to improve risk stratification of SSc patients. The current study underscores the need for implementing speckle tracking strain analysis in larger systemic sclerosis cohort studies, investigating risk stratification and potential protective effects of anti-arrhythmic strategies.

The current study was a cross-sectional analysis and therefore a causal relationship between impaired 2D speckle tracking derived strain and impaired functional capacity and ventricular arrhythmias in SSc patients could not be established. Moreover, the current population included SSc patients with preserved functional capacity and low prevalence of pulmonary hypertension and the results of the present study can not be extrapolated to SSc patients with severe cardiopulmonary involvement. Lastly, microvascular and macrovascular ischemia were not fully documented, since all patients had no clinical evidence of myocardial ischemia (neither during CPET) and invasive evaluations and/or vasoreactivity tests were therefore not performed. Future studies are required to evaluate the impact of both microvascular or macrovascular ischemia on 2D speckle tracking derived multi-directional strain in SSc patients.

In conclusion, patients with SSc are associated with LV systolic dysfunction measured by 2D speckle tracking strain analysis. Importantly, LV global longitudinal and circumferential strains independently predicted impaired functional capacity measured by CPET and ventricular arrhythmias detected by 24-hour ECG Holter monitoring. The use of this novel imaging technique may therefore improve risk stratification and monitoring of the cardiovascular involvement in patients with SSc.

References

(1)   Bryan C, Knight C, Black CM, Silman AJ. Prediction of five-year survival following presentation with scleroderma: development of a simple model using three disease factors at first visit. Arthritis Rheum 1999;42:2660-5.

(2)   Tyndall AJ, Bannert B, Vonk M et al. Causes and risk factors for death in systemic sclerosis: a study from the EULAR Scleroderma Trials and Research (EUSTAR) database. Ann Rheum Dis 2010;69:1809-15.

(3)   Follansbee WP, Miller TR, Cirtoss EI et al. A controlled clinicopathologic study of myocardial fibrosis in systemic sclerosis (scleroderma). J Rheumatol 1990;17:656-62.

(4)   Allanore Y, Meune C, Vonk MC et al. Prevalence and factors associated with left ventricular dysfunction in the EULAR Scleroderma Trial and Research group (EUSTAR) database of patients with systemic sclerosis. Ann Rheum Dis 2010;69:218-21.

(5)   Mele D, Censi S, La Corte R et al. Abnormalities of left ventricular function in asymptomatic patients with systemic sclerosis using Doppler measures of myocardial strain. J Am Soc Echocardiogr 2008;21:1257-64.

(6)   Kepez A, Akdogan A, Sade LE et al. Detection of subclinical cardiac involvement in systemic sclerosis by echocardiographic strain imaging. Echocardiography 2008;25:191-7.

(7)   D'Andrea A, Stisi S, Bellissimo S et al. Early impairment of myocardial function in systemic sclerosis: Non-invasive assessment by Doppler myocardial and strain rate imaging. Eur J Echocardiogr 2005;6:407-18.

(8)   Blessberger H, Binder T. Two dimensional speckle tracking echocardiography: basic principles. Heart 2010;96:716-22.

(9)   Schuerwegh AJ, Schouffoer AA, Beaart-van deVoorde LJ, Tromp FJ, Ninaber MK, de Jong Z, Vliet Vlieland TP. Yearly, Standardized, comprehensive Assessment and Treatment Advice for Patients with Systemic Sclerosis (SSc): Feasibility of a Day Care Program. Arthritis Rheum 2009;60(s10):1144.

(10)   Schouffoer AA, Ninaber MK, Beaart-van de Voorde LJ, van der Giesen FJ, de Jong Z, Stolk J, Voskuyl AE, Scherptong RW, van Laar JC, Schuerwegh AJ, Huizinga TW, Vliet Vlieland TP. A randomised comparison of a multidisciplinary team care program with usual care in patients with systemic sclerosis. Art Res Ther 2011;63(6):909-17.

(11)   Clements P, Lachenbruch P, Siebold J et al. Inter and intraobserver variability of total skin thickness score (modified Rodnan TSS) in systemic sclerosis. J Rheumatol 1995;1281-5.

(12)   LeRoy EC, Black C, Fleischmajer R et al. Scleroderma (systemic sclerosis): classification, subsets and pathogenesis. J Rheumatol 1988;15:202-5.

(13)   Miller MR, Hankinson J, Brusasco V et al. Standardisation of spirometry. Eur Respir J 2005;26:319-38.

3

(14) Wanger J, Clausen JL, Coates A et al. Standardisation of the measurement of lung volumes. Eur Respir J 2005;26:511-22.

(15) MacIntyre N, Crapo RO, Viegi G et al. Standardisation of the single-breath determination of carbon monoxide uptake in the lung. Eur Respir J 2005;26:720-35.

(16) Lang RM, Bierig M, Devereux RB et al. Recommendations for chamber quantification: a report from the American Society of Echocardiography's Guidelines and Standards Committee and the Chamber Quantification Writing Group, developed in conjunction with the European Association of Echocardiography, a branch of the European Society of Cardiology. J Am Soc Echocardiogr 2005;18:1440-63.

(17) Nagueh SF, Appleton CP, Gillebert TC et al. Recommendations for the evaluation of left ventricular diastolic function by echocardiography. J Am Soc Echocardiogr 2009;22:107-33.

(18) McQuillan BM, Picard MH, Leavitt M, Weyman AE. Clinical correlates and reference intervals for pulmonary artery systolic pressure among echocardiographically normal subjects. Circulation 2001;104:2797-802.

(19) Kircher BJ, Himelman RB, Schiller NB. Noninvasive estimation of right atrial pressure from the inspiratory collapse of the inferior vena cava. Am J Cardiol 1990;66:493-6.

(20) Delgado V, Ypenburg C, van Bommel RJ et al. Assessment of left ventricular dyssynchrony by speckle tracking strain imaging comparison between longitudinal, circumferential, and radial strain in cardiac resynchronization therapy. J Am Coll Cardiol 2008;51:1944-52.

(21) ATS/ACCP Statement on Cardiopulmonary Exercise Testing. Am J Respir Crit Care Med 2003;167:211-77.

(22) Smedema JP, Snoep G, van Kroonenburgh MP et al. Evaluation of the accuracy of gadolinium-enhanced cardiovascular magnetic resonance in the diagnosis of cardiac sarcoidosis. J Am Coll Cardiol 2005;45:1683-90.

(23) de Groote P, Gressin V, Hachulla E et al. Evaluation of cardiac abnormalities by Doppler echocardiography in a large nationwide multicentric cohort of patients with systemic sclerosis. Ann Rheum Dis 2008;67:31-6.

(24) Follansbee WP, Curtiss EI, Medsger TA et al. Physiologic abnormalities of cardiac function in progressive systemic sclerosis with diffuse scleroderma. N Engl J Med 1984;310:142-8.

(25) Tzelepis GE, Kelekis NL, Plastiras SC et al. Pattern and distribution of myocardial fibrosis in systemic sclerosis: A delayed enhanced magnetic resonance imaging study. Arthritis Rheum 2007;56:3827-36.

(26) Hachulla AL, Launay D, Gaxotte V et al. Cardiac magnetic resonance imaging in systemic sclerosis: a cross-sectional observational study of 52 patients. Ann Rheum Dis 2009;68:1878-84.

(27) Sudduth CD, Strange C, Cook WR et al. Failure of the circulatory system limits exercise performance in patients with systemic sclerosis. Am J Med 1993;95:413-8.

(28) Alkotob ML, Soltani P, Sheatt MA et al. Reduced exercise capacity and stress-induced pulmonary hypertension in patients With scleroderma. Chest 2006;130:176-81.

(29)   Walkey AJ, Ieong M, Alikhan M, Farber HW. Cardiopulmonary exercise testing with right-heart catheterization in patients with systemic sclerosis. J Rheumatol 2010;37:1871-7.

(30)   Kovacs G, Maier R, Aberer E et al. Borderline pulmonary arterial pressure is associated with decreased exercise capacity in scleroderma. Am J Respir Crit Care Med 2009;180:881-6.

(31)   Schwaiblmair M, Behr J, Fruhmann G. Cardiorespiratory responses to incremental exercise in patients with systemic sclerosis. Chest 1996;110:1520-5.

(32)   John BK, James RS, Darya T et al. Prognostic importance of cardiac arrhythmias in systemic sclerosis. Am J Med 1988;84:1007-15.

Chapter 4

Impact of pulmonary fibrosis and elevated pulmonary pressures on right ventricular function in patients with systemic sclerosis

Kai Hang Yiu, Maarten K. Ninaber,* Lucia J. Kroft, Anne A. Schouffoer, Jan Stolk, Hans U. Scherer, Jessica Meijs, Jeska de Vries-Bouwstra, Hung Fat Tse, Victoria Delgado, Jeroen J. Bax, Tom W.J. Huizinga and Nina Ajmone Marsan

* K.H. Yiu and M.K. Ninaber contributed equally to the manuscript and share first author.

Abstract

Objectives: Right ventricular (RV) dysfunction is of great prognostic value in patients with systemic sclerosis (SSc). The aim of the present study was to assess in these patients the relationship between pulmonary fibrosis and elevated pulmonary pressure (PHT) with RV function.

Methods: A total of 102 SSc patients who underwent thoracic computed tomography and transthoracic echocardiography, were included. Speckle tracking-derived RV free wall strain was used to assess RV function.

Results: A total of 51 (50%) SSc patients did not have pulmonary fibrosis or PHT, 32 (31%) patients had pulmonary fibrosis but no PHT and the remaining 19 (19%) had both pulmonary fibrosis and PHT. Patients with both pulmonary fibrosis and PHT had the most impaired RV free wall strain (-16.8±3.1%) compared with patients with pulmonary fibrosis and no PHT (-21.5±3.6%) and patients with no pulmonary fibrosis and no PHT (-24.0±4.4%). All 3 SSc groups showed impaired RV free wall strain compared with controls (-28.0±4.2%). Importantly, multivariate regression analysis demonstrated that pulmonary fibrosis and left ventricular ejection fraction were independently associated with impaired RV free wall strain in SSc patients.

Conclusion: SSc patients show impaired RV function compared with controls. Both pulmonary fibrosis and PHT are independently associated with RV dysfunction.

Introduction

Right ventricular (RV) dysfunction is not uncommon in patients with systemic sclerosis (SSc) and cardiovascular involvement is one of the leading causes of mortality in these patients (1-3). Potential mechanisms leading to RV dysfunction in SSc include a primary involvement of the RV myocardium (fibrosis) or RV pressure overload secondary to interstitial lung disease and elevated pulmonary pressure (PHT) (4;5). However, limited studies have been performed so far to elucidate the role of these factors in the development of RV dysfunction.

Echocardiography is systematically performed in patients with SSc in order to evaluate and monitor cardiac function and pulmonary pressures. However, assessment of the RV performance by echocardiography is particularly challenging due to the complex geometry of RV cavity, to the significant influence of the loading conditions and to the less definite endocardial border. Therefore, conventional echocardiographic measures of RV dimension and function rely often on inadequate geometric assumptions and are hampered by a low reproducibility (6). Recent advances in echocardiography using two-dimensional (2D) speckle tracking analysis have allowed direct assessment of the intrinsic myocardial deformation (strain), independent of specific geometrical assumptions or loading conditions. Echocardiographic speckle tracking-derived strain has been therefore proposed as a sensitive and accurate measure of regional and global RV systolic function (7).

The aim of the present study was to assess RV systolic function using 2D speckle tracking-derived strain echocardiography in a large cohort of SSc patients, and to identify the potential role of pulmonary fibrosis and PHT in the development of RV dysfunction in these patients.

Patients and methods

Patients and protocol

The current study included 102 consecutive patients with SSc referred to the department of Rheumatology, Leiden University Medical Center. The patients were recruited from a study evaluating the outcomes of diagnostic multidisciplinary health-care program, as previously described (8;9).

All patients underwent an extensive screening, including detailed physical examination, a Modified Rodnan Skin Score assessment (10), laboratory testing (including erythrocyte

sedimentation rate, anti-nuclear, anti-topoisomerase I and anti-centromere antibodies assessments), and pulmonary function testing (PFT). Patients were classified as limited cutaneous systemic sclerosis (lSSc) or diffuse cutaneous systemic sclerosis (dSSc), according to the classification system described by LeRoy et al. (11). Furthermore, all SSc patients included in this analysis also underwent a thoracic computed tomography (CT) for detailed evaluation of the presence and extent of pulmonary fibrosis. In addition, transthoracic echocardiography was performed to evaluate conventional parameters of cardiac function and to assess subclinical RV systolic dysfunction using 2D speckle tracking strain echocardiography. The physicians who analyzed these studies were blinded to the clinical status of the patients.

A total of 36 normal individuals (1:3 ratio with SSc patients) matched for age and gender (51±12 vs.54±14 years, p=0.22, and female gender 69% vs. 76%, p=0.51) were included as a control group for comparison. These subjects were referred for an echocardiographic assessment for atypical chest pain, palpitations, or syncope without murmur and all of them showed normal cardiac structure and function and normal pulmonary pressures.

The study protocol was approved by the Ethics Committee of the Leiden University Medical Center all participants provided written informed consent.

Pulmonary function testing

PFT was performed in all SSc patients including spirometry and carbon monoxide (DLCO) transfer studies according to the American Thoracic Society/European Respiratory Society recommendations and expressed as percentage predicted (12;13).

Thoracic computed tomography

Non-contrast high-resolution CT imaging of the chest was performed using a Toshiba Aquilion 64 CT scanner (Toshiba Medical System, Otawara, Japan). Scan parameters were: slice collimation 64 x 0.5 mm, tube voltage 120 kV, tube current 110–220 mA (dependent on weight), rotation time 0.4 sec, helical pitch 53. Data was reconstructed as 0.5 mm/0.4 mm slices. Two observers (LK and AS), scored the CT investigations in consensus. Observers were blinded for clinical information. The images were scored as previously described (14). Briefly, three chest levels were identified at the level of the aortic arch, the carina and 1 cm above the diaphragm. In particular, a total of 9 areas were assessed including (i) right

upper lobe at aortic level, (ii) left upper lobe at aortic level, (iii) right upper lobe at carina level (vi) right lower lobe at carina level, (v) left upper lobe at carina level, (vi) left lower lobe at carina level, (vii) right middle lobe at diaphragmatic level (viii) right lower lobe at diaphragmatic level, (ix) left lower lobe at diaphragmatic level. Each lobe of the lung was scored on a scale of 0–5 (reticulation and/or honeycombing), depending on the percentage of each lobe involved (0 = no fibrosis, 1 = interlobular septal thickening, 2 = honeycombing with or without septal thickening involving <25% of the lobe, 3 = honeycombing with or without septal thickening involving 25–49% of the lobe, 4 = honeycombing with or without septal thickening involving 50–75% of the lobe, 5 = honeycombing with or without septal thickening involving >75% of the lobe. The scores for each lobe were added (maximum score of 45) for data analysis of pulmonary fibrosis score. Patients with a total thoracic CT fibrosis score of ≥7 were considered to have clinical relevant pulmonary fibrosis, since a score of ≥7 was only observed when there was honeycombing in at least one lobe besides septal thickening.

Conventional 2-dimensional echocardiography

All SSc patients and controls were imaged using a commercially available system (Vingmed Vivid 7, General Electric Vingmed Ultrasound, Milwaukee, USA). Images were obtained using a 3.5-MHz transducer and digitally stored in cine-loop format. Subsequent offline analysis was performed using EchoPAC version 111.0.0 (General Electric – Vingmed, Horten, Norway). LV volumes and ejection fraction (EF) were measured according to biplane Simpson's method as currently recommended (15). RV end-diastolic area (RVEDA) was also measured as recommended from the apical 4-chamber view, and tricuspid annular plane systolic excursion (TAPSE) was measured at the level of the RV free wall to evaluate RV systolic function. In particular, the M-mode cursor was placed through the tricuspid annulus at the free wall and the total displacement of the RV base from end-diastole to end-systole was measured (16).

Evaluation of LV diastolic function was based on the pulsed-wave Doppler of mitral valve inflow as recommended by the American Society of Echocardiography (17), measuring peak early (E) and late (A) diastolic velocities, their ratio (E/A) and the E wave deceleration. Using tissue Doppler imaging, the early diastolic velocity (E') measured at the level of the LV basal lateral segment. In addition, E/E' ratio was calculated as an estimation of LV filling pressure (18). LV diastolic dysfunction was therefore categorized as previously described:

normal, mild, moderate and severe (17). Pulmonary arterial systolic pressure (PASP) was estimated by RV systolic pressure, which was calculated from the tricuspid regurgitation peak gradient using Bernoulli equation, and adding right atrial pressure estimated by the dimension and the degree of inferior vena cava respiratory collapse (19). Patients were considered to have PHT if PASP was >35 mmHg (6;11).

Therefore, based on the evaluation of the CT scan and the conventional echocardiogram, SSc patients were categorized into the following subgroups: (1) no pulmonary fibrosis and no PHT, (2) pulmonary fibrosis and no PHT and (3) pulmonary fibrosis and PHT.

2-dimensional speckle tracking right ventricular strain analysis

Two-dimensional speckle tracking analysis is a novel echocardiographic technique which evaluates myocardial deformation by tracking natural myocardial acoustic markers (speckles) in a frame-to-frame basis within the cardiac cycle. RV longitudinal strain, evaluating the shortening (= negative % values) and lengthening (back to initial length = zero, or stretching = positive % values) of the RV myocardial free wall, was assessed by 2D speckle tracking echocardiography from the apical 4-chamber view. The endocardial border of the RV was manually traced with the region of interest width adjusted to include the entire myocardium. The RV free wall was divided into 3 levels (basal, mid and apical) and subsequently 3 segmental strain curves were obtained (Figure 4.1). RV free wall longitudinal strain was calculated as the average of peak systolic strain values of the 3 segments of the free wall, representing an accurate measure of global RV systolic function. Frame rate ranged from 50 to 100 frames/s.

For the measure of RV free wall longitudinal strain, 15 patients were randomly identified for assessment of intra-observer and inter-observer reproducibility. According to Bland-Altman analysis, intra-observer reproducibility was good, with mean differences of -0.59±3.17% and coefficients of variation of 5.4%. Additionally, the intraclass correlation coefficient was 0.89 (95% CI 0.73–0.96). Inter-observer variability was also good, with mean differences of -0.23±2.21%, a coefficient of variation of 9.6% and an intraclass correlation coefficient of 0.95 (95% CI 0.88–0.98).
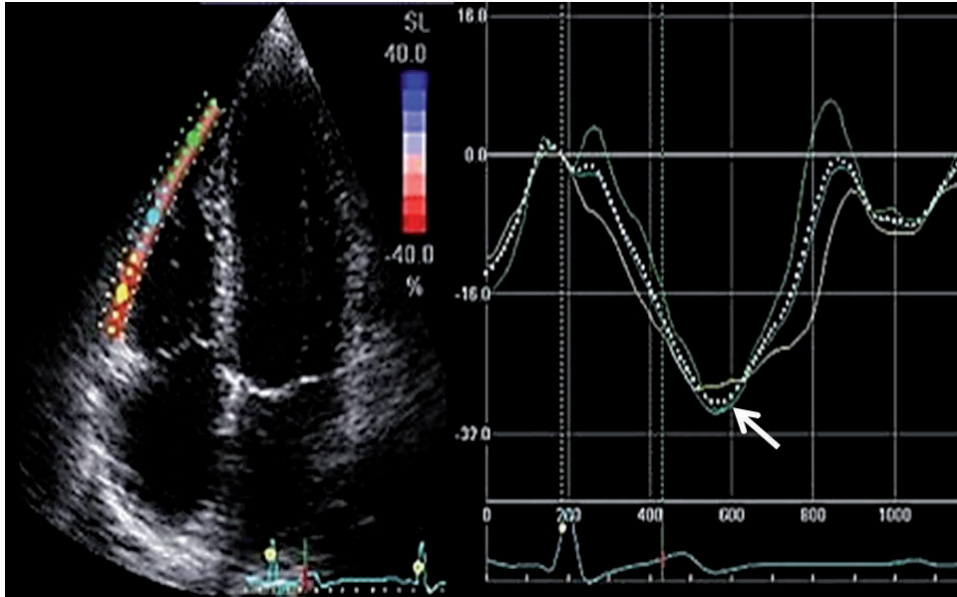
Figure 4.1   Right ventricular (RV) free wall strain assessment by 2-dimensional speckle-tracking echocardiography calculated from the apical 4-chamber view (left panel).
Each color denotes the strain curve of the 3 RV free wall segments and the white dotted line represents the average RV free wall strain. In this example RV free wall strain is -25.0% as indicated by the arrow.

Statistical analysis

Continuous variables are presented as mean ± standard deviation. Categorical data are presented as frequencies and percentages. Continuous variables were tested for normal distribution with the Kolmogorov-Smirnov test. Statistical comparisons were performed by using Student's T test for continuous variables, and chi-square test for binary variables. One-way analysis of variance (ANOVA) with post-hoc test by Bonferroni was used to examine the differences among groups. Correlations between clinical parameters, pulmonary function, thoracic CT pulmonary fibrosis score and echocardiography parameters with RV free wall strain were expressed in terms of Pearson's correlation coefficient. Univariate linear regression analysis was used to identify potential determinants of RV free wall strain. The final multivariate model to identify determinants of RV free wall strain was obtained using the enter method by including parameters with a p-value <0.10 in univariate analysis and excluding parameters with significant collinearity. All statistical analysis were performed using the statistical package SPSS for windows (Version 17.0, SPSS, Chicago, USA). A p-value <0.05 was considered to be statistically significant.

Results

Clinical characteristics of the patients

The average CT pulmonary fibrosis score was 8.1±7.4. A total of 51 (50%) patients did not have pulmonary fibrosis and did not have PHT, 32 (31%) patients had pulmonary fibrosis but no PHT and the remaining 19 (19%) had pulmonary fibrosis and PHT. Clinical characteristics of the 3 groups are shown in Table 4.1. Age, gender, dSSc, Modified Rodnan Skin Score and blood pressure were similar between the 3 groups of SSc patients. Patients with pulmonary fibrosis and PHT had a longer duration of the disease (since onset of skin manifestation) compared with the remaining two groups of patients. Auto-antibodies (anti-nuclear, anti-topoisomerase and anti-centromere), current immunosuppressive and cardiovascular medications were also similar between the different groups. Moreover, SSc patients with pulmonary fibrosis and PHT had the lowest forced vital capacity (FVC)% and DLCO% compared with the remaining two groups of patients. However, the FVC% and DLCO% did not differ significantly between SSc patients with pulmonary fibrosis and no PHT and SSc patients with no pulmonary fibrosis and no PHT.

Echocardiographic characteristics of the patients

Conventional echocardiographic parameters of LV systolic and diastolic function of SSc patients (divided in the 3 subgroups) and controls are shown in Table 4.2. No significant differences were noted in LV end-diastolic volume (92±24 ml vs. 95±16 ml, p=0.41), LV end-systolic volume (34±12 ml vs. 36±9 ml, p=0.44), and LVEF (62±7% vs. 62±7%, P=0.92) between overall SSc patients and controls. However, estimated PASP (30±11 mmHg vs. 20±6 mmHg, p<0.01) was significantly higher in SSc patients as compared to controls, while E/E' ratio (12.2±3.9 vs. 8.5±2.1, p<0.01) and LV diastolic dysfunction grade (60% vs. 14%, p<0.01) were significantly impaired in these patients.

When comparing the 3 different groups of SSc patients (Table 4.2), all groups showed similar values of conventional echocardiographic parameters including LV and RV systolic function. According to the definition, SSc patients with pulmonary fibrosis and PHT showed significantly higher PASP as compared to the other 2 groups.

However, when using speckle tracking-derived strain for the analysis of RV function, significant differences among the groups were observed. In particular, RV free wall strain

Table 4.1 Clinical characteristics of the 102 patients with systemic sclerosis (SSc) divided in patients with (1) no pulmonary fibrosis and no pulmonary hypertension (PHT), (2) pulmonary fibrosis and no PHT (3) both pulmonary fibrosis and PHT

	No pulmonary fibrosis and no PHT (n=51)	Pulmonary fibrosis and no PHT (n=32)	Pulmonary fibrosis and PHT (n=19)	p-value
Age (yrs)	51±13	58±12	58±15	**<0.01**
Female gender, n (%)	34 (77)	19 (70)	11 (73)	0.81
Diffuse type of SSc	24 (47)	16 (50)	12 (63)	0.48
Time since diagnosis, yrs	5.6±8.3	4.9±4.6	9.9±7.6	**0.046**
Time since onset of Raynaud's, yrs	10.8±12.2	10.0±8.7	13.6±10.1	**0.50**
Time since onset of skin manifestation, yrs	6.2±8.2	5.6±4.7	11.8±8.4[†‡]	**<0.01**
Modified Rodnan Skin Score	5.0±5.5	5.2±5.8	8.1±6.8	0.33
Systolic blood pressure, mmHg	120±22	113±13	125±17	0.37
Diastolic blood pressure, mmHg	73±9	72±12	73±11	0.95
Systemic hypertension	5 (12)	3 (12)	0 (0)	0.52
Immune markers				
Anti-nuclear, n (%)	40 (91)	24 (89)	12 (80)	0.52
Anti-topoisomerase, n (%)	12 (27)	10 (37)	6 (43)	0.48
Anti-centromere, n (%)	3 (7)	2 (7)	7 (8)	0.45
Chronic kidney disease, n (%)	2 (5)	5 (20)	1 (10)	0.13
Pulmonary function test				
FVC% predicted	96.5±16.1	91.5±15.6	65.1±10.8[†‡]	**<0.01**
DLCO% predicted	69.0±14.5	61.0±14.7	45.1±10.9[†‡]	**<0.01**
CT pulmonary fibrosis score	2.4±2.6	12.3±3.9	16.6±7.9[†‡]	**<0.01**
Current immunosuppressive medication (%)				
Corticosteroids, n (%)	2 (4)	11 (34)	7 (37)	<0.01
Methotrexate, n (%)	4 (8)	3 (9)	1 (5)	0.87
Azathioprine, n (%)	2 (4)	3 (9)	3 (16)	0.24
Current cardiovascular medications (%)				
Calcium antagonists, n (%)	21 (41)	12 (38)	10 (53)	0.56
ACE inhibitors, n (%)	4 (8)	3 (9)	1 (5)	0.87

ACE, angiotensin converting-enzyme; dSSc, diffuse systemic sclerosis; CT, computed tomography; DLCO, diffusion lung capacity for carbon monoxide; ESR, erythrocyte sedimentation rate; FVC, forced vital capacity; PHT, pulmonary arterial hypertension; Chronic kidney disease was defined as an estimated glomerular filtration clearance rate <60 ml/min/1,73m^2 for more than 3 months.
[†] p<0.05 vs. patients no pulmonary fibrosis and no PHT; [‡] p<0.05 vs. patients with pulmonary fibrosis and no PHT.

was significantly impaired (less negative values) in SSc patients compared with controls (-21.9±4.7% vs. -28.0±4.2%, p<0.01). Furthermore among the 3 groups of SSc patients, patients with pulmonary fibrosis and PHT had the most impaired RV free wall strain (-16.8±3.1%) compared with patients with pulmonary fibrosis and no PHT (-21.5±3.6%) and patients with no pulmonary fibrosis and no PHT (-24.0±4.4%) (Figure 4.2). Moreover, SSc

Table 4.2   Conventional echocardiographic characteristics of left and right ventricular performance in SSc patients and controls

	Controls (n=36)	SSc patients (n=102)			p-value
		No pulmonary fibrosis and no PHT (n=51)	Pulmonary fibrosis and no PHT (n=32)	Pulmonary fibrosis and PHT (n=19)	
LV end diastolic volume (ml)	95±16	89±21	98±29	90±24	0.22
LV end systolic volume (ml)	36±9	33±10	36±14	35±12	0.65
LV ejection fraction (%)	62±7	62±7	64±7	61±7	0.30
LV diastolic function, n (%)					
Normal	31 (86)	17 (33)	15 (47)	9 (47)	0.17
Mild	4 (11)	12 (26)	5 (16)	8 (42)	
Moderate	1 (3)	13 (29)	8 (42)	1 (5)	
Severe	0 (0)	6 (12)	4 (11)	1 (5)	
E/E' ratio	8.5±2.1	11.9±4.2	12.2±3.1	13.3±4.4	0.60
RVDA (ml)	18.3±2.4	17.3±3.5	17.9±3.8	19.8±4.2[†]	0.053
TAPSE (cm)	2.3±0.2	2.1±0.2	2.1±0.3	2.0±0.2	0.08
PASP (mmHg)	20±6	26±5	28±6	47±10[†‡]	**<0.01**

LV, left ventricular; PASP, pulmonary arterial systolic pressure; PHT, pulmonary arterial hypertension; RVDA, right ventricular end-diastolic area; TAPSE, tricuspid annular plane systolic excursion.
[†] p<0.05 vs. patients no fibrosis and no PHT; [‡] p<0.05 vs. patients with fibrosis and no PHT.
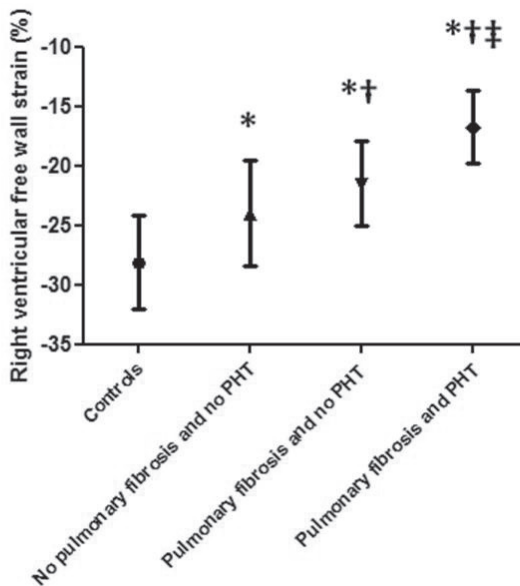

Figure 4.2   Right ventricular free wall strain in controls and patients with SSc (3 subgroups including [1] no pulmonary fibrosis and no PHT, [2] pulmonary fibrosis and no PHT and [3] pulmonary fibrosis and PHT). * p<0.05 vs. control; [†] p<0.05 vs. patients no pulmonary fibrosis and no PHT; [‡] p<0.05 vs. patients with pulmonary fibrosis and no PHT.

patients with pulmonary fibrosis and no PHT showed significantly more impaired RV free wall strain as compared to patients with no pulmonary fibrosis and no PHT. Importantly, RV free wall strain was significantly more impaired in SSc patients with no pulmonary fibrosis and no PHT as compared to controls.

Correlates of right ventricular free wall strain

Univariate linear regression analysis revealed that age, FVC%, DLCO%, CT pulmonary fibrosis score, CT evidence of pulmonary fibrosis, LVEF and PASP were significantly associated with impaired RV free wall strain. To avoid multicollinearity, only DLCO% was entered into the model. At multivariate analysis, CT evidence of pulmonary fibrosis, LVEF and PASP were independently associated with impaired RV free wall strain (Table 4.3).

Table 4.3   Univariate and multivariate linear regression models for RV free wall strain in patients with SSc

	Univariate		Multivariate	
	β (CI)	p-value	β (CI)	p-value
Age (yrs)	0.09 (0.03–0.16)	**<0.01**	0.02 (-0.04–0.09)	0.53
Female gender, n (%)	1.44 (-0.72–3.60)	0.19		
Diffuse type of SSc	0.90 (-0.97–2.76)	0.34		
Time since diagnosis	0.12 (-0.01–0.24)	0.07	0.03 (-0.23–0.29)	0.82
Time since onset of Raynaud's	0.02 (-0.07–0.11)	0.61		
Time since onset of skin manifestation	0.12 (-0.01–0.24)	0.06	0.01 (-0.25–0.25)	0.98
Modified Rodnan Skin Score	0.06 (-0.07–0.19)	0.36		
Systolic blood pressure	0.03 (-0.02–0.08)	0.18		
Diastolic blood pressure	0.05 (-0.05–0.14)	0.35		
Pulmonary function test:				
FVC% predicted	-0.08 (-0.13–-0.03)	<0.01		
DLCO% predicted	-0.11 (-0.16–-0.06)	<0.01	-0.03 (-0.08–0.03)	0.35
CT pulmonary fibrosis score	0.28 (0.17–0.40)	<0.01		
Pulmonary fibrosis (CT pulmonary fibrosis score >7)	3.93 (2.22–5.64)	<0.01	2.18 (0.25–4.11)	**0.03**
LV ejection fraction	-0.15 (-0.29–-0.02)	0.02	-0.12 (-0.24–-0.01)	**0.04**
E/E' ratio	0.15 (-0.14–0.43)	0.30		
PASP	0.23 (0.16–0.31)	<0.01	-0.03 (-0.08–-0.03)	**0.03**

Abbreviations as in Tables 4.1 and 4.2.

Discussion

The main findings of the present study can be summarized as follows: 1) despite no significant differences in conventional echocardiographic parameters, RV free wall strain assessed by 2D speckle tracking echocardiography was significantly impaired (less negative) in patients with SSc as compared to controls; 2) in particular, patients with pulmonary fibrosis and PHT showed the most impaired RV free wall strain, followed by patients with pulmonary fibrosis and no PHT. Of interest, patients without pulmonary fibrosis and no PHT had the most preserved RV free wall strain, although remaining significantly impaired as compared to controls; 3) CT evidence of pulmonary fibrosis, PASP and LVEF were independently associated with impaired RV free wall strain.

Impaired right ventricular function in SSc patients

The exact prevalence of RV dysfunction in SSc patients is currently unknown (20). Echocardiography is the most widely available and applied method to evaluate RV function in these patients. Since the contraction of RV occurs mainly along the longitudinal axis (21), the assessment of systolic displacement of the tricuspid annulus towards the apex along the longitudinal plane, the so-called TAPSE, is one of the most frequently used echocardiographic methods to estimate RV systolic function. However, initial small studies have applied TAPSE in SSc patients with contradictive results: some studies showed impaired TAPSE in SSC patients as compared to controls (22;23) while other studies showed similar values (24). In the present study, TAPSE was not significantly different between SSc patients and controls, although it showed a trend of being more impaired in a most advanced stage of the disease (in patients with pulmonary fibrosis and PHT). A possible explanation of these results might be that TAPSE reflects the contraction of a single RV segment (basal part of RV free wall next to tricuspid annulus) and may not accurately represent global RV systolic function (25). Furthermore, this measure is probably not sensitive enough to identify subtle RV myocardial dysfunction and is therefore significantly impaired only at a late stage of the disease. A diagnostic technique that could overcome these limitations and allow an early and accurate diagnosis RV dysfunction in SSc patients would therefore be of great clinical importance for patient management.

2D echocardiographic speckle tracking strain analysis has been proposed as a sensitive tool to detect subtle LV dysfunction in patients with SSc (26). However, the value of this technique for the assessment of RV function in SSc patients is largely unknown. The present study,

using this novel echocardiographic technique in a large cohort of patients, demonstrated significantly more impaired RV function in patients with SSc (with apparently normal RV dimension and TAPSE) as compared with matched controls. In particular, patients with pulmonary fibrosis and PHT showed the most impaired RV free wall strain as compared with patients with pulmonary fibrosis and no PHT and patients without either condition. Of similar importance, SSc patients without pulmonary fibrosis or PHT still showed a significantly impaired RV free wall strain as compared with controls, suggesting the ability of this technique to diagnose subclinical direct myocardial involvement of the RV by SSc, with important implications in the clinical decision-making regarding the follow-up/monitor of cardiac function and potential early treatment. Similar results were also observed in initial studies which showed impaired RV function as detected by speckle tracking derived strain in SSc patients with no PHT (27-29).

Independent association of PASP, pulmonary fibrosis and LVEF with impaired RV function

Initial studies have suggested a close relationship between PHT and the development of RV dysfunction in SSc patients. In a study involving 98 patients with connective tissue disease (91 patients with SSc), RV function measured by Tei-index significantly correlated with pulmonary pressure derived by right heart catheterization (30). Pulmonary pressures were also correlated with tissue-Doppler imaging-derived RV strain rate among 23 patients with SSc (31). These findings are further confirmed by the present study, where PASP independently contributed to the presence of impaired RV function, suggesting the detrimental effect of elevated PASP on RV performance by pressure-overload, either due to interstitial lung disease or to pulmonary arterial hypertension.

Similarly, various types of pulmonary disease are associated with RV dysfunction. In a study involving 434 patients with severe pulmonary disease, RV dysfunction was present in 66% of patients and the prevalence was similar between the different groups (alpha1-antitrypsin deficiency emphysema, chronic obstructive airway disease, cystic fibrosis and idiopathic pulmonary fibrosis) (32). Another study also demonstrated that in patients with interstitial lung disease (n=22), RV dysfunction was common and significantly correlated with exercise capacity (33). The association between pulmonary fibrosis and RV dysfunction in patients with SSc has not been explored. The present study demonstrated in a large cohort that patients with pulmonary fibrosis, detected by high-resolution CT thorax, had impaired RV

free wall strain, even without associated PHT. In addition, presence of pulmonary fibrosis was independently associated with RV dysfunction after multivariate adjustment. A potential explanation of this finding is that pulmonary fibrosis may be associated with mild/latent or dynamic PHT, which could not be detected by a single echocardiography measurement (34). In addition, patients with pulmonary fibrosis have been shown to be more likely to have systemic involvement, and are therefore probably at higher risk for a significant direct myocardial involvement contributing to RV dysfunction (35). These hypotheses, however, require further studies.

In the current study, LVEF was also independently associated with RV free wall strain in patients with SSc. Only limited data are available on the relationship between LV and RV function in SSc patients. In a study of 42 SSc patients, 16 of them showed impaired RV ejection fraction and 8 of them had concomitant LV diastolic dysfunction (2). The concomitant presence of RV and LV dysfunction can be explained by a primary myocardial involvement, which is common in patients with SSc and can occur simultaneously in both RV and LV, leading to biventricular dysfunction (36). In addition, RV and LV performance are closely related as they share a common ventricular septum and RV epicardial fibers are contiguous with LV epicardial fibers. This inter-ventricular interaction can play a significant role in SSc patients, particularly since RV dilatation and elevated PASP may influence LV filling and subsequently LV diastolic and systolic function (37).

Limitations

The cross-sectional design of the study precluded the establishment of causal relationship between 2D speckle tracking derived RV free wall strain with pulmonary fibrosis and PASP in patients with SSc. In addition, PASP was estimated with echocardiography and right heart catheterization was not systematically available, since it was performed only at the discretion of the treating physician after joint discussion within the PHT working group. Therefore, PASP measured in the present study was considered to be a general measure of RV overload. Also in this analysis, tissue Doppler imaging derived measures of RV function were not performed. However, 2D speckle tracking analysis should be considered more accurate for RV function assessment since it overcomes the main limitation of tissue Doppler imaging which is the dependency of the insonation angle, often significant in the visualization of the RV free/wall (29). Finally, the findings of the present study should be confirmed in larger prospective studies eventually exploring also the prognostic value of these measures.

Conclusion

Patients with SSc showed impaired RV function as assessed by 2D speckle tracking derived strain as compared to controls. CT evidence of pulmonary fibrosis, PASP and LVEF were independently associated with impaired RV free wall strain.

4

References

(1) Hachulla AL, Launay D, Gaxotte V et al. Cardiac magnetic resonance imaging in systemic sclerosis: a cross-sectional observational study of 52 patients. Ann Rheum Dis 2009;68:1878-84.

(2) Meune C, Allanore Y, Devaux JY et al. High prevalence of right ventricular systolic dysfunction in early systemic sclerosis. J Rheumatol 2004;31:1941-5.

(3) Meune C, Avouac J, Wahbi K et al. Cardiac involvement in systemic sclerosis assessed by tissue-doppler echocardiography during routine care: A controlled study of 100 consecutive patients. Arthritis Rheum 2008;58:1803-9.

(4) Giunta A, Tirri E, Maione S et al. Right ventricular diastolic abnormalities in systemic sclerosis. Relation to left ventricular involvement and pulmonary hypertension. Ann Rheum Dis 2000;59:94-8.

(5) Overbeek MJ, Lankhaar JW, Westerhof N et al. Right ventricular contractility in systemic sclerosis-associated and idiopathic pulmonary arterial hypertension. Eur Respir J 2008;31:1160-6.

(6) Rudski LG, Lai WW, Afilalo J et al. Guidelines for the echocardiographic assessment of the right heart in adults: a report from the American Society of Echocardiography endorsed by the European Association of Echocardiography, a registered branch of the European Society of Cardiology, and the Canadian Society of Echocardiography. J Am Soc Echocardiogr 2010;23:685-713.

(7) Blessberger H, Binder T. Non-invasive imaging: Two dimensional speckle tracking echocardiography: basic principles. Heart 2010;96:716-22.

(8) Schouffoer AA, Ninaber MK, Beaart-van de Voorde LJ et al. Randomized comparison of a multidisciplinary team care program with usual care in patients with systemic sclerosis. Arthritis Care Res (Hoboken) 2011; 63: 909-17.

(9) Schuerwegh AJ, Schouffoer AA, Beaart-van deVoorde LJ et al. Yearly, standardized, comprehensive assessment and treatment advice for patients with systemic sclerosis (SSc): feasibility of a day care program [abstract]. Arthritis Rheum 2009;60 Suppl:S427-8.

(10) Clements P, Lachenbruch P, Siebold J et al. Inter and intraobserver variability of total skin thickness score (modified Rodnan TSS) in systemic sclerosis. J Rheumatol 1995;22:1281-5.

(11) LeRoy EC, Black C, Fleischmajer R et al. Scleroderma (systemic sclerosis): classification, subsets and pathogenesis. J Rheumatol 1988;15:202-5.

(12) Macintyre N, Crapo RO, Viegi G et al. Standardisation of the single-breath determination of carbon monoxide uptake in the lung. Eur Respir J 2005;26:720-35.

(13) Wanger J, Clausen JL, Coates A et al. Standardisation of the measurement of lung volumes. Eur Respir J 2005;26:511-22.

(14) Kazerooni EA, Martinez FJ, Flint A et al. Thin-section CT obtained at 10-mm increments versus limited three-level thin-section CT for idiopathic pulmonary fibrosis: correlation with pathologic scoring. AJR Am J Roentgenol 1997;169:977-83.

(15) Lang RM, Bierig M, Devereux RB et al. Recommendations for chamber quantification: a report from the American Society of Echocardiography's Guidelines and Standards Committee and the Chamber Quantification Writing Group, developed in conjunction with the European Association of Echocardiography, a branch of the European Society of Cardiology. J Am Soc Echocardiogr 2005;18:1440-63.

(16) Hammarstrom E, Wranne B, Pinto FJ, Puryear J, Popp RL. Tricuspid annular motion. J Am Soc Echocardiogr 1991;4:131-9.

(17) Nagueh SF, Appleton CP, Gillebert TC et al. Recommendations for the evaluation of left ventricular diastolic function by echocardiography. J Am Soc Echocardiogr 2009;22:107-33.

(18) McQuillan BM, Picard MH, Leavitt M, Weyman AE. Clinical correlates and reference intervals for pulmonary artery systolic pressure among echocardiographically normal subjects. Circulation 2001;104:2797-802.

(19) Kircher BJ, Himelman RB, Schiller NB. Noninvasive estimation of right atrial pressure from the inspiratory collapse of the inferior vena cava. Am J Cardiol 1990;66:493-6.

(20) Giusca S, Dambrauskaite V, Scheurwegs C et al. Deformation imaging describes right ventricular function better than longitudinal displacement of the tricuspid ring. Heart 2010;96:281-8.

(21) Rushmer RF, Crystal DK, Wagner C. The functional anatomy of ventricular contraction. Circ Res 1953;1(2):162-70.

(22) Lee CY, Chang SM, Hsiao SH et al. Right heart function and scleroderma: insights from tricuspid annular plane systolic excursion. Echocardiography 2007;24:118-25.

(23) Mathai SC, Sibley CT, Forfia PR et al. Tricuspid annular plane systolic excursion is a robust outcome measure in systemic sclerosis-associated pulmonary arterial hypertension. J Rheumatol 2011;38:2410-8.

(24) Serra W, Chetta A, Santilli D et al. Echocardiography may help detect pulmonary vasculopathy in the early stages of pulmonary artery hypertension associated with systemic sclerosis. Cardiovasc Ultrasound 2010;8:25.

(25) Focardi M, Cameli M, Carbone SF, Massoni A, De Vito R, Lisi M, Mondillo S. Traditional and innovative echocardiographic parameters for the analysis of right ventricular performance in comparison with cardiac magnetic resonance. Eur Heart J Cardiovasc Imaging 2015;16(1):47-52.

(26) Yiu KH, Schouffoer AA, Marsan NA et al. Left ventricular dysfunction assessed by speckle-tracking strain analysis in patients with systemic sclerosis: relationship to functional capacity and ventricular arrhythmias. Arthritis Rheum 2011;63:3969-78.

(27) Matias C, Isla LP, Vasconcelos M et al. Speckle-tracking-derived strain and strain-rate analysis: a technique for the evaluation of early alterations in right ventricle systolic function in patients with systemic sclerosis and normal pulmonary artery pressure. J Cardiovasc Med (Hagerstown) 2009;10:129-34.

(28) Schattke S, Knebel F, Grohmann A et al. Early right ventricular systolic dysfunction in patients with systemic sclerosis without pulmonary hypertension: a Doppler Tissue and Speckle Tracking echocardiography study. Cardiovasc Ultrasound 2010;8:3.

(29) Durmus E, Sunbul M, Tigen K et al. Right ventricular and atrial functions in systemic sclerosis patients without pulmonary hypertension: Speckle-tracking echocardiographic study. Herz 2015;(40)4:709-15

(30) Vonk MC, Sander MH, van den Hoogen FH, van Riel PL, Verheugt FW, van Dijk AP. Right ventricle Tei-index: a tool to increase the accuracy of non-invasive detection of pulmonary arterial hypertension in connective tissue diseases. Eur J Echocardiogr 2007;8:317-21.

(31) D'Andrea A, Stisi S, Bellissimo S et al. Early impairment of myocardial function in systemic sclerosis: non-invasive assessment by Doppler myocardial and strain rate imaging. Eur J Echocardiogr 2005;6:407-18.

(32) Vizza CD, Lynch JP, Ochoa LL, Richardson G, Trulock EP. Right and left ventricular dysfunction in patients with severe pulmonary disease. Chest 1998;113:576-83.

(33) Giannakoulas G, Karamitsos TD, Pitsiou G, Karvounis HI. Right ventricular dysfunction and functional limitation in idiopathic pulmonary fibrosis. Eur Respir J 2008;31:219-20.

(34) Huez S, Roufosse F, Vachiery JL et al. Isolated right ventricular dysfunction in systemic sclerosis: latent pulmonary hypertension? Eur Respir J 2007;30:928-36.

(35) McNearney TA, Reveille JD, Fischbach M et al. Pulmonary involvement in systemic sclerosis: associations with genetic, serologic, sociodemographic, and behavioral factors. Arthritis Rheum 2007;57:318-26.

(36) Allanore Y, Meune C. Primary myocardial involvement in systemic sclerosis: evidence for a microvascular origin. Clin Exp Rheumatol 2010;28:S48-S53.

(37) Valsangiacomo Buechel ER, Mertens LL. Imaging the right heart: the use of integrated multimodality imaging. Eur Heart J 2012;33:949-60.

Increased respiratory drive relates to severity of dyspnea in systemic sclerosis

Maarten K. Ninaber, Willem B.G.J. Hamersma,
Annemie J.M. Schuerwegh and Jan Stolk

Abstract

Background: Dyspnea may be a presenting symptom in progressive systemic sclerosis (SSc). Respiratory drive (mouth occlusion pressure, MOP, at rest and during CO_2 rebreathing, 7% CO_2, 93% O_2) is a major determinant of dyspnea and may relate to the magnitude of dyspnea.

Methods: In a prospective design, MOP at 0.1 sec (P0.1) was measured in 73 SSc patients while breathing room air and during CO_2 rebreathing. An abnormal V'E/P0.1 is defined as <8 L/min/cmH$_2$O. Dyspnea scores were assessed by a shortness of breath questionnaire (UCSD dyspnea scale).

Results: Mean P0.1 in patients with normal V'E/P0.1 (n=45) was 1.1±0.04 and 1.6±0.08 cmH$_2$O in patients with abnormal V'E/P0.1 (n=28), p<0.001. ΔP0.1/Δ PetCO$_2$ differed significantly between these groups (0.45 versus 0.75 cmH$_2$O/mmHg, p<0.001), but no significant difference was present in ΔV'E/ΔPetCO$_2$. V'E/P0.1 showed the highest significant correlation with the UCSD dyspnea score (r=-0.76, p<0.001). UCSD cut-off value for abnormal V'E/P0.1 was 8.5 (sensitivity 93%, specificity 96%, area under the curve 0.98).

Conclusions: In SSc patients an abnormal V'E/P0.1 better relates to the severity of dyspnea than traditional lung function parameters and can easily be assessed at first outpatient consultation.

Background

Systemic sclerosis (SSc) is a rare, heterogeneous condition of unknown etiology characterized by microvascular injury and deposition of excess collagen in skin and internal organs (1). Principle subsets of SSc include limited cutaneous SSc (lcSSc) and diffuse cutaneous SSc (dcSSc) (2). Importantly, progressive systemic sclerosis may involve interstitial lung disease (ILD) resulting into a restrictive lung function pattern abnormality (1). In addition, pulmonary arterial hypertension (PAH) may arise in the course of the disease (1). Validated measures to monitor progression of SSc are necessary for clinical trials and routine care of patients with SSc. Dyspnea as a presenting symptom occurs in 20% of all newly diagnosed SSc patients and 70% of patients with SSc complicated by ILD or PAH patients complain of dyspnea (1). Importantly, early recognition of disease progression related to organ damage and initation of treatment may improve health-related outcomes. Lung volumes and gas transfer studies are related to disease severity in SSc (1) and used for initation of treatment and evaluation. However, whether the magnitude of dyspnea relates to these pulmonary function tests is not known.

The impedance of the respiratory system is influenced by lung and chest wall compliance and respiratory flow resistance (3). An increased respiratory impedance is recognized as the most frequent cause of dyspnea (3). Other respiratory abnormalities resulting into dyspnea may include hypoxia, respiratory muscle weakness or pulmonary vasculopathy (pulmonary embolisms, pulmonary arterial hypertension). In progressive SSc, dyspnea may arise from an increased impedance of the respiratory system caused by ILD. In SSc, ILD or limited chest wall excursions due to a thickened thoracic skin is considered to cause this increased impedance (4;5). Furthermore, dyspnea may result from an inappropriate ventilatory response upon the chemoreflex drive at rest and to hypercapnia (6;7).

To assess the ventilatory output as an index of the respiratory drive, resting ventilation (V'E) and tidal volumes can be evaluated (8). Ventilation, however, is an imperfect output parameter of the respiratory drive since it is affected by alterations in the impedance of the respiratory system (i.e. mechanical properties of the lung and chest wall) independently of changes in respiratory sensitivity to hypercapnia (3;6;9). To assess the respiratory drive, mouth occlusion pressures (MOP) as an index of the output can be measured (3). Important advantages of this technique include the reproducibility within each subject and reported values independent of age (10). In a study of normal subjects and patients with ILD, a V'E/ P0.1 greater than 8 l/min/cmH$_2$O sharply separated a normal from an abnormal response

(10). Therefore, in patients who report dyspnea and who have concomitant ILD, a low V'E to a high P0.1 (i.e. low V'E/P0.1) is expected.

In addition to V'E/P0.1 at rest, the respiratory drive to hypercapnia (P0.1 to CO_2, i.e. $\Delta P0.1/\Delta PetCO_2$) provides insight into the central chemoreflex drive to hypercapnia (11-13). In patients with ILD and dyspnea, the central chemoreflex drive may result into a falsely low ventilatory response to hypercapnic stimulation (7). To overcome this, the central chemoreflex drive to hypercapnia may be assessed by mouth occlusion pressures ($\Delta P0.1/\Delta PetCO_2$) (6;11;12).

Based on the above we hypothesized that in patients with SSc the respiratory drive, as measured by P0.1, V'E/P0.1 and mouth occlusion pressures to CO_2 rebreathing, may better relate to the magnitude of reported dyspnea than the severity of gas transfer or lung volume impairment as measured by PFTs. Furthermore, we hypothesized that the respiratory drive to hypercapnia is increased in SSc patients who reported dyspnea.

Methods

Patients

We prospectively screened SSc patients referred to an outpatient targeted health care program. All patients underwent an intensive screening procedure which included PFTs, serum laboratory testing, echocardiography, high-resolution chest CT scanning (HRCT) and a cardiopulmonary exercise test (CPET). Furthermore, all patients consulted a rheumatologist, cardiologist and a pulmonologist. All tests were done in one or two consecutive days. Patients were classified as limited systemic sclerosis (lcSSc) or diffuse systemic sclerosis (dcSSc) according to the LeRoy criteria (2).

Ethics

The local Medical Ethical Committee of the Leiden University Medical Center approved the protocol. A written informed consent was obtained from each patient prior to enrollment.

Standard pulmonary function testing

PFTs were measured in all SSc patients including spirometry and gas transfer studies and expressed as percentage predicted (14;15). Total lung capacity (TLC) was measured by the multiple breath helium dilution method and diffusion capacity for carbon monoxide (DLCO) by the single breath carbon monoxide method (14;15).

Measuring mouth occlusion pressures during resting ventilation and CO_2 rebreathing

Subjects were seated comfortably, attached to the mouthpiece with a noseclip in place. At randomized intervals, and without the subject's knowledge, the inspiratory side of the rebreathing circuit was occluded during late expiration. The pressure generated at 0.1 s after the onset of inspiration was obtained in each subject during several minutes with a minimum of 10 measurements prior to the rebreathing test (3). Thereafter, occlusion pressures were measured simultaneously during CO_2 rebreathing at randomized intervals (3;16). The slope of this curve was used as an index of the respiratory drive to hypercapnia (i.e. central chemoreflex drive) and reported as $\Delta P0.1/\Delta PetCO_2$ (3;16)

Measuring the hyperoxic ventilatory response to hypercapnia (HCVR)

We used a simple rebreathing technique according to Read's rebreathing technique, which consisted of a rebreathing bag filled with a gas mixture (7% CO2 and 93% O_2) (17). In the rebreathing bag, a total volume of approximately twice the measured vital capacity of the patient was used.

Under hyperoxia the ventilatory response to hypercapnia (HCVR) represents the central chemoreflex response only, assuming that the peripheral chemoreflex drive is suppressed by hyperoxia (16;17). Equilibrium of pressures between CO_2 in cerebral blood and end-tidal PCO_2 exhalation at the mouth ($PetCO_2$) is expected not to occur before recirculation of cerebral blood flow (17). Respiratory volumes were recorded by a turbine volume measuring device (Oxycon-Pro, Jaeger). The Oxycon Pro was calibrated according to the instruction manual before each test (Oxycon instruction manual ver. 4.5. Erich Jaeger GmbH, Hoechberg, Germany) (18). Oxygen and CO_2 analyzers were calibrated with room air and certified calibration gases at 180 kPa (16% O_2, 5% CO_2 and 79% N_2). The flow turbine (Triple V, Erich Jaeger GmbH, Hoechberg, Germany) was calibrated with a 3.00 liter 5530 series calibration

syringe (Hans Rudolph, Inc, Kansas City, USA). Both gas and volume calibration were repeated until the difference between consecutive calibrations was less than 1%. Therefore, measurements were not considered to be influenced under hyperoxia. Expired gas at the mouth was sampled continuously and analyzed for $PetCO_2$ by a fast-response infrared analyzer. The software calculated tidal volumes, inspiratory and expiratory times, minute ventilation, and $PetCO_2$ on a breath-by-breath basis. The hyperoxic ventilatory response to hypercapnia (HCVR) was measured during several minutes after equilibrium between the end-tidal CO_2 and mixed venous CO_2. In this phase, a linear increase in V'E with respect to $PetCO_2$ was observed. The slope of this curve was used as the index of the ventilatory central chemosensitivity and reported as $\Delta V'E/\Delta PetCO_2$ (17).

UCSD shortness of breath questionnaire

We used a previously validated shortness of breath questionnaire which evaluates in 24-items self-reported shortness of breath while performing a variety of activities of daily living (19). It was administered by MKN prior to the MOP and rebreathing study while the subject sitting comfortably.

Statistical analysis

Statistical analysis was performed with the SPSS 20.0 package (SPSS, Inc., Chicago, IL, USA). Continuous variables are expressed as mean value ± standard deviations. P-values <0.05 were considered significant. Categorical data are presented as frequencies and percentages. Statistical comparisons were performed by using Student's T-test for continuous variables, and chi square test for binary variables. Correlations between clinical parameters, pulmonary function tests, were expressed in terms of Pearson's or Spearman's correlation coefficient when appropriate. The receiver operating characteristic (ROC) curve was used to evaluate the optimal cut-off value for the UCSD dyspnea score in relation to an abnormal V'E/P0.1.

Results

In total, 73 SSc patients were prospectively evaluated by measuring PFTs, MOP and the hyperoxic ventilatory response to hypercapnia (HCVR). Patients were classified by their V'E/P0.1 according to Scott GC and Burki NK [10], where ≥8 l/min/cmH_2O was defined as normal.

Anthropometric and lung function data are presented in Table 5.1. In the group with a V'E/P0.1 ≥8 L/min/cmH20, lcSSc patients were significantly more present. In all patients with an abnormal V'E/P0.1 (<8 L/min/cmH$_2$O), spirometric and gas transfer studies were significantly lower. All SSc patients were normocapnic at rest (PaCO$_2$=5.24±0.41 kPa).

Table 5.1   Anthropometric and pulmonary function data of 73 SSc patients classified by V'E/P0.1 ≥8 l/min/cmH$_2$O (10)

	V'E/P0.1 <8 l/min/cmH$_2$O N=28	V'E/P0.1 ≥8 l/min/cmH$_2$O N=45	P-value*
Age (yrs)	54.4 (11.8)	50.9 (14.4)	0.25
Female sex (%)	26 (93)	37 (82)	0.11
Height (cm)	164 (7.2)	171 (8.7)	0.002
Weight (kg)	67.1 (15.3)	69.8 (12.8)	0.43
BMI (cm/kg2)	24.8 (5.4)	23.9 (3.7)	0.48
lcSSc subtype (%)	10 (36)	34 (76)	0.02
PaO$_2$ (kPa)	10.4 (0.36)	10.6 (0.29)	0.58
PaCO$_2$ (kPa)	5.31 (0.41)	5.18 (0.43)	0.25
FVC (% pred)	92.1 (19.9)	111.1 (19.7)	0.001
DLCOc SB (% pred)	57.7 (15.8)	70.7 (15.1)	0.001
TLC-He (% pred)	81.5 (16.6)	95.4 (13.5)	<0.001
FRC/TLC (%)	53 (17)	56 (7)	0.23

* P-value expressed for student T-test.
PaO$_2$ (partial arterial oxygen pressure, kPa); PaCO$_2$ (partial arterial carbon dioxide pressure, kPa); FVC (forced vital capacity, % pred); DLCOc SB (diffusion capacity for carbon monoxide single breath, % pred); TLC-He (total lung capacity, helium-dilution, % pred); FRC/TLC (ratio of functional residual capacity and TLC, %).

Indices of MOP differed significantly between the two groups (Table 5.2). In contrast, there was no difference in the hyperoxic ventilatory response to hypercapnia. In our study, patients with a normal V'E/P0.1 had a mean ΔP0.1/ΔPetCO$_2$ of 0.45±0.19 cmH$_2$O /mmHg, which differed significantly from patients with an abnormal V'E/P0.1. The latter group had an increased respiratory drive to hypercapnia (mean ΔP0.1/ΔPetCO$_2$ 0.75±0.42 cmH$_2$O/ mmHg).

All pulmonary function test parameters correlated inversely and significantly with the UCSD shortness of breath questionnaire (coefficient of correlation ranging from -0.39 to -0.49). V'E/P0.1, however, showed the highest significant correlation with the UCSD dyspnea score (r=-0.76, p<0.001, Figure 5.1). The cut-off value in UCSD dyspnea score for an abnormal V'E/P0.1 was 8.5 (sensitivity 93%, specificity 96%, area under the curve 0.98).

Table 5.2   Indices of MOP, CO_2 rebreathing and the UCSD dyspnea score (19) of 73 SSc patients

	V'E/P0.1 <8 l/min/cmH$_2$O N=28	V'E/P0.1 ≥8 l/min/cmH$_2$O N=45	P-value*
UCSD SOBQ	13 (3.5)	2.2 (2.7)	<0.001
P0.1	1.60 (0.57)	1.10 (0.31)	<0.001
V'E	8.7 (2.3)	11.6 (3.5)	<0.001
V'E/P0.1	5.68 (1.24)	10.83 (2.46)	<0.001
ΔV'E/ΔPetCO$_2$	2.31 (2.0)	2.49 (1.76)	0.71
(ΔV'E/FVC)/ΔPetCO$_2$	0.93 (0.72)	0.57 (0.51)	0.07
ΔP0.1/ΔPetCO$_2$	0.75 (0.42)	0.45 (0.19)	0.01

* P-value expressed for student T-test.
UCSD SOBQ (shortness of breath questionnaire; score range 0–120); P0.1 (mouth occlusion pressure at 0.1 second; cmH$_2$O); V'E (minute ventilation; L/min); V'E/P0.1 (central inspiratory neuromuscular respiratory drive; L/min/cmH$_2$O); ΔV'E/ΔPetCO$_2$ (hyperoxic ventilatory response to hypercapnia; L/min/mmHg); (ΔV'E/FVC)/ΔPetCO$_2$ (hyperoxic ventilatory response to hypercapnia, corrected for FVC; FVC/min/mmHg); ΔP0.1/ΔPetCO$_2$ (slope of occlusion pressure to hypercapnia; cmH$_2$O/mmHg).
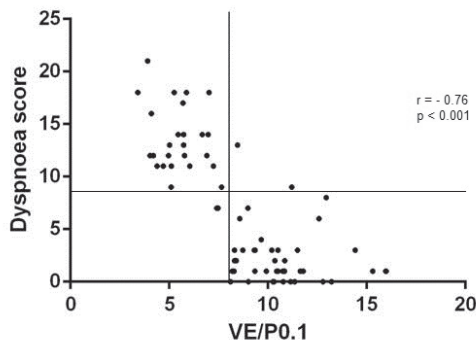

Figure 5.1   Correlation between the UCSD dyspnea score (19) and V'E/P0.1 in 73 prospectively screened SSc patients.
Vertical line set at V'E/P0.1 = 8 L/min/cmH$_2$O. Horizontal line set at UCSD 8.5.

Discussion

We report that in SSc patients with an abnormal inspiratory respiratory drive (V'E/P0.1 <8 L/min/cmH$_2$O) the sensation of dyspnea as measured by the UCSD dyspnea score differed from SSc patients with a normal respiratory drive. In addition, with a cut-off value of 8.5, the dyspnea score showed a high sensitivity and specificity for an abnormal V'E/P0.1. Furthermore, an abnormal V'E/P0.1 better relates to the magnitude of dyspnea than traditional lung function parameters and in these SSc patients an increased central

chemoreflex drive to CO_2 is present. Therefore, at first outpatient consultation, SSc patients complaining of dyspnea can easily be classified by using mouth occlusion pressures.

We showed that the level of dyspnea perception measured by the UCSD shortness of breath questionnaire (19) had a strong inverse correlation with the inspiratory neuromuscular drive as measured by V'E/P0.1 (Figure 5.1). A high dyspnea score and an increased respiratory drive to hypercapnia suggest that the work of breathing is increased due to an increased respiratory impedance (7;10). An increased activation of central respiratory centers results not only into an increase in minute ventilation but also into an increased perception of dyspnea (20). The basis for this awareness originates from the exchange in information between the motor and sensory cortex and is referred to as corollary discharge (20). Although the work of breathing is not the sole cause of dyspnea, increased effort as a result from an increased mechanical load causes a heightened sense of respiratory effort. Consequently, this may explain the strong correlation between the dyspnea score and the respiratory drive in the present study. This drive can be easily measured using mouth occlusion pressures at rest. As our results indicate, it better relates to dyspnea than impairment in lung volumes or gas transfer and may be present before significant impairment in these function tests arises. Therefore, measurement of the neuromuscular inspiratory drive may function in clinical practice in SSc patients complaining of dyspnea as a screening tool for detection of ILD or PAH.

Ventilation and its components, tidal volume and breathing frequency, depend on the compliance of the respiratory system and airway resistance (3;9-11). Importantly, one would like to differentiate patients who will not breathe because of central or neuromuscular inadequacy from those who cannot breathe because of mechanical abnormalities of the chest. The ventilatory response to hypercapnia is known for its large variability and reported responses may vary from 2.0 to 4.7 L/min/mmHg (3;17). Although a correction by FVC will lead to less variability (reported values vary from 0.42 to 0.94 FVC/min/mmHg (3), measuring the respiratory drive in patients affected by ILD using ventilatory parameters remains troublesome.

The mouth occlusion pressure generated by the inspiratory muscles at functional residual capacity (P0.1) has been proposed as a useful test to avoid these disadvantages (3;9-11). It is independent of flow resistance and respiratory compliance and less variability is observed in various subjects (3;10). Taken this together, we argue that ventilation and its components, may not represent an accurate output of the respiratory drive in our patients.

In daily practice, measuring P0.1 is very simple to apply and joined with a rebreathing bag, measurement of CO_2 responsiveness is possible. In normal subjects, P0.1 values of 0.75–1.5 cmH_2O have been described (3;10). In addition, normal V'E/P0.1 is defined by ≥ 8 L/min/cmH_2O, as evaluated by Scott and Burki (10). The responsiveness to hypercapnia by measuring P0.1 (ΔP0.1/ΔPetCO$_2$) in normal subjects is reported to be 0.17–0.49 cmH_2O /mmHg (3;16). This is in agreement with our results of SSc patients with a normal V'E/P0.1 (Table 5.2, mean ΔP0.1/ΔPetCO$_2$ 0.45 cmH_2O/mmHg). Thus, in these SSc patients, the respiratory compliance and airflow resistance did not affect occlusion pressures or the responsiveness to hypercapnia and is therefore considered to be normal. Furthermore, our data of mouth occlusion pressures during resting minute ventilation and during CO_2 rebreathing in patients with normal V'E/P0.1 are consistent with those of others (3;7;10;16;21). However, in the present study no significant difference was seen in ΔV'E/ΔPetCO$_2$ between the groups as classified by V'E/P0.1 (Table 5.2). Since there was a significant difference present between these groups using mouth occlusion pressures, minute ventilation may not represent the neuromuscular drive adequately in SSc patients with an increased respiratory impedance.

Although our reported values of the respiratory drive, as measured by P0.1, were approximately similar, differences from those previously reported by Walterspacher et al. are present (21). Potential reasons may include the differences in degree of restrictive lung function as measured by FVC % predicted. Our SSc patients with an abnormal V'E/P0.1 had mildly reduced FVC % predicted and may have preserved inspiratory muscle function. Furthermore, our SSc patients did not avoid activities provoking dyspnea resulting into deconditioning and muscle wasting. Secondly, they did not use immunosuppressive agents affecting respiratory muscle function (prednisone). Finally, polyneuropathy, which may cause an impaired respiratory muscle function, was not likely in our patients. Therefore, respiratory drive was considered to be appropriate in our SSc population.

In our study, patients with a low V'E/P0.1 had an increased responsiveness to hypercapnia which suggests an increased central respiratory drive (Table 5.2). This group was characterized by fewer limited SSc patients, a lower forced vital capacity, more impaired gas transfer and a lower lung volume (Table 5.1). Importantly, the majority of these patients had evidence of interstitial lung disease on their HRCT and some patients had an elevated tricuspid insufficiency gradient (data not shown). The disease duration did not differ between these groups. The difference in V'E/P0.1 between the groups are related to SSc disease severity and therefore influence the impedance of the respiratory system. Consequently, differences in V'E/P0.1 were observed.

Similar results are reported by Gorini and coworkers in normocapnic ILD patients without SSc (7). This contrasts to the concept of gradual down-regulation in central respiratory sensitivity for carbon dioxide in scleroderma patients (4). DiMarco and coworkers concluded that in patients with ILD, non-chemical, and presumably neural, mechanisms, both increase respiratory drive and alter the breathing pattern (22).

Several factors may influence the central sensitivity to CO_2 as measured by the ventilatory response to hypercapnia, such as the hormonal status, sex, age, use of sedative agents and caffeine (8;17). However, these factors will generally not result into an abnormal V'E/P0.1 since the compliance of the respiratory system or airway resistance is not affected.

Some considerations may apply to our study. First, we evaluated MOP and CO_2 rebreathing in patients with systemic sclerosis. We used a dataset of normal values for normal resting minute ventilation as a function of occlusion pressures (V'E/P0.1) (10). As reported by others a value higher than 8 L/min/cmH$_2$O, independent of age or sex, identifies subjects with normal PFTs and therefore provides a reliable index of respiratory drive (3;10). Consequently, we restricted our measurements in a patient group, only classified by V'E/P0.1. Our study contained 73 patients, which was similar to previous studies evaluating mouth occlusion pressures (3;10), and considered to be sufficient for group difference statistics. Despite the relatively mild range in low dyspnea scores (range 0–21; Figure 5.1), a significant difference in V'E/P0.1 and ΔP0.1/ΔPetCO$_2$ was present (Table 5.2), indicating the sensitivity of the mouth occlusion pressure test. Furthermore, assessing V'E/P0.1 to an additional load such as exercise may have increased this difference since airflow resistance will increase and consequently the impedance of the respiratory system.

Secondly, we did not measure the sensation of dyspnea, as assessed at rest by the UCSD questionnaire, during CO_2 rebreathing. To evaluate the relationship between the intensity of dyspnea and respiratory chemosensitivity may have strengthened our results, however this questionnaire was not designed to be administered during a rebreathing or exercise test.

In summary, the results of the present study show that patients with systemic sclerosis display a substantial variability in the ventilatory response to hypercapnia. In contrast, mouth occlusion pressures, independent of respiratory compliance or airflow resistance, provide an accurate outcome parameter in combination with minute ventilation as an initial evaluation for mild dyspnea. They better relate to the magnitude of patient reported dyspnea than traditional lung function parameters such as FVC or DLCO % predicted. Furthermore, in our SSc patients with an abnormal V'E/P0.1, an increased respiratory drive to hypercapnia was

5

present. Since dyspnea is one of the most frequently reported symptoms at first consultation in SSc, an easy test to discriminate between normal or abnormal respiratory mechanics would be obligatory. Therefore, we suggest that an abnormal V'E/P0.1 in combination with reported dyspnea indicates further assessment of respiratory involvement in SSc patients.

References

(1)   Black CM. Scleroderma. Br J Hosp Med 1979;22(1):28, 30, 32-28, 30, 33.

(2)   Leroy EC, Black C, Fleischmajer R, Jablonska S, Krieg T, Medsger TA, Jr. et al. Scleroderma (systemic sclerosis): classification, subsets and pathogenesis. J Rheumatol 1988;15(2):202-5.

(3)   Whitelaw WA, Derenne JP, Milic-Emili J. Occlusion pressure as a measure of respiratory center output in conscious man. Respir Physiol 1975;23(2):181-99.

(4)   Nageh TT, Du Bois RM. Non-invasive ventilation in hypercapnic respiratory failure secondary to sclerodermic chest wall restriction. Respir Med 1998;92(9):1170-2.

(5)   Pugazhenthi M, Cooper D, Ratnakant BS, Postlethwaite A, Carbone L. Hypercapnic respiratory failure in systemic sclerosis. J Clin Rheumatol 2003;9(1):43-6.

(6)   Cherniack RM, Snidal DP. The effect of obstruction to breathing on the ventilatory response to CO2. J Clin Invest 1956;35(11):1286-90.

(7)   Gorini M, Spinelli A, Ginanni R, Duranti R, Gigliotti F, Arcangeli P et al. Neural respiratory drive and neuromuscular coupling during CO2 rebreathing in patients with chronic interstitial lung disease. Chest 1989;96(4):824-30.

(8)   Patrick JM, Howard A. The influence of age, sex, body size and lung size on the control and pattern of breathing during CO 2 inhalation in Caucasians. Respir Physiol 1972;16(3):337-50.

(9)   Milic-Emili J, Whitelaw WA, Derenne JP. New tests to assess lung function: occlusion pressure--a simple measure of the respiratory center's output. N Engl J Med 1975;293(20):1029-30.

(10)   Scott GC, Burki NK. The relationship of resting ventilation to mouth occlusion pressure. An index of resting respiratory function. Chest 1990;98(4):900-6.

(11)   Pride NB. Applied physiology of the respiratory pump. Prax Klin Pneumol 1988;42 Suppl 2:807-11.

(12)   Grassino A, Perrault JL, Jean-Francois R, Whitelaw W. [Neural control of respiration. II- Methods of clinical evaluation]. Union Med Can 1983;112(2):137-44.

(13)   Jordan C. Automatic method for measuring mouth occlusion pressure response to carbon dioxide inhalation. Med Biol Eng Comput 1981;19(3):279-86.

(14)   MacIntyre N, Crapo RO, Viegi G, Johnson DC, van der Grinten CP, Brusasco V et al. Standardisation of the single-breath determination of carbon monoxide uptake in the lung. Eur Respir J 2005;26(4):720-35.

(15)   Miller MR, Hankinson J, Brusasco V, Burgos F, Casaburi R, Coates A et al. Standardisation of spirometry. Eur Respir J 2005;26(2):319-38.

(16)   Montes de OM, Celli BR. Mouth occlusion pressure, CO2 response and hypercapnia in severe chronic obstructive pulmonary disease. Eur Respir J 1998;12(3):666-71.

(17)   Read DJ. A clinical method for assessing the ventilatory response to carbon dioxide. Australas Ann Med 1967;16(1):20-32.

5

(18)   Rietjens GJ, Kuipers H, Kester AD, Keizer HA. Validation of a computerized metabolic measurement system (Oxycon-Pro) during low and high intensity exercise. Int J Sports Med 2001;22(4):291-4.

(19)   Eakin EG, Resnikoff PM, Prewitt LM, Ries AL, Kaplan RM. Validation of a new dyspnea measure: the UCSD Shortness of Breath Questionnaire. University of California, San Diego. Chest 1998 March;113(3):619-24.

(20)   Nishino T. Dyspnoea: underlying mechanisms and treatment. Br J Anaesth 2011;106(4):463-74.

(21)   Walterspacher S, Schlager D, Walker DJ, Muller-Quernheim J, Windisch W, Kabitz HJ. Respiratory muscle function in interstitial lung disease. Eur Respir J 2013;42(1):211-9.

(22)   DiMarco AF, Kelsen SG, Cherniack NS, Gothe B. Occlusion pressure and breathing pattern in patients with interstitial lung disease. Am Rev Respir Dis 1983;127(4):425-30.

5

Chapter 6

The global peripheral chemoreflex drive in patients with systemic sclerosis: a rebreathing and exercise study

Maarten K. Ninaber, Willem B.G.J. Hamersma, Anne A. Schouffoer,
Emily F.A. van 't Wout and Jan Stolk

Abstract

Background: Exercise intolerance (EI) in systemic sclerosis (SSc) is difficult to manage by the clinician. The peripheral chemoreflex drive compensates for metabolic acidosis during exercise and may be related to EI.

Aim: To assess the global peripheral chemoreflex drive (GPCD) in patients with SSc at rest and during exercise.

Methods: Consecutively tested SSc patients (n=49) were evaluated by pulmonary function tests, carbon dioxide (CO_2) rebreathing studies and non-invasive cardiopulmonary exercise testing (CPET). Results of their CO_2 rebreathing tests were compared with those of controls (n=32). Respiratory compensation for metabolic acidosis during CPET was defined by the occurrence of a sharp increase in minute ventilation (VdotE) and the ventilatory equivalent for CO_2 (VdotE/VdotCO_2) at the end of the isocapnic buffer phase. Euoxic (eVHR) and hyperoxic (hVHR) ventilatory responses to hypercapnia were measured and its difference (eVHR-hVHR) was considered to reflect the GPCD.

Results: In 45 patients with SSc, CPET results showed respiratory compensation at the occurrence of metabolic acidosis. eVHR-hVHR in patients with diffuse cutaneous SSc (dcSSc) differed significantly from that in patients with limited cutaneous SSc (lcSSc) and from that in controls (0.47±0.38 (dcSSc) *versus* 0.90±0.77 (lcSSc) and 0.90±0.49 (controls) L/min/mmHg; p=0.04 and p=0.03, respectively).

Conclusions: Respiratory compensation for metabolic acidosis occurred in all patients. However, the GPCD was diminished in dcSSc patients, suggesting an altered control of breathing. Its assessment may help the clinician to better understand reported exercise intolerance and exertional dyspnea in dcSSc patients.

Background

Typically, progressive systemic sclerosis (SSc) may involve interstitial lung disease (ILD) and pulmonary hypertension (PH) (1). In some cases of progressive SSc, however, thoracic wall involvement may arise and manifest as an impairment in chest wall excursions caused by thickened thoracic skin, referred to as "sclerodermic chest wall" (2). The impedance of the respiratory system is influenced by lung and chest wall compliance and respiratory flow resistance (2;3). In progressive SSc, dyspnea may arise from an increased impedance of the respiratory system caused by ILD. In SSc, ILD or limited chest wall excursions due to a thickened thoracic skin is considered to cause this increased impedance. Consequently, ventilatory impairment as a result of restriction may occur, resulting in alveolar carbon dioxide (CO_2) retention and subsequently in hypercapnic respiratory failure (2;3). It has been postulated that hypercapnic respiratory failure and exercise intolerance (EI) may, in contrast, involve a gradual down-regulation in central and peripheral chemosensitivity, resulting in slightly chronic elevated arterial partial carbon dioxide pressures ($PaCO_2$) and reported dyspnea during exercise (2;3). Therefore respiratory failure and EI in SSc may include not only increased respiratory impedance (i.e. reduced respiratory compliance and/or increased flow resistance), but also a diminished peripheral chemoreflex drive. Moreover, an absent peripheral chemoreflex drive itself may induce an early onset of metabolic acidosis and therefore an exercise intolerance and reported exertional dyspnea (4;5).

The peripheral chemoreflex drive plays an important role in the control of breathing (4;5). It not only ensures oxygen homeostasis, but also helps maintain CO_2 levels at rest and during exercise (4-6). Activation by peripheral chemoreceptors has been implicated in ventilatory compensation for metabolic acidosis during exercise (4-6). This ventilatory compensation is reflected in a sharp increase in the ventilatory equivalent for CO_2 (VdotE/VdotCO$_2$) at the end of the isocapnic buffer phase and a decrease in end-tidal pCO_2 (6).

The pathophysiology of SSc is complex, involving immune activation and widespread vascular injury (7-9). Although SSc is primarily a microvascular disorder with perivascular cellular infiltrates that consist of macrophages, T cells and B cells, with a predominance of CD4+ T cells, macrovascular involvement has been reported as well (7-9). The carotid bodies, the site of the peripheral chemoreflex to oxygen, CO_2 and pH, contain a complex microvascular anatomy in a macrovascular environment. SSc-related inflammatory and fibrotic responses may cause a diminished peripheral chemoreflex, which may result into an increased susceptibility to EI and consequently reported dyspnea during exercise (4-6;10). We

therefore hypothesized that the peripheral chemoreflex drive in normocapnic SSc patients is diminished at rest and during exercise. We obtained CO_2 rebreathing studies in SSc patients and healthy controls, and all SSc patients performed a cardiopulmonary exercise test (CPET).

Methods

Ethics

The local Medical Ethical Committee of the Leiden University Medical Center approved the protocol. Written informed consent was obtained from each participant prior to enrolment in the study.

Patients and healthy controls

We consecutively tested 49 SSc patients referred to an outpatient health care program. All patients were included in the study and underwent pulmonary function tests (PFTs), CO_2 rebreathing tests at rest and non-invasive incremental CPET on a bicycle according to Wasserman (6). No patients were excluded. All tests were done in one day or on two consecutive days between April 2010 and January 2012. Patients were classified as having limited cutaneous sclerosis (lcSSc) or diffuse cutaneous systemic sclerosis (dcSSc) according to the LeRoy criteria (11). All healthy controls performed the CO_2 rebreathing tests at rest only; PFTs were expected to be normal.

Euoxic (eVHR) and hyperoxic (hVHR) ventilatory response to hypercapnia at rest

CO_2 rebreathing tests were first obtained in all subjects. To assess the global peripheral chemoreflex drive (GPCD), we assessed the ventilatory response to hypercapnia under both euoxic (eVHR) and hyperoxic (hVHR) conditions as previously described (12). Briefly, under hyperoxia, the peripheral chemoreflex drive is considered to be suppressed for at least 30 minutes (13;14). The central chemoreflex drive to hypercapnia can therefore best be assessed for several minutes during hyperoxia. When the ventilatory response to hypercapnia under euoxia is measured, the total chemoreflex drive consists of both central and peripheral chemoreflex drives (15-17). These drives are then assumed to be additive (14;17). Thus, when the inspiratory fraction of oxygen in room air is kept constant at a level of 21%, the global

contribution of the peripheral chemoreceptor to total ventilatory response to hypercapnia can be evaluated by calculating eVHR minus hVHR (eVHR-hVHR) (12;14-17).

In SSc, increased respiratory impedance may be present as a result of ILD, thoracic wall involvement or increased flow resistance (2;3;18). However, because we measured eVHR and hVHR in a single SSc patient on the same day with a limited time interval, we did not consider the respiratory impedance to influence the peripheral chemoreflex loop gain (eVHR-hVHR). As a result, the GPCD may be compared between SSc patients and controls, irrespective of increased respiratory impedance.

Non-invasive CPET

Symptom-limited, noninvasive incremental CPET (without arterial blood gas sampling) was next performed under physician supervision in all SSc patients (19). To evaluate the presence of a peripheral chemoreflex drive during exercise, we monitored minute ventilation (VdotE) and VdotE/VdotCO$_2$ continuously by breath-by-breath analysis. The anaerobic threshold was determined by use of the lowest ventilatory equivalent for oxygen (VdotE/VdotO$_2$) or the V-slope method whenever appropriate (19). Normally, when exercise continues until the occurrence of metabolic acidosis (i.e. at the end of the isocapnic buffer phase), a sharp increase in VdotE/VdotCO$_2$ provides ventilatory compensation which reflects an active peripheral chemoreflex drive (Figure 6.1). In all CPET results, this response was scored qualitatively as being either present or absent (6;10). Since this response is expected in all healthy controls, they did not undergo CPET.

Statistical analysis

Statistical analysis was performed with the SPSS 20.0 package (SPSS, Inc., Chicago, IL, USA). Continuous variables are expressed as the mean value ± standard deviation. P-values <0.05 were considered significant. Categorical data are presented as frequencies and percentages. Statistical comparisons were performed by using the Student's t-test for continuous variables and the chi-square test for binary variables.
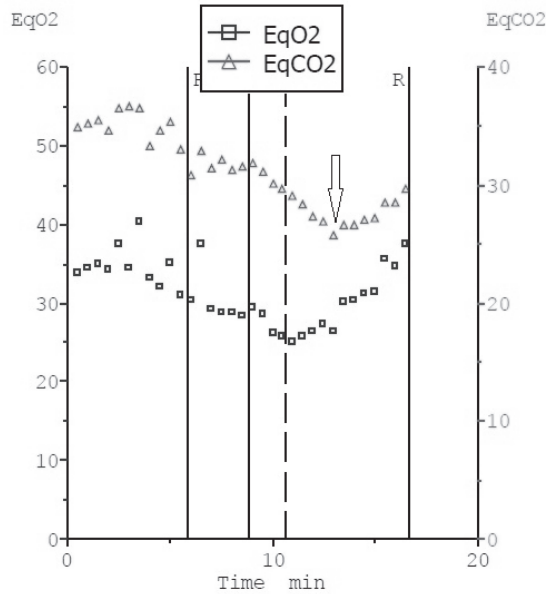
Figure 6.1   Example of a sharp increase (arrow) in the ventilatory equivalent for CO_2, providing ventilatory compensation for metabolic acidosis in a single patient with systemic sclerosis.
EqO_2, ventilatory equivalent for O_2; $EqCO_2$, ventilator equivalent for CO_2.

Results

Study population characteristics

Our 49 SSc patients were extensively characterized (Table 6.1). LcSSc patients (n=20) differed significantly from patients with dcSSc (n=29) with respect to disease duration, duration of skin disease, modified Rodnan skin score, onset of Raynaud phenomenon, and current and previous treatment.

Pulmonary function tests

DcSSc patients differed significantly from lcSSc patients in predicted forced vital capacity (FVC%; p=0.034) and total lung capacity, helium dilution method (TLC-He%; p=0.034) (Table 6.2). Furthermore, gas transfer (DLCO single breath method) was impaired in both groups, although it was not significantly different. These parameters may indicate the presence of increased respiratory impedance and therefore ILD, PH or both.

Table 6.1 Clinical characteristics of 49 SSc patients and 32 healthy controls

	lcSSc n=20	dcSSc n=29	Controls n=32	p-value*
Sex, female, no. (%)	18 (90)	18 (62)	16 (50)	0.35
Age, years, mean (SD)	57.1 (8.8)	49.1 (12.2)	45.4 (15.8)	0.65
Ethnicity, no.				
Caucasian	19	22	32	-
Hispanic	1	2	-	-
African	0	1	-	-
Asian	0	2	-	-
Disease duration, years, median (IQR)	10.1 (8.1)	4.7 (4.5)	-	0.009
Skin duration, years, median (IQR)	11.7 (9.3)	6.1 (6.4)	-	0.022
Onset of Raynaud phenomenon, months, median (IQR)	14.8 (11.2)	8.5 (8.9)	-	0.039
MRSS (0–51), mean (SD)	3.9 (4.1)	7.8 (6.8)	-	0.003
Current treatment, no. (%)			-	
Methotrexate	0 (0)	6 (19)		<0.001
Prednisone	1 (0.04)	4 (13)		0.008
Azathioprine	0 (0)	4 (13)		0.002
Previous treatment, no. (%)			-	
Cyclophosphamide	0 (0)	14 (45)		<0.001
Stem cell transplantation	0 (0)	10 (32)		<0.001
Methotrexate	2 (8)	15 (48)		<0.001
Prednisone	2 (8)	11 (35)		0.002

SSc, systemic sclerosis; lcSSc, limited cutaneous systemic sclerosis; dcSSc, diffuse cutaneous systemic sclerosis; SD, standard deviation; IQR, interquartile range; MRSS, modified Rodnan skin score. * Chi square, Student t-test, Mann Whitney U test or Fisher exact test where appropriate between limited and diffuse SSc.

6

Table 6.2 Pulmonary functions tests and ventilatory responses to hypercapnia

	lcSSc n=20	dcSSc n=29	Controls n=32	p-value
FVC (% pred)	101 (21)	84 (20)	-	0.034*
DLCOcSB (% pred)	63 (19)	57 (15)	-	0.19*
TLC-He (% pred)	91 (21)	80 (16)	-	0.034*
eVHR	2.59 (1.27)	1.87 (0.75)	3.08 (0.75)	<0.001#
hVHR	1.70 (0.98)	1.41 (0.62)	2.46 (0.91)	<0.001#
eVHR-hVHR	0.90 (0.77)	0.47 (0.38)	0.90 (0.49)	0.04#$

* P-value expressed for Student t-test between lcSSc and dcSSc. # P-value expressed for Student t-test between dcSSc and controls. $ P-value expressed for Student t-test between lcSSc and dcSSc. lcSSc, limited cutaneous systemic sclerosis; dcSSc, diffuse cutaneous systemic sclerosis; FVC, forced vital capacity (L); % pred, percentage predicted; DLCOcSB, carbon monoxide gas transfer factor corrected for hemoglobin, single breath method (mmol/min/kPa); TLC-He, total lung capacity, helium-dilution method (L); eVHR, euoxic ventilatory response to hypercapnia (L/min/mmHg); hVHR, hyperoxic ventilatory response to hypercapnia (L/min/mmHg); eVHR-hVHR, global peripheral chemoreflex drive (L/min/mmHg).

Euoxic and hyperoxic ventilatory response to hypercapnia

In healthy controls, the mean eVHR was 3.08±0.75 L/min/mmHg and differed significantly from that in dcSSc patients (1.87±0.75 L/min/mmHg; p<0.001). Similarly, the mean hVHR in controls differed significantly from that in dcSSc patients (2.46±0.91 *versus* 1.41±0.62 L/min/mmHg; p<0.001), but not from that in lcSSc patients (1.70±0.98 L/min/mmHg; p=0.11).

Global peripheral chemoreflex drive (eVHR-hVHR) in dcSSc patients was diminished and differed significantly from that in lcSSc patients (0.47±0.38 in dcSSc *versus* 0.90±0.77 in lcSSc; p=0.04) and from that in healthy controls (0.47±0.38 in dcSSc *versus* 0.90±0.49 L/min/mmHg in healthy controls; p=0.03). Figure 6.2 presents the mean (eVHR-hVHR) response in all subjects.

Furthermore, in 14 of 29 (48%) dcSSc patients, previous treatment consisted of autologous hematopoietic stem cell transplantation, which had a significant impact on the modified Rodnan skin score and on Raynaud phenomenon. In 15 dcSSc patients who were not treated with stem cells, the GPCD was significantly diminished compared with 14 stem-cell-treated dcSSc patients (0.27±0.23 and 0.64±0.42 L/min/mmHg, respectively, p=0.008).
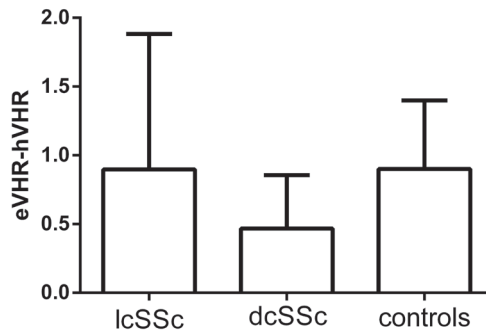

Figure 6.2   Mean (eVHR-hVHR) response to hypercapnia in L/min/mmHg in all subjects.
eVHR, euoxic ventilatory response to hypercapnia; hVHR, hyperoxic response to hypercapnia; dcSSc, diffuse cutaneous systemic sclerosis; lcSSc, limited cutaneous systemic sclerosis.

Non-invasive CPET

In total, 45 SSc patients (20 lcSSc, 25 dcSSc) reached metabolic acidosis during incremental exercise (end of isocapnic buffer phase). Four SSc patients (all dcSSc) discontinued their exercise before reaching anaerobic threshold and reported exertional dyspnea. In all CPET results for these 45 SSc patients, ventilatory compensation to metabolic acidosis occurred

by means of a sharp increase in VdotE and VdotE/VdotCO$_2$ (i.e. Figure 6.1, data not shown) (19). Within these 45 SSc patients, peak aerobic capacity (VdotO$_{2peak}$), a parameter of exercise tolerance, did not differ between lcSSc and dcSSc patients (data not shown).

Discussion

In progressive SSc, the global peripheral chemoreflex drive may be altered. Our results show the presence of an active peripheral chemoreflex drive during maximal exercise in all patients with SSc, as indicated by ventilatory compensation for metabolic acidosis. However, the global peripheral chemoreflex drive, as measured by the difference in eVHR and hVHR, was diminished in our dcSSc patients compared with that in healthy controls.

This is the first study on the hypercapnic ventilatory response to evaluate the peripheral chemoreflex drive in patients with SSc. In the present study, global assessment of CO$_2$ responsiveness was used to characterize different populations. We used room air in a rebreathing bag and kept the inspired fraction of oxygen during the euoxic rebreathing test constant at a level of 21% (12). However, some considerations may apply to the methods used in the present study. First, age, sex, status of menstrual phase and ethnicity all affect the ventilatory response to CO$_2$ (20). In our study, age and sex were not significantly different between SSc patients and healthy subjects. Furthermore, the ventilatory response did not significantly differ between healthy male and female SSc patients in the eVHR and hVHR tests (data not shown). Therefore, taking these results together, we believe that these issues did not contribute significantly to differences in ventilatory responses. Second, some dcSSc patients were previously treated with high-dose cyclophosphamide and autologous hematopoietic stem cell transplantation. Such treatment was not given to patients with lcSSc and may have contributed to the variability in ventilatory responses.

We used the concept of testing the GPCD by subtracting ventilatory responses to different oxygen supplies, as previously suggested by Duffin (17). In mammals, the carotid bodies are responsible for 95% of the ventilatory response to hypoxemia (21) and 30% of the response to arterial hypercapnia. In patients with resected bilateral carotid bodies, a 20–40% decrease in ventilatory response to euoxic hypercapnia is observed (10) Under euoxia, the peripheral chemoreflex drive is less active than when measured under hypoxia and considered to be 50–80% of total peripheral chemoreceptor sensitivity (10;15;16;20). In a previous study, we evaluated the peripheral chemoreflex drive in paraganglioma patients by subtracting

the hyperoxic from the euoxic ventilatory response to CO_2 (11). Furthermore, by using different levels of oxygen it was possible to determine the quantitative contribution of the chemoreceptors to ventilation at different levels of peripheral chemoreceptor stimulation (16;22). Consequently, the GPCD to CO_2 could be estimated from the difference in the euoxic and hyperoxic slopes (11;15-17). We therefore designated peripheral chemoreflex sensitivity under euoxia minus the hyperoxic ventilatory response (eVHR-hVHR) as the global peripheral chemoreflex drive.

In the setting of ILD or PH, minute ventilation may be strongly influenced by increased respiratory impedance (i.e. reduced respiratory compliance and/or increased flow resistance). In our study, lcSSc and dcSSc patients differed significantly in global peripheral chemoreflex function. Moreover, since both eVHR and hVHR are measured in the same patient and within a limited time period, respiratory impedance is considered not to influence the peripheral chemoreflex loop gain (eVHR-hVHR). Therefore, a difference in the GPCD between lcSSc and dcSSc patients may be derived from our rebreathing studies.

In addition to its measurement during rebreathing studies, the peripheral chemoreflex function can be assessed during exercise (6;10). When the exercise work rate is high enough to produce metabolic acidosis, the increase in ventilatory response is only – and strongly – mediated by the peripheral chemoreceptors (6). Thus, in the setting of an absent carotid body function, respiratory compensation for metabolic acidosis does not occur (6;10). In all of our SSc patients, including dcSSc patients, a ventilatory compensatory response at the end of the isocapnic buffer phase occurred as a result of the presence of a peripheral chemoreflex drive. However, quantitatively, as our results from the rebreathing studies indicate, a diminished ventilatory response is present in dcSSc patients compared with that in healthy controls, suggesting an altered GPCD in the absence of metabolic acidosis.

Our results may be explained by two mechanisms. First, SSc is considered to be an inflammatory disease (8;9). Anti-inflammatory treatment by autologous stem cell transplantation may have reduced the level of inflammation in carotid bodies, as indicated by our results in dcSSc patients. In dcSSc patients treated with autologous hematopoietic stem cell transplantation, a significant difference was present in the GPCD compared with that in dcSSc patients without such treatment. Therefore, this drive may have been altered positively by stem cell transplantation, suggesting an impact on carotid body vascularization and consequently its function. Second, widespread atherosclerosis is present not only in lcSSc patients, but also in dcSSc patients, and may involve the carotid arteries and bodies (8;9).

In subjects affected by widespread atherosclerosis, carotid body parenchyma may show degenerative changes; we speculate that atrophy may influence carotid body function (i.e. peripheral chemoreceptors) (7-9). We did not, however, measure carotid artery intima thickness. Furthermore, serum lipid spectrum was not significantly different between lcSSc and dcSSc patients.

Conclusions

In summary, our results show that in all SSc patients, ventilatory compensation for metabolic acidosis occurs as a result of an active peripheral chemoreflex drive. The global peripheral chemoreflex drive was, however, diminished in dcSSc patients compared with that in healthy controls, suggesting an altered chemoreflex control of breathing in these patients. This may help the clinician to better understand reported exercise intolerance and exertional dyspnea in dcSSc patients.

6

References

(1)   Black CM. Scleroderma. Br J Hosp Med 1979;22(1):28, 30, 32-28, 30, 33.

(2)   Nageh TT, du Bois RM. Non-invasive ventilation in hypercapnic respiratory failure secondary to sclerodermic chest wall restriction. Respir Med 1998;92(9):1170-2.

(3)   Pugazhenthi M, Cooper D, Ratnakant BS, Postlethwaite A, Carbone L. Hypercapnic respiratory failure in systemic sclerosis. J Clin Rheumatol 2003;9(1):43-6.

(4)   Dejours P. Chemoreflexes in breathing. Physiol Rev 1962;42:335-58.

(5)   Prabhakar NR, Peng YJ. Peripheral chemoreceptors in health and disease. J Appl Physiol (1985) 2004;96(1):359-66.

(6)   Wasserman K. Breathing during exercise. N Engl J Med 1978;298(14):780-5.

(7)   Lowe P, Heath D, Smith P. Relation between histological age-changes in the carotid body and atherosclerosis in the carotid arteries. J Laryngol Otol 1987;101(12):1271-5.

(8)   Au K, Singh MK, Bodukam V, Bae S, Maranian P, Ogawa R et al. Atherosclerosis in systemic sclerosis: a systematic review and meta-analysis. Arthritis Rheum 2011;63(7):2078-90.

(9)   Matucci-Cerinic M, Kahaleh B, Wigley FM. Review: evidence that systemic sclerosis is a vascular disease. Arthritis Rheum 2013;65(8):1953-62.

(10)   Lugliani R, Whipp BJ, Seard C, Wasserman K. Effect of bilateral carotid-body resection on ventilatory control at rest and during exercise in man. N Engl J Med 1971;285(20):1105-11.

(11)   LeRoy EC, Black C, Fleischmajer R, Jablonska S, Krieg T, Medsger TA, Jr. et al. Scleroderma (systemic sclerosis): classification, subsets and pathogenesis. J Rheumatol 1988;15(2):202-5.

(12)   van Hulsteijn LT, van DN, Ninaber MK, Romijn JA, van Dijk JG, van Kralingen KW et al. Carotid body tumors are not associated with an increased risk for sleep-disordered breathing. Sleep Breath 2014;18(1):103-9.

(13)   Becker H, Polo O, McNamara SG, Berthon-Jones M, Sullivan CE. Ventilatory response to isocapnic hyperoxia. J Appl Physiol (1985) 1995;78(2):696-701.

(14)   Caruana-Montaldo B, Gleeson K, Zwillich CW. The control of breathing in clinical practice. Chest 2000;117(1):205-25.

(15)   Poulin MJ, Cunningham DA, Paterson DH, Kowalchuk JM, Smith WD. Ventilatory sensitivity to CO2 in hyperoxia and hypoxia in older aged humans. J Appl Physiol (1985) 1993;75(5):2209-16.

(16)   Poulin MJ, Cunningham DA, Paterson DH. Dynamics of the ventilatory response to step changes in end-tidal PCO2 in older humans. Can J Appl Physiol 1997;22(4):368-83.

(17)   Duffin J. The chemoreflex control of breathing and its measurement. Can J Anaesth 1990;37(8):933-42.

(18) Whitelaw WA, Derenne JP, Milic-Emili J. Occlusion pressure as a measure of respiratory center output in conscious man. Respir Physiol 1975;23(2):181-99.

(19) Albouaini K, Egred M, Alahmar A, Wright DJ. Cardiopulmonary exercise testing and its application. Postgrad Med J 2007;83(985):675-82.

(20) Patrick JM, Howard A. The influence of age, sex, body size and lung size on the control and pattern of breathing during CO 2 inhalation in Caucasians. Respir Physiol 1972;16(3):337-50.

(21) Gonzalez C, Almaraz L, Obeso A, Rigual R. Oxygen and acid chemoreception in the carotid body chemoreceptors. Trends Neurosci 1992;15(4):146-53.

(22) Morelli C, Badr MS, Mateika JH. Ventilatory responses to carbon dioxide at low and high levels of oxygen are elevated after episodic hypoxia in men compared with women. J Appl Physiol (1985) 2004;97(5):1673-80.

6

Chapter 7

Lung structure and function relation in systemic sclerosis: application of lung densitometry

Maarten K. Ninaber, Jan Stolk, Jasper Smit, Ernest J. Le Roy,
Lucia J. Kroft, M. Els Bakker, Jeska K. de Vries Bouwstra,
Anne A. Schouffoer, Marius Staring and Berend C. Stoel

Abstract

Introduction: Interstitial lung disease occurs frequently in patients with systemic sclerosis (SSc). Quantitative computed tomography (CT) densitometry using the percentile density method may provide a sensitive assessment of lung structure for monitoring parenchymal damage. Therefore, we aimed to evaluate the optimal percentile density score in SSc by quantitative CT densitometry, against pulmonary function.

Material and methods: We investigated 41 SSc patients by chest CT scan, spirometry and gas transfer tests. Lung volumes and the nth percentile density (between 1 and 99%) of the entire lungs were calculated from CT histograms. The nth percentile density is defined as the threshold value of densities expressed in Hounsfield units. A prerequisite for an optimal percentage was its correlation with baseline DLCO % predicted. Two patients showed distinct changes in lung function 2 years after baseline. We obtained CT scans from these patients and performed progression analysis.

Results: Regression analysis for the relation between DLCO % predicted and the nth percentile density was optimal at 85% (Perc85). There was significant agreement between Perc85 and DLCO % predicted (R=-0.49, p=0.001) and FVC % predicted (R=-0.64, p<0.001). Two patients showed a marked change in Perc85 over a two year period, but the localisation of change differed clearly.

Conclusions: We identified Perc85 as optimal lung density parameter, which correlated significantly with DLCO and FVC, confirming a lung parenchymal structure-function relation in SSc. This provides support for future studies to determine whether structural changes do precede lung function decline.

Introduction

Clinical risk assessment of organ manifestations in systemic sclerosis (SSc) has revealed that interstitial lung disease (ILD) is present in 53% of cases with diffuse cutaneous SSc (dcSSC) and in 35% of cases with limited cutaneous SSc (lcSSc) (1). For evaluating the response to treatment of ILD, pulmonary function tests (PFTs) such as the diffusion capacity for carbon monoxide (DLCO) and forced vital capacity (FVC) are key outcome measures. However, these measures are affected by pulmonary vascular changes and chest wall skin stiffening, respectively (1). Therefore, more specific measures of lung parenchymal involvement of ILD may provide additional structural information.

Currently, chest high-resolution computed tomography (HRCT) is considered the most accurate noninvasive imaging method for ILD assessment. Both severity and extent of ILD are usually estimated by semi-quantitative scoring of a limited number of cross-sectional slices through the lungs (2;3). However, visual scoring has limited reproducibility, because of its subjective nature, and is time-consuming, thereby constraining the number of slices that can be assessed. HRCT data provide a means to quantitatively analyze the structure of the whole lung, since inflammation, ground glass opacities and fibrosis can be quantified by lung densitometry. Therefore, objective quantitative techniques by CT densitometry may provide a more sensitive measurement, similar to what has been proven in assessing progression of pulmonary emphysema by the percentile density method (4). Since these quantitative techniques are automated, it is feasible to quantify the entire lungs instead of only a limited number of slices, with a smaller chance of missing pathological changes.

Previously, Camiciotolli et al. (5) reported that lung density histogram parameters are more reproducible than visual assessment of HRCT and are more closely related to functional, exercise and quality-of-life impairment in SSc. In their evaluation of each patient, they calculated the average global density of the lung and included kurtosis and skewness of the density histogram of the whole lung. However, this analysis did not provide a single overall score for the structure of the lungs and, more importantly, lung density values were not corrected for lung volume. In a recent report, the same investigators clearly demonstrated the need for volume correction of density parameters (6). By a so-called sponge model (7), in which the lungs are considered mass preserving (i.e. the total lung mass is constant during breathing), density values can be corrected in a relatively simple calculation. Volume-corrected lung density parameters calculated by specific software may be useful outcome

7

measures in evaluating the progression of ILD and the response to treatment. Therefore, the aim of this study was to identify the optimal volume correction and percentage threshold for the percentile density method in SSc.

Material and methods

Patients

We investigated 41 patients with SSc who were referred consecutively to our tertiary outpatient targeted multidisciplinary healthcare program. As part of this program, all patients underwent, among other tests, PFTs and an HRCT scan of the thorax; they were instructed to take their usual medication before scanning. Included patients were classified as lcSSc or dcSSc according to Leroy EC et al. (8). The local Medical Ethical Committee approved the protocol. Written informed consent was obtained from each patient prior to enrolment. In two individual patients PFTs (both FVC and DLCO) significantly changed during clinical follow-up. To analyze this we performed additional CT scans.

Pulmonary function testing

All SSc patients had lung volume, spirometry and gas transfer studies. These PFTs included inspiratory vital capacity, total lung capacity, FVC, forced expiratory volume in one second and single-breath DLCO. Results are expressed as a percentage of the predicted value (9;10).

Computed tomography

All patients were scanned during full inspiration without contrast enhancement by the same CT scanner (Aquilion 64, Toshiba Medical Systems, Otawara, Japan), calibrated according to the manufacturer's guidelines. The standardized protocol comprised the following: tube voltage = 120 kVp; tube current = 140 mA without modulation; rotation time = 0.4 sec; collimation = 64 x 0.5 mm; helical beam pitch = 0.8. Axial slices were reconstructed for visual ILD scoring with 0.5 mm slices with 0.4 mm increment and lung kernel (FC30), and for densitometry with 5mm thick slices with an increment of 2.5 mm and smooth kernel (FC03).

Image analysis

Images were processed by Pulmo-CMS software (version 2.1, Medis medical imaging systems BV, Leiden, the Netherlands) (11). The CT scans were first recalibrated on the basis of densities measured in extrathoracic air and blood in the descending aorta (12). After automated lung contour detection with user correction options was complete, lung volumes and the nth percentile density of the entire lungs were calculated. The nth percentile density is defined as the threshold value of densities expressed in Hounsfield units (HU), below which n% of all lung voxels in the CT images are distributed (as schematically illustrated in Figure 7.1). In order to optimize the percentile method, we calculated all percentile densities by using percentages between 5% and 95% (Perc5–Perc95) with increments of 5%.
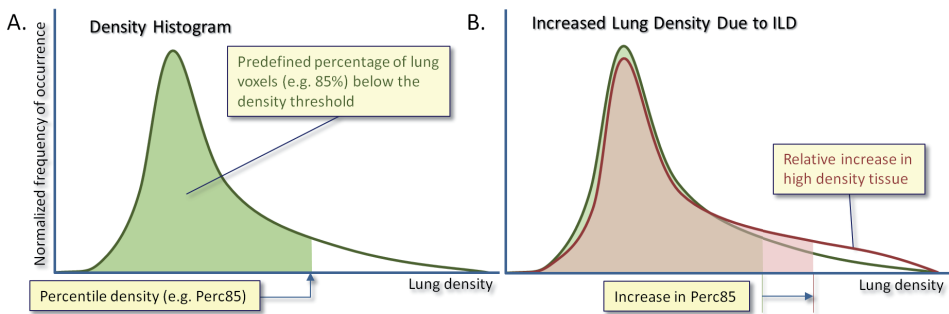

Figure 7.1   Schematic graph of the definition of the nth percentile density.
A, A normalized histogram of lung densities is shown (i.e., with a total area under the curve of 100%). The percentile density threshold is chosen in such a way that a predefined percentage (e.g., n=85) of all lung voxels (3D pixels) contains densities lower than the threshold, indicated by the green area. **B**, Because of interstitial lung disease (ILD), certain lung densities increase, causing the normalized histogram to change shape, where there are relatively more voxels with higher densities (green curve: normal density distribution; red curve: shifted distribution with increased densities). As a result, the percentile density has increased.

Subclinical parenchymal lung disease was previously defined as high attenuation areas (% HAAs) within the lung fields having a CT attenuation value between -600 and -260 HU (13). For comparison, we therefore performed a similar analysis in our data set of lung densities. Finally, an experienced chest radiologist (LK) scored all CT scans visually according to the Kazerooni scoring system (3).

Statistical analysis

Optimization of the percentile density method was based on the correlation between n^{th} percentile density and DLCO, which should be as high as possible. This was investigated by regression analysis, with DLCO as the dependent variable and one of the nth percentile densities as the independent variable. Lung volume was entered as a covariate to correct for different lung sizes. The partial correlation coefficient was then plotted against the percentage n. The statistical analysis was performed by using SPSS version 20.0.2, with a programmability extension for python scripting. The relation between the percentile and the correlation coefficient was automatically plotted by using Matplotlib (14).

Using the optimal percentage for the percentile density method, we investigated the cross-sectional correlations with the remaining lung function parameters. In addition, we studied the correlation of % HAA with the cross-sectional DLCO % predicted and FVC % predicted.

Progression map analysis

We noticed distinct changes in the FVC % predicted and DLCO % predicted during clinical follow-up of our patient population. Therefore we obtained CT scans from these patients and performed a recently published progression analysis between baseline and follow-up CT scans (15). Local changes in lung density were computed by progression analysis (15). Corresponding locations in the CT scans between baseline and follow-up were obtained by non-rigid intensity-based image registration using elastix (16). After we corrected for lung volume differences with the sponge model, local changes in lung density were calculated and displayed (15).

Results

The clinical characteristics of the 41 SSc patients (LcSSc: n=15) in this prospective cross-sectional study are shown in Table 7.1.

Determination of the optimal percentage

From the regression analysis (with CT-derived lung volume as a covariate), we found that the relation between the gas transfer factor DLCO (as % predicted) and the nth percentile density was optimal at 85% (Perc85), with a partial correlation coefficient of -0.32, as shown

Table 7.1 Clinical data of SSc patients

	LcSSc	DcSSc
Demographic data and serology		
Number of patients (n=41)	15	26
Age	54.7 (14.5)	48.7 (11.3)
Sex (female)	11 (73)	20 (83)
Disease duration, years	5.8 (7.4)	4.6 (3.5)
Onset of Raynaud, years	12.7 (11.3)	7.1 (4.8)
Caucasian origin (y/n)	13 (87)	18 (69)
Modified Rodnan skin score	6 (4–9)	9 (5–15)
Number of patients with:		
Antinuclear antibodies	14	21
Anti-centromere antibodies	7	4
Anti-Scl-70	2	16
Overall treatment		
ASCT	0 (0)	9 (22)
Cyclophosphamide	0 (0)	11 (27)
Methotrexate	3 (7)	5 (12)
Rituximab	0 (0)	5 (12)
Mycophenolate – Mofetil	1 (2)	4 (10)
Azathioprine	1 (2)	0 (0)
Pulmonary function		
FVC, L	3.34 (0.76)	3.37 (0.99)
FVC, % predicted	104.7 (26.5)	90.7 (19.5)
DLCO, mL/min/mmHg	5.67 (1.23)	6.06 (2.22)
DLCO, % predicted	67.7 (12.4)	64.0 (14.6)
FVC/DLCO	0.67 (0.17)	0.68 (0.19)

Data presented as mean (SD) or as median (25–75th percentile), n (%). LcSSc, limited cutaneous systemic sclerosis; DcSSc, diffuse cutaneous systemic sclerosis; ASCT, autologous stem cell transplantation; FVC, forced vital capacity; DLCO, single breath diffusion capacity of the lung for carbon monoxide.

in Figure 7.2. The slope between Perc85 and DLCO was -0.069 (95% confidence interval: -1.36 to -0.001).

Relation between structure and function

In the remainder of this report, Perc85 is used as the optimal parameter. There was a moderate agreement between Perc85 and both DLCO % predicted (R=-0.49, p=0.001) and FVC % predicted (R=-0.64, p<0.001) (Figure 7.3A and 7.3B, respectively). Kazerooni scores correlated significantly with Perc85 (R=0.56, p<0.01). For the alternative densitometric method by % HAA, Spearman's correlation with DLCO % predicted was R=-0.48 (p=0.002) and with FVC % predicted was -0.62 (p<0.001).
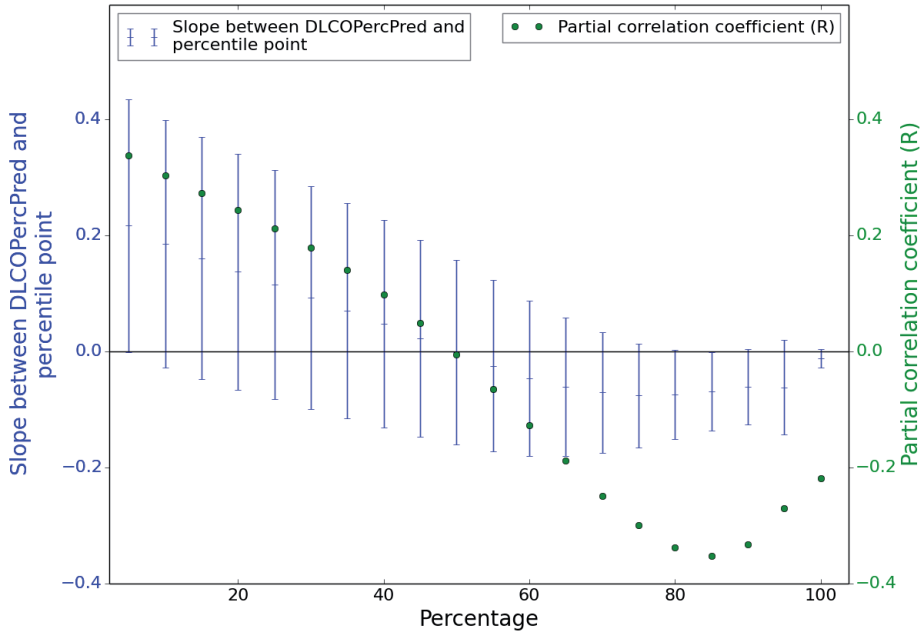
Figure 7.2   Partial correlation between percentile density and DLCO % predicted, against the percentage used for defining the percentile density.
For each percentage, the slope is plotted with 95% confidence intervals (blue error bars). The corresponding partial correlation coefficient is indicated by green dots. Lung volume during CT scanning was entered in the regression analysis as a covariate.shifted distribution with increased densities). As a result, the percentile density has increased.

Prospective application in individual study data: progression map analysis

Two isolated individuals in our SSc population showed marked change in their clinical course. After the observed change in their FVC (+24 and +8% pred) and DLCO (+11 and +5% pred), we decided to image their lungs by a similar CT scan. These data were not part of our cross-sectional study. Details of the two patients with diffuse SSc were analyzed extensively by local progression analysis (15). Figure 7.4 shows a local decrease lung density (in HU) in both patients, albeit in different locations in the lung and with different patterns. Both patients had ground glass densities that partly resolved after one year, in patient B this returned to the average values of the study population.
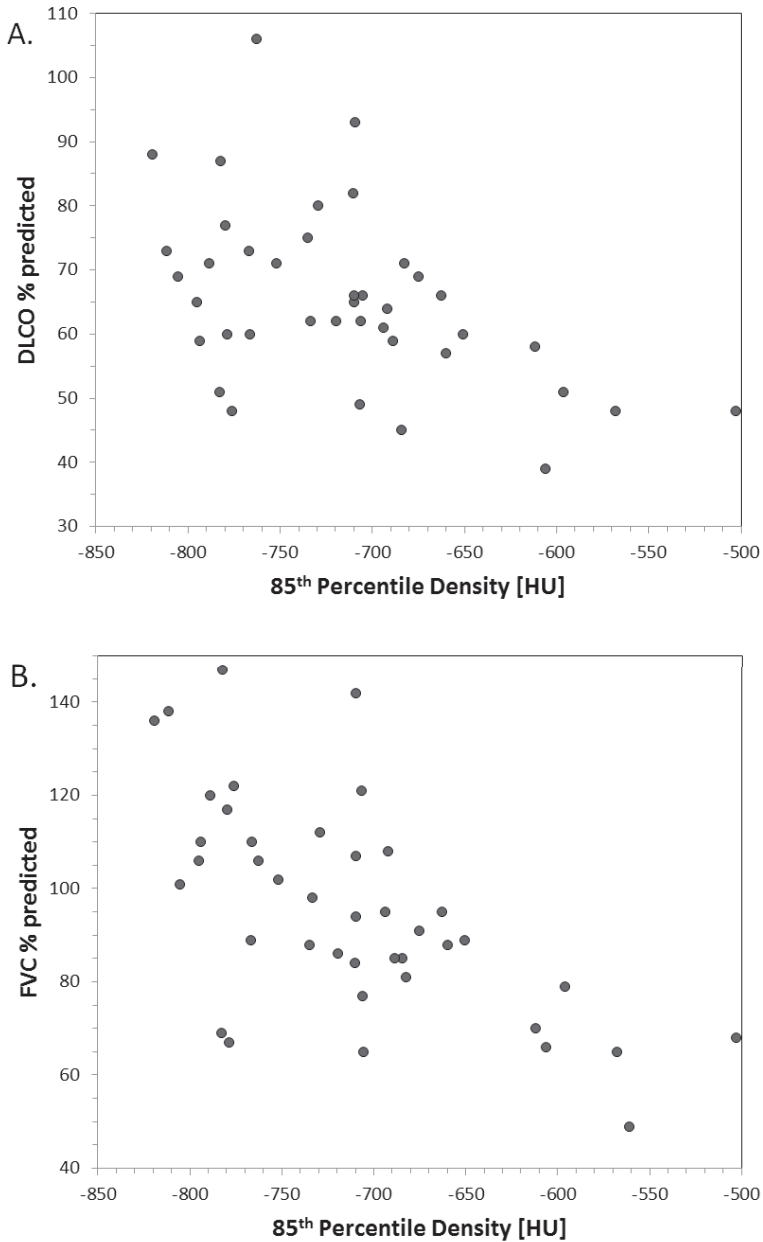
Figure 7.3   Correlation between lung structure and function.
A, Correlation between volume-corrected 85th percentile density and CO diffusion capacity (R=-0.49, p=0.001).
B, Correlation between volume-corrected 85th percentile density and forced vital capacity (R=-0.64, p<0.001).
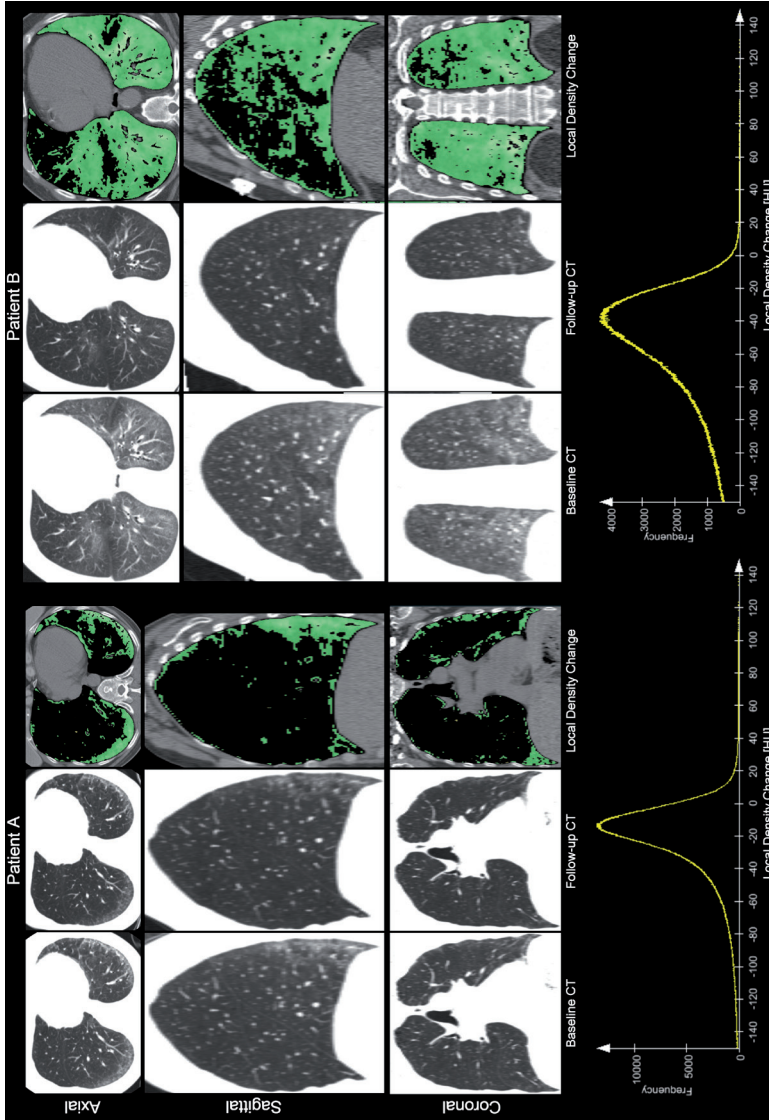
Figure 7.4   Local progression analysis for two patients with marked change in their clinical course.
For each patient, the axial sagittal and coronal CT images are shown: in the first column, the baseline CT scans are shown; in the second column, the CT scans at follow-up are shown and are elastically transformed to match the baseline scans, by image registration; the third column shows the local difference in density after volume correction. The green areas indicate significant changes in local densities (the brightness of the green overlay corresponds to the size of the density change). At the bottom, the histograms of the local density changes for each voxel are shown, where a positive change indicates a density increase and a negative change a density decrease. Both patients show a clear decrease in densities, but with clearly different local patterns.

Discussion

We studied the lung tissue structure by histogram analysis of lung densities obtained from CT images of patients with SSc. We report that the 85th percentile density score (Perc85) represents the most informative density parameter to assess lung parenchyma in SSc. Perc85 significantly correlated with DLCO as a measure of gas transfer. Interestingly, the lower percentile densities showed a positive relation between density and DLCO, indicating that low lung densities in SSc are accompanied by relatively high gas transfer values. Higher percentile densities showed the opposite, i.e., higher lung densities are associated with a relatively low gas transfer. This suggests that changes in lung density correlate with clinically relevant functional changes in patients with various severities of SSc. Indeed, two cases with marked improvement in FVC and DLCO related to a marked decline in Perc85.

The analysis of lung structure by densitometry of CT images provides a rapid and operator-independent assessment of lung pathology in SSc. Percentile density analysis of the histogram of tissue densities for both lungs is new in the analysis of ILD. The Perc85 point contains all densities present in the histogram between the density of air (-1000 HU) and the Hounsfield unit at which 85% of the densities in the histogram is captured. We considered DLCO rather than FVC as the most appropriate functional parameter for determining the optimal percentile density, although FVC is the most frequently reported outcome parameter in SSc for analysis of ILD (17;18). By using FVC only for the ultimate evaluation of the optimized parameter, we avoided introducing bias. Therefore, we calculated the correlation between DLCO % predicted of our SSc patients and all percentiles of the density histogram of each CT scan, which were corrected for lung volume. Again, this resulted in the 85th percentile density as the optimum lung density for analysis of lung structure.

Interestingly, two patients had a substantial change in both FVC and Perc85. By application of recently developed software (15), we demonstrated that areas with a decrease in lung density over time can be identified in the lungs, suggesting an improvement in the quality of lung tissue, and that these were accompanied by an increase in FVC and DLCO. Data from these two patients suggest that small changes in lung density do precede changes in their FVC and DLCO. However, assessment of a larger number of patients and a longer time interval are needed in future studies to confirm this observation and to evaluate the clinical benefit of lung densitometry.

The present study has some limitations. The range of lung function restriction was rather limited. A wider range of lung function restriction is needed to elucidate whether Perc85 will

7

be able to detect changes in lung density over the entire severity spectrum of SSc. Validation of lung density against quantitative pathology scores of SSc-affected lung tissue is almost impossible. Unlike in pulmonary emphysema, no quantitative pathology score is available that can be used in the analysis of lobectomy or pneumonectomy tissue specimens from SSc patients (19). However, some studies have used qualitative pathology scores on open lung biopsy specimens from ILD patients, and these related significantly to lung HRCT scores (3;20). Furthermore, we found that one such score, published by Kazerooni (3), correlated significantly with Perc85. The latter may suggest a possible correlation between a pathology score and our Perc85 score for lung tissue structure.

Conclusions

We identified an optimal lung density parameter, Perc85, which correlated significantly with gas transfer in the lung and may be used to assess clinically relevant changes in lung structure that coincide with changes in lung function. Future studies are needed to determine whether a change in Perc85 will precede changes in FVC and gas transfer to support clinical decision making on early treatment intervention in SSc patients.

References

(1)   Walker UA, Tyndall A, Czirjak L, Denton C, Farge-Bancel D, Kowal-Bielecka O et al. Clinical risk assessment of organ manifestations in systemic sclerosis: a report from the EULAR Scleroderma Trials And Research group database. Ann Rheum Dis 2007;66(6):754-63.

(2)   Goh NS, Desai SR, Veeraraghavan S, Hansell DM, Copley SJ, Maher TM et al. Interstitial lung disease in systemic sclerosis: a simple staging system. Am J Respir Crit Care Med 2008;177(11):1248-54.

(3)   Kazerooni EA, Martinez FJ, Flint A, Jamadar DA, Gross BH, Spizarny DL et al. Thin-section CT obtained at 10-mm increments versus limited three-level thin-section CT for idiopathic pulmonary fibrosis: correlation with pathologic scoring. AJR Am J Roentgenol 1997;169(4):977-83.

(4)   Parr DG, Stoel BC, Stolk J, Stockley RA. Validation of computed tomographic lung densitometry for monitoring emphysema in alpha1-antitrypsin deficiency. Thorax 2006;61(6):485-90.

(5)   Camiciottoli G, Orlandi I, Bartolucci M, Meoni E, Nacci F, Diciotti S et al. Lung CT densitometry in systemic sclerosis: correlation with lung function, exercise testing, and quality of life. Chest 2007;131(3):672-81.

(6)   Camiciottoli G, Diciotti S, Bartolucci M, Orlandi I, Bigazzi F, Matucci-Cerinic M et al. Whole-lung volume and density in spirometrically-gated inspiratory and expiratory CT in systemic sclerosis: correlation with static volumes at pulmonary function tests. Sarcoidosis Vasc Diffuse Lung Dis 2013;30(1):17-27.

(7)   Stoel BC, Putter H, Bakker ME, Dirksen A, Stockley RA, Piitulainen E et al. Volume correction in computed tomography densitometry for follow-up studies on pulmonary emphysema. Proc Am Thorac Soc 2008;5(9):919-24.

(8)   LeRoy EC, Medsger TA, Jr. Criteria for the classification of early systemic sclerosis. J Rheumatol 2001;28(7):1573-6.

(9)   Macintyre N, Crapo RO, Viegi G, Johnson DC, van der Grinten CP, Brusasco V et al. Standardisation of the single-breath determination of carbon monoxide uptake in the lung. Eur Respir J 2005;26(4):720-35.

(10)   Miller MR, Hankinson J, Brusasco V, Burgos F, Casaburi R, Coates A et al. Standardisation of spirometry. Eur Respir J 2005;26(2):319-38.

(11)   Stoel BC, Stolk J. Optimization and standardization of lung densitometry in the assessment of pulmonary emphysema. Invest Radiol 2004;39(11):681-8.

(12)   Parr DG, Stoel BC, Stolk J, Nightingale PG, Stockley RA. Influence of calibration on densitometric studies of emphysema progression using computed tomography. Am J Respir Crit Care Med 2004;170(8):883-90.

(13)   Lederer DJ, Enright PL, Kawut SM, Hoffman EA, Hunninghake G, van Beek EJ et al. Cigarette smoking is associated with subclinical parenchymal lung disease: the Multi-Ethnic Study of Atherosclerosis (MESA)-lung study. Am J Respir Crit Care Med 2009;180(5):407-14.

7

(14) Hunter J. Matplotlib: A 2D graphics environment. Computing in Science and Engineering 2007; 9(3):90-9.

(15) Staring M, Bakker ME, Stolk J, Shamonin DP, Reiber JH, Stoel BC. Towards local progression estimation of pulmonary emphysema using CT. Med Phys 2014;41(2):021905.

(16) Klein S, Staring M, Murphy K, Viergever MA, Pluim JP. elastix: a toolbox for intensity-based medical image registration. IEEE Trans Med Imaging 2010;29(1):196-205.

(17) Tashkin DP, Elashoff R, Clements PJ, Goldin J, Roth MD, Furst DE et al. Cyclophosphamide versus placebo in scleroderma lung disease. N Engl J Med 2006 22;354(25):2655-66.

(18) Solomon JJ, Olson AL, Fischer A, Bull T, Brown KK, Raghu G. Scleroderma lung disease. Eur Respir Rev 2013;22(127):6-19.

(19) Gould GA, MacNee W, McLean A, Warren PM, Redpath A, Best JJ et al. CT measurements of lung density in life can quantitate distal airspace enlargement--an essential defining feature of human emphysema. Am Rev Respir Dis 1988;137(2):380-92.

(20) Sahin H, Brown KK, Curran-Everett D, Hale V, Cool CD, Vourlekis JS et al. Chronic hypersensitivity pneumonitis: CT features comparison with pathologic evidence of fibrosis and survival. Radiology 2007;244(2):591-8.

7

Chapter 8

General discussion

The burden of complicating interstitial lung disease and pulmonary vasculopathy in systemic sclerosis

Systemic sclerosis is a clinically heterogeneous, multi-system autoimmune disorder. Patients with SSc usually have proliferative small artery and obliterative microvascular disease, plus inflammation and fibrosis affecting not only the skin, but importantly, also the lungs. Pulmonary involvement is very common in SSc and most often consists of interstitial lung disease (ILD) and pulmonary vascular disease leading to pulmonary (arterial) hypertension (PAH). These complications of the disease are the leading cause of disease related morbidity and mortality (1) and mortality from pulmonary disease in SSc can be as high as 33% (2).

Clinical signs of pulmonary involvement in SSc may include shortness of breath on exertion and, eventually, at rest. Additionally, patients may exhibit a non-productive cough, chest pain and dyspnoea. These symptoms are highly prevalent; dyspnoea is present in SSc in 93% of all cases (3). However, the prevalence of respiratory symptoms has been shown to be similar in SSc patients with and without concurrent lung disease (4). Traditionally, pulmonary function testing, echocardiography and high-resolution chest CT play a key role in the evaluation of dyspnoea and pulmonary complications. Frequently, patients can be well characterised using these tests, i.e. into a limited and extensive disease (5;6). However, these examinations may not always elucidate subclinical disease. Consequently, there is a need for non-invasive (bio)markers of complicating ILD and PAH in SSc, even in subclinical cases. Predictive models of major organ complications, in particular the lungs, are essential and may be used as clinical tools for patients risk stratification and could facilitate clinical interventional studies. In this thesis, several of these (bio)markers are addressed.

A different approach to dyspnea evaluation at rest and during exercise in SSc

Progressive systemic sclerosis may involve ILD and PAH and results into dyspnea at rest and on exertion. Dyspnea as a presenting occurs in 20% of all newly diagnosed SSc patients and in 93% of patients with complicating ILD and/or PAH (3). In all of these patients the mechanics of the respiratory system are involved. These mechanics, i.e. the impedance of the respiratory system, are influenced by lung and chest wall compliance and respiratory flow resistance (7). An increased respiratory impedance is recognized as the most frequent cause of dyspnea. In SSc, ILD or limited chest wall excursions cause an increased respiratory impedance. Other causes of dyspnea may include hypoxia, respiratory muscle weakness and pulmonary vasculopathy.

Traditionally, dyspnea is initially evaluated by the pulmonary physician using pulmonary function tests (spirometry, carbon monoxide gas transfer studies and body plethysmography) (8). However, in SSc, dyspnea may also arise from an inappropriate ventilatory response upon the chemoreflex drive at rest and to hypercapnia (9;10). To assess this ventilatory response, resting ventilation and tidal volumes can be evaluated. Ventilation, however, is an imperfect output parameter of the respiratory drive since it is affected by alterations in the impedance of the respiratory system (i.e. mechanical properties of the lung and chest wall). Mouth occlusion pressures (MOP, P0.1), as an index output parameter of the respiratory drive, provide not only a high reproducibility within each subject but also independency of age and sex (11). In all subjects, a relation between resting ventilation and MOP (V'E/P0.1) higher than 8 L/min sharply separates a normal from an abnormal response (11). In addition, the respiratory drive to hypercapnia (P0.1 to CO_2, i.e. $\Delta P0.1/\Delta CO_2$) provides insight into the central chemoreflex drive (9). These simple tests showed in our SSc population a distinct different response from normal reported values (Chapter 5, this thesis). Furthermore, an increased respiratory impedance could be depicted from our results in contrast to pulmonary function tests, which did not show any abnormality. Therefore, MOP at rest and during hypercapnia provide an easy to perform initial screening test in patients with SSc complaining of dyspnea.

In addition to mouth occlusion pressures and the measurement of the central chemoreflex drive, the peripheral chemoreflex drive plays an important role in resting ventilation and during exercise (12;13). Exercise intolerance in systemic sclerosis is a determinant of the disease and has a major impact on the quality of life (14). Moreover, the peripheral chemoreflex plays an important role in the control of breathing at rest and during exercise (15;16). Reported dyspnea at rest and during exercise may not only influenced by an increased respiratory impedance, but also by a diminished peripheral chemoreflex drive. This drive may be assessed by the difference between the ventilatory response to hypercapnia under euoxic (eVHR) and hyperoxic conditions (hVHR), i.e. eVHR-hVHR (Chapter 6 this thesis) and in addition, by cardiopulmonary exercise testing (CPET). In the latter, the occurrence of an ventilatory response in the setting of metabolic acidosis represents an active peripheral chemoreflex drive (16). In SSc, the peripheral chemoreflex drive showed to be significantly different between patients with limited cutaneous SSc and diffuse cutaneous SSc. Possible explanations include the reduction in the level of inflammation in by autologous stem-cell transplantation in a subgroup of diffuse cutaneous SSc patients (17) consequently affecting the carotid body vascularization and its function. Secondly, carotid body parenchyma may be negatively affected by the well-known widespread atherosclerosis in SSc (18-20).

8

135

Dyspnea evaluation in SSc can be challenging, in particular when both ILD and PAH are present. However, simple tests to detect whether the mechanical properties of the respiratory system are involved are necessary to guide further examination. Furthermore, these tests as described in Chapter 5 and 6 are even applicable in the most severely affected SSc patients who cannot produce reliable flow-volume curves. We therefore advocate the use of these tests early in clinical practice, not as a replacement of spirometry and gas transfer studies, but more as complementary, in order to facilitate best personalized medicine.

Analysis of non-invasive resting and exercise physiology to detect pulmonary vasculopathy in SSc

Recently, two-dimensional (2-D) speckle tracking strain analysis was proposed as a sensitive and accurate method for the evaluation of subclinical myocardial dysfunction (21). In short, this technique allows the assessment of left ventricular (LV) and right ventricular (RV) myocardial deformation by tracking the acoustic markers (speckles) in a frame-to-frame basis within the cardiac cycle (22). In Chapter 3 and 4 this technique is applied in SSc patients in whom subclinical cardiovascular involvement can occur in up to 70% (23). Concerning the left, ventricle 2-D speckle strain analysis revealed LV systolic dysfunction despite normal LV ejection fraction and normal LV dimensions. Furthermore, LV global longitudinal and circumferential strains were independently associated with oxygen uptake. This study demonstrated that LV global longitudinal and circumferential strains were significantly correlated with maximum aerobic capacity (VO_2% predicted), independent of age, SSc subtype, and lung function. Thus, this observation indirectly provided evidence that LV dysfunction contributes to an impaired functional capacity in patients with SSc. This novel technique therefore represents a valuable tool to improve the risk stratification among SSc patients.

In the RV study (the evaluation of RV dysfunction in relation to pulmonary hypertension and pulmonary fibrosis in SSc patients), free wall strain was significantly impaired in patients with SSc compared to controls. In particular patients with pulmonary fibrosis and ILD showed the most impaired free wall strain. A potential explanation for the findings in the RV study is that pulmonary fibrosis may be associated with mild/latent or dynamic pulmonary hypertension, which could not be detected by a single echocardiographic measurement (24). In addition, patients with pulmonary fibrosis have been shown to be more likely to have systemic involvement, and are therefore probably at higher risk for a significant direct myocardial involvement contributing to RV dysfunction (25).

In addition to echocardiographic studies, chapter 5 has a focus on the contribution to risk stratification among SSc patients by analysing the oxygen pulse slope in a cardiopulmonary exercise test (CPET). The oxygen pulse, which normalizes oxygen consumption for heart rate, is widely used as an indirect measurement for cardiac stroke volume (SV) (26) and is correlated with invasively measured SV (27). In SSc, a novel analysis of the $V'O_2$/HR slope to exercise in the clinical evaluation of systemic sclerosis patients showed that a breakpoint in the $V'O_2$/HR slope was preceded by a breakpoint in the slope of pulmonary arterial pressures against oxygen uptake. This suggests that the increase in pulmonary pressures results in a change in heart rate response to maintain sufficient cardiac output. In patients with a breakpoint in the $V'O_2$/HR slope, peak oxygen uptake was limited and differed significantly compared to patients without a breakpoint. Importantly, in patients with normal SPAP at rest, non-invasive CPET identified patients with a $V'O_2$/HR slope not fitting in the normal range (i.e. pathologic $V'O_2$/HR slope). In the evaluation of SSc patients, analysis of the $V'O_2$/HR slope may therefore reveal important information extending that of Doppler echocardiography in resting patients. Taken together, these patients may be at risk for developing pulmonary vasculopathy and ultimately pulmonary hypertension.

In patients with exercise induced pulmonary hypertension (EIPAH), two different groups were defined by the nature of their mPAP response to exercise (28). Data during exercise were analyzed using best-fit two-segment plots of mPAP versus oxygen uptake. Patients with severe EIPAH and resting PAH showed a "plateau" physiology. In these patients mPAP will increase as well as PVR during exercise until the cardiac output is compromised and starts to fall. Eventually, with a decline in cardiac output as a result of right ventricular dysfunction, PAP will not further increase or even fall resulting in a compensatory tachycardia. In contrast, patients with mild to moderate EIPAH showed a "take-off" physiology, suggesting pulmonary vasoconstriction during incremental exercise (28;29). In these patients, mPAP further increases in which the cardiac output does not decrease. Therefore, it seems plausible that patients with PAH of varying duration and severity will exhibit different mPAP responses to exercise. Likewise, different comparable $V'O_2$/HR slopes may be expected in these patients. Since different mPAP responses in patients with varying PAH or EIPAH are present, different $V'O_2$/HR responses are likely to occur. In other words, pulmonary vasculopathy, as reflected by a sudden increase in pulmonary pressures, may result into a breakpoint in the $V'O_2$/HR slope during non-invasive CPET. Consequently, the pulmonary vasculature may be more affected in patients showing a pathologic $V'O_2$/HR slope compared to patients without a pathologic $V'O_2$/HR slope.

8

Our novel analysis of the V'O$_2$/HR slope showed that SSc patients with a breakpoint in this slope are characterized by a decreased oxygen uptake and exercise capacity. This breakpoint is preceded by a sudden increase in pulmonary arterial pressures and may therefore reflect an inadequate increase or even decrease in stroke volumes. Importantly, non-invasive CPET identified patients with a pathologic V'O$_2$/HR slope despite normal echocardiographic pulmonary pressures at rest. These patients may have a compromised pulmonary vasculature and are at risk for developing pulmonary vasculopathy and ultimately pulmonary hypertension. To assess the predictive value of the V'O$_2$/HR breakpoint analysis, analysis of serial CPET and echocardiography in patients with normal SPAP and a pathologic V'O$_2$/HR slope or with a V'O$_2$/HR breakpoint are needed. Our analysis implies the analysis of the V'O$_2$/HR slope in every newly diagnosed SSc patient. Since a compromised pulmonary vasculature is not restricted to systemic sclerosis, our novel analysis may also be applicable to other types of lung disease coinciding with cardiovascular malfunction.

Lung densitometry as a quantitative measurement for interstitial lung disease assessment

The analysis of lung structure by densitometry of CT images provides a rapid and an operator-independent assessment of lung pathology. In our SSc population, the 85th percentile density score (Perc85) represented the most informative density parameter to assess lung parenchyma in SSc. It significantly correlated with DLCO, suggesting that changes in lung density correlate with clinical relevant functional changes in patients. In particular, two patients showed a substantial change in both their FVC and Perc85. By the application of specific software, progression maps were made showing areas with a decrease in lung density over time. These decreases were accompanied by increases in FVC. Interestingly, lung densitometry may show changes in lung density which may precede changes in functional parameters such as FVC. Since HRCT is considered the most accurate non-invasive imaging method for ILD assessment, quantitative assessment tools are necessary. However, only semi-quantitative scoring methods are currently used to determine the severity and extent of ILD. Visual scoring has limited reproducibility and is time-consuming (5;30). A quantitative tool may help the clinician to decide which patient will benefit from a treatment intervention. Furthermore, it allows treatment evaluation and early clinical decision making.

Conclusions and future perspectives

Recent cohort studies have demonstrated an improvement in the overall survival among SSc patients who were analysed for pulmonary involvement in a standardized manner (1;31). More recent cohorts showed reduced mortality and better disease outcome. Steen et al. analysed mortality and causes of death among SSc patients studied in a single centre dividing the subjects into groups based on the 5-year time periods between 1972 and 1997 within which they had their first assessment (1). Ten year survival from disease diagnosis showed improvement from 54% in the 1972–76 group to 66% in the 1987–91 group. In addition, systematic annual screening of organ-based complications and greater awareness of these manifestations has substantially increased accurate organ ascertainment and improved survival. Therefore we hope that the assessment methods and techniques presented in this thesis may better help the clinician if and when to start with immunomodulating agents and/or stem cell transplantation in SSc.

This thesis has focused on the relation between pulmonary structural abnormalities and its relation with pulmonary and cardiac function tests. Better ascertainment of lung and cardiac involvement is of particular interest, since treatment allocation has been traditionally based on the extent and type of its involvement. We showed that novel speckle tracking echocardiography can detect subtle myocardial abnormalities and has highly correlated with reduced aerobic capacity and the presence of pulmonary hypertension with or without ILD. Secondly, we demonstrated that during exercise our novel analysis of the oxygen pulse slope revealed clearly the onset of a sudden increase in pulmonary pressures which were also highly correlated with aerobic capacity and therefore survival. Finally, we presented a novel technique in the assessment of CT images, providing a quantitative, reproducible manner to evaluate the extent of SSc associated ILD.

Current evaluations of therapies focus on patient survival or markers of chronic disease progression (e.g. change in FVC). However, therapeutic research has been limited by the lack of consensus on and the validation of outcome measures that reliably assess treatment response. The outcome measures in Rheumatology (OMERACT) filter is a dynamic structure through which an instrument's performance can be evaluated under three points of examination: validity, discrimination and feasibility (32;33). Changes in FVC, as an example, have been shown to be reproducible in SSc-ILD but not in other forms of connective tissue related- ILD (CTD-ILD) (34). There are confounding issues of (pulmonary) vasculopathy, chest wall impairment and systemic disease activity that may coexist in CTD-

8

ILD. Nevertheless, FVC remains a reliable and sensitive parameter to reflect the contribution of parenchymal disease.

Although cohort studies remain a cornerstone in studying outcome of rare and heterogeneous diseases such as SSc, they should ideally be contemporary with prospective standardized data collection. This has significant implications for the cost and utility of descriptive clinical research. As such, the novel techniques described in this thesis may contribute to better identification of SSc patients at risk for developing clinically important pulmonary and cardiac complications. This would facilitate the clinician in clinical decision making and treatment evaluation in a "personalized care setting" for the SSc patient. However, since clinical research always evolves future studies on the organ ascertainment may include an integral analysis of all rest and exercise parameters involved in the detection of PH and ILD. In addition, the predictive value of quantitative CT densitometry (evaluating lung parenchyma and vessels) on the change in pulmonary and cardiac function tests is of particular interest. Therefore, we aim to focus on these themes in the coming years.

References

(1)   Steen VD, Medsger TA. Changes in causes of death in systemic sclerosis, 1972-2002. Ann Rheum Dis 2007;66(7):940-4.

(2)   Wells AU, Steen V, Valentini G. Pulmonary complications: one of the most challenging complications of systemic sclerosis. Rheumatology (Oxford) 2009;48 Suppl 3:iii40-iii44.

(3)   Khanna D, Tseng CH, Farmani N, Steen V, Furst DE, Clements PJ et al. Clinical course of lung physiology in patients with scleroderma and interstitial lung disease: analysis of the Scleroderma Lung Study Placebo Group. Arthritis Rheum 2011;63(10):3078-85.

(4)   Battle RW, Davitt MA, Cooper SM, Buckley LM, Leib ES, Beglin PA et al. Prevalence of pulmonary hypertension in limited and diffuse scleroderma. Chest 1996;110(6):1515-9.

(5)   Goh NS, Desai SR, Veeraraghavan S, Hansell DM, Copley SJ, Maher TM et al. Interstitial lung disease in systemic sclerosis: a simple staging system. Am J Respir Crit Care Med 2008;177(11):1248-54.

(6)   Schreiber BE, Valerio CJ, Keir GJ, Handler C, Wells AU, Denton CP et al. Improving the detection of pulmonary hypertension in systemic sclerosis using pulmonary function tests. Arthritis Rheum 2011;63(11):3531-9.

(7)   Whitelaw WA, Derenne JP, Milic-Emili J. Occlusion pressure as a measure of respiratory center output in conscious man. Respir Physiol 1975;23(2):181-99.

(8)   Nishino T. Dyspnoea: underlying mechanisms and treatment. Br J Anaesth 2011;106(4):463-74.

(9)   Cherniack RM, SNIDAL DP. The effect of obstruction to breathing on the ventilatory response to CO_2. J Clin Invest 1956;35(11):1286-90.

(10)   Gorini M, Spinelli A, Ginanni R, Duranti R, Gigliotti F, Arcangeli P et al. Neural respiratory drive and neuromuscular coupling during CO_2 rebreathing in patients with chronic interstitial lung disease. Chest 1989;96(4):824-30.

(11)   Scott GC, Burki NK. The relationship of resting ventilation to mouth occlusion pressure. An index of resting respiratory function. Chest 1990;98(4):900-6.

(12)   Wasserman K, Cox TA, Sietsema KE. Ventilatory regulation of arterial H(+) (pH) during exercise. Respir Physiol Neurobiol 2014;190:142-8.

(13)   Wasserman K. Breathing during exercise. N Engl J Med 1978;298(14):780-5.

(14)   Schouffoer A, Ninaber M, Beaart-van de Voorde L, van der Giesen F, de Jong Z, Stolk J et al. Randomized Comparison of a Multidisciplinary Team Care Program With Usual Care in Patients With Systemic Sclerosis. Arthritis Care & Research 2011;63(6):909-17.

(15)   Prabhakar NR, Peng YJ. Peripheral chemoreceptors in health and disease. J Appl Physiol (1985) 2004;96(1):359-66.

(16)   Lugliani R, Whipp BJ, Seard C, Wasserman K. Effect of bilateral carotid-body resection on ventilatory control at rest and during exercise in man. N Engl J Med 1971;285(20):1105-11.

8

(17)   van Laar JM, Farge D, Sont JK, Naraghi K, Marjanovic Z, Larghero J et al. Autologous hematopoietic stem cell transplantation vs intravenous pulse cyclophosphamide in diffuse cutaneous systemic sclerosis: a randomized clinical trial. JAMA 2014;311(24):2490-8.

(18)   Lowe P, Heath D, Smith P. Relation between histological age-changes in the carotid body and atherosclerosis in the carotid arteries. J Laryngol Otol 1987;101(12):1271-5.

(19)   Matucci-Cerinic M, Kahaleh B, Wigley FM. Review: evidence that systemic sclerosis is a vascular disease. Arthritis Rheum 2013;65(8):1953-62.

(20)   Au K, Singh MK, Bodukam V, Bae S, Maranian P, Ogawa R et al. Atherosclerosis in systemic sclerosis: a systematic review and meta-analysis. Arthritis Rheum 2011;63(7):2078-90.

(21)   Blessberger H, Binder T. NON-invasive imaging: Two dimensional speckle tracking echocardiography: basic principles. Heart 2010;96(9):716-22.

(22)   Delgado V, Ypenburg C, van Bommel RJ, Tops LF, Mollema SA, Marsan NA et al. Assessment of left ventricular dyssynchrony by speckle tracking strain imaging comparison between longitudinal, circumferential, and radial strain in cardiac resynchronization therapy. J Am Coll Cardiol 2008;51(20):1944-52.

(23)   Walker UA, Tyndall A, Czirjak L, Denton C, Farge-Bancel D, Kowal-Bielecka O et al. Clinical risk assessment of organ manifestations in systemic sclerosis: a report from the EULAR Scleroderma Trials And Research group database. Ann Rheum Dis 2007;66(6):754-63.

(24)   Huez S, Roufosse F, Vachiery JL, Pavelescu A, Derumeaux G, Wautrecht JC et al. Isolated right ventricular dysfunction in systemic sclerosis: latent pulmonary hypertension? Eur Respir J 2007;30(5):928-36.

(25)   McNearney TA, Reveille JD, Fischbach M, Friedman AW, Lisse JR, Goel N et al. Pulmonary involvement in systemic sclerosis: associations with genetic, serologic, sociodemographic, and behavioral factors. Arthritis Rheum 2007;57(2):318-26.

(26)   Whipp BJ, Higgenbotham MB, Cobb FC. Estimating exercise stroke volume from asymptotic oxygen pulse in humans. J Appl Physiol (1985) 1996;81(6):2674-9.

(27)   Walkey AJ, Ieong M, Alikhan M, Farber HW. Cardiopulmonary exercise testing with right-heart catheterization in patients with systemic sclerosis. J Rheumatol 2010;37(9):1871-7.

(28)   Tolle JJ, Waxman AB, Van Horn TL, Pappagianopoulos PP, Systrom DM. Exercise-induced pulmonary arterial hypertension. Circulation 2008;118(21):2183-9.

(29)   Waxman AB. Exercise physiology and pulmonary arterial hypertension. Prog Cardiovasc Dis 2012;55(2):172-9.

(30)   Kazerooni EA, Martinez FJ, Flint A, Jamadar DA, Gross BH, Spizarny DL et al. Thin-section CT obtained at 10-mm increments versus limited three-level thin-section CT for idiopathic pulmonary fibrosis: correlation with pathologic scoring. AJR Am J Roentgenol 1997;169(4):977-83.

(31) Ferri C, Valentini G, Cozzi F, Sebastiani M, Michelassi C, La MG et al. Systemic sclerosis: demographic, clinical, and serologic features and survival in 1,012 Italian patients. Medicine (Baltimore) 2002;81(2):139-53.

(32) Saketkoo LA, Mittoo S, Huscher D, Khanna D, Dellaripa PF, Distler O et al. Connective tissue disease related interstitial lung diseases and idiopathic pulmonary fibrosis: provisional core sets of domains and instruments for use in clinical trials. Thorax 2014;69(5):428-36.

(33) Saketkoo LA, Mittoo S, Frankel S, LeSage D, Sarver C, Phillips K et al. Reconciling healthcare professional and patient perspectives in the development of disease activity and response criteria in connective tissue disease-related interstitial lung diseases. J Rheumatol 2014;41(4):792-8.

(34) Tashkin DP, Elashoff R, Clements PJ, Goldin J, Roth MD, Furst DE et al. Cyclophosphamide versus placebo in scleroderma lung disease. N Engl J Med 2006;354(25):2655-66.

8

Chapter 9

Summary

Summary

This thesis describes the clinical assessment of complicating interstitial lung disease (ILD) and pulmonary vasculopathy (PV) in patients with systemic sclerosis (SSc). In **chapter 2, 3 and 4** exercise test derived and echocardiographic parameters for the presence of ILD and/ or PV are described. In **chapter 5 and 6** patient-reported dyspnea and exercise intolerance are studied and in **chapter 7** lung densitometry is performed to assess the lung function-structure relationship in SSc.

Systemic sclerosis is a systemic autoimmune disease that is characterised by endothelial dysfunction resulting in a small-vessel vasculopathy, fibroblast dysfunction with resultant excessive collagen production and fibrosis. The classification of SSc is based on the extent of skin involvement into diffuse cutaneous sclerosis (dcSSc) and limited cutaneous sclerosis (lcSSc). While virtually any organ system may be involved in the disease process, fibrotic and vascular pulmonary manifestations of SSc, including ILD and pulmonary hypertension (PH), are the leading cause of death. Better ascertainment of lung and cardiac involvement is of particular interest, since treatment allocation has been traditionally based on the extent and type of its involvement.

In **chapter 2** the oxygen pulse slope ($V'O_2/HR$) is studied in patients with SSc during cardiopulmonary exercise testing (CPET). The oxygen pulse normalizes oxygen consumption for heart rate and is widely used as an indirect measurement of cardiac stroke volume (SV). In our experience, SSc patients may show an abnormal $V'O_2/HR$ slope containing a breakpoint despite normal pulmonary pressures measured at rest using Doppler echocardiography (DE). We hypothesized that a compromised pulmonary vasculature may lead to an increase in pulmonary pressures and an decreased oxygen uptake. The resulting heart rate increase as a function of the oxygen uptake ($V'O_2/HR$) may therefore show a breakpoint in the slope reflecting a disproportional heart rate increase. In two SSc patient populations (Graz, Austria and Leiden, the Netherlands) $V'O_2/HR$ slopes were analysed for breakpoints. In the Austrian SSc population simultaneous right heart catheterisation was performed allowing direct comparison between heart rate and pulmonary pressure increase as a function of oxygen uptake during exercise. In the Austrian CPETS a breakpoint in the $V'O_2/mPAP$ preceded the breakpoint in the V'O2/HR slope. In the Leiden CPETs peak oxygen uptake was significantly lower CPETs containing a $V'O_2/HR$ breakpoint. Furthermore, several pathologic $V'O_2/HR$ slopes were observed despite normal resting pulmonary pressures measured by DE. Whether these patients will develop pulmonary hypertension at rest is an interesting focus for further research.

Chapter 3 and 4 describe the use of a new available echocardiographic tool to assess the myocardial velocity and deformation (strain) by tissue Doppler imaging. This two-dimensional speckle-tracking strain analysis has been proposed for the evaluation of left ventricular (LV) regional and global strain in 3 orthogonal directions (longitudinal, circumferential and radial). Right ventricular (RV) function was assessed by speckle-tracking derived RV free wall strain. The relation between LV systolic dysfunction as measured by this technique and functional capacity (peak oxygen uptake during CPET) as well as ventricular arrhythmias was evaluated in **chapter 3**. Each strain was independently associated with peak oxygen uptake. Furthermore each strain was associated with abnormal Holter electrocardiography results. In **chapter 4** the potential role of pulmonary fibrosis and pulmonary hypertension (PHT) in the development of RV dysfunction was evaluated. Compared to controls SSc patients without pulmonary fibrosis and PHT had an impaired RV free wall strain. Both pulmonary fibrosis and PHT were independently associated with impaired RV free wall strain and therefore RV dysfunction. The findings of both LV and RV strain analysis in SSc should be explored in larger prospective studies to assess the prognostic value of these measures.

In **chapter 5 and 6** frequently reported problems by SSc patients are described: dyspnea and exercise intolerance. Dyspnea may arise in SSc by complicating interstitial lung disease and/or pulmonary hypertension. An increased respiratory impedance, which is influenced by the lung and chest wall compliance as well as respiratory flow resistance, is recognized as the most frequent cause of dyspnea. To assess dyspnea in SSc, mouth occlusion pressures as an index of central respiratory output (i.e. the respiratory drive), were measured in **chapter 5**. In addition, they were obtained during CO_2 rebreathing and related to pulmonary function tests. Normal values of mouth occlusion pressures (V'E/P0.1>8 l/min/cm H2O) are independent of age and sex. Furthermore, the technique has a high reproducibility within each subject. In SSc patients an abnormal V'E/P0.1 response provided a better correlation with severity of dyspnea than traditional lung function parameters. Furthermore, in these patients, $\Delta P0.1/\Delta PetCO_2$, as an index of the central chemoreceptor response to hypercapnia, was significantly higher than in SSc patients with normal mouth occlusion pressure responses. Since it sharply demarcates a normal from a high (i.e. abnormal) impedance of the respiratory system, mouth occlusion pressures (V'E/P0.1) can be easily assess as a first diagnostic test in the outpatient clinic. In **chapter 6** the peripheral chemoreflex drive is studied in SSc in relation to patient-reported exercise intolerance. The peripheral chemoreflex drive plays an important role in the control of breathing at rest and during exercise. Activation of this

9

drive has been implicated in the ventilatory compensation for metabolic acidosis during exercise. This activation is reflected by an sharp increase in the ventilator equivalent for CO_2 at the end of the isocapnic buffer phase and decrease in end-tidal pCO_2. In addition to an exercise test, the peripheral chemoreflex drive is assessed by the difference between the euoxic and hyperoxic ventilatory response to hypercapnia (eVHR-hVHR). Since SSc is primarily a microvascular disorder, SSc-related inflammatory and fibrotic responses in the carotid body may cause a diminished peripheral chemoreflex. In all SSc patients, respiratory compensation for metabolic acidosis occurred. However, eVHR-hVHR differed significantly between limited cutaneous and diffuse cutaneous patients, suggesting an altered control of breathing in these patients. This may help the clinician to better understand reported exercise intolerance and exertional dyspnea in diffuse cutaneous SSc patients.

In **chapter 7** lung structure and lung function relationship is studied by lung densitometry and pulmonary function tests. Data from a high-relation CT scan of the thorax (HRCT) provide a means to quantitatively analyze the structure of the whole lung, since inflammation, ground glass opacities and fibrosis can be quantified by lung densitometry. Therefore, objective quantitative techniques by CT densitometry may provide a more sensitive measurement than visual scoring as currently is done by the radiologist. In SSc, we evaluated the optimal percentile density score in SSc by quantitative CT densitometry, against pulmonary function. Lung volumes and the nth percentile density (between 1 and 99%) of the entire lungs were calculated from CT histograms. The nth percentile density is defined as the threshold value of densities expressed in Hounsfield units. A prerequisite for an optimal percentage was its correlation with baseline DLCO% predicted. Regression analysis for the relation between DLCO% predicted and the nth percentile density was optimal at 85% (Perc85). There was significant agreement between Perc85 and DLCO % predicted and FVC % predicted. Of interest, two patients showed a marked change in Perc85 over a two year period, but the localisation of change differed clearly. We conclude that we identified Perc85 as optimal lung density parameter, which correlated significantly with DLCO and FVC, confirming a lung parenchymal structure-function relation in SSc. This provides support for future studies to determine whether structural changes do precede lung function decline.

9
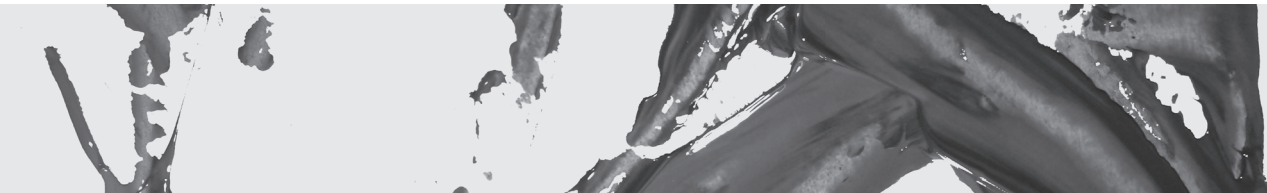
Samenvatting

Samenvatting

Dit proefschrift beschrijft de klinische evaluatie van complicerende interstitiële longaandoeningen (ILD) en pulmonale vasculopathie (PV) bij patiënten met systemische sclerose (SSc). In **hoofdstuk 2, 3 en 4** worden parameters beschreven voor de aanwezigheid van ILD en/of PV, afgeleid uit een inspanningstest en een echo cor. In **hoofdstuk 5 en 6** worden patiënt-gerapporteerde kortademigheid en inspanningsintolerantie beschreven en in **hoofdstuk 7** wordt longdensitometrie toegepast om de longfunctiestructuurrelatie in SSc beoordelen.

Systemische sclerose is een auto-immuunziekte die wordt gekenmerkt door endotheliale disfunctie resulterend in een vasculopathie die met name de kleinere vaten betreft. Voorts is er een fibroblastdysfunctie met als resultaat excessieve collageendepositie en interstitiële fibrose. De classificatie van SSc is gebaseerd op de mate van aangedaan huidoppervlak en wordt onderverdeeld in diffuse cutane sclerose (dcSSc) en beperkte cutane sclerose (lcSSc). Hoewel vrijwel elk orgaansysteem betrokken kan zijn bij het ziekteproces, zijn fibrotische en pulmonaire vasculaire uitingen van SSc (ILD en pulmonaire hypertensie (PH)), de voornaamste doodsoorzaak. Betere evaluatie van pulmonale en cardiale betrokkenheid is van bijzonder belang, omdat het besluit om te behandelen van oudsher gebaseerd is op de omvang en de aard van deze betrokkenheid.

In **hoofdstuk 2** wordt de zuurstofpolshelling (V'O$_2$/HR) onderzocht bij patiënten met SSc gedurende een cardiopulmonale inspanningstest (CPET). De zuurstofpols normaliseert zuurstofverbruik voor de hartslag en wordt veel gebruikt als een indirecte meting van het slagvolume (SV). In onze ervaring, kunnen SSc-patiënten een abnormale V'O$_2$/HR-helling met een breekpunt hebben, ondanks normale pulmonaaldrukken gemeten in rust met behulp van Doppler echocardiografie (DE). Onze hypothese was dat een gecompromitteerde pulmonale vasculatuur kan leiden tot een toename van pulmonaaldrukken en een verminderde zuurstofopname. De hartslagtoename als een functie van de zuurstofopname (V'O$_2$/HR) kan dan ook een breekpunt in de helling bevatten, hetgeen een disproportionele hartslagtoename weerspiegelt. In twee SSc-patiëntpopulaties (Graz, Oostenrijk en Leiden, Nederland) werden V'O$_2$/HR-hellingen geanalyseerd op breekpunten. In de Oostenrijkse SSc-populatie werd gelijktijdig een rechtse hartkatheterisatie uitgevoerd waardoor een directe vergelijking tussen de hartslag en de pulmonale drukverhoging als functie van de zuurstofopname tijdens inspanning mogelijk werd. In de Oostenrijkse CPET's viel bijzonder op dat een breekpunt in de V'O$_2$/mPAP-helling een breekpunt in de V'O$_2$/HR-helling voorafging. In de Leidse SSc-populatie bleek de piek-zuurstofopname aanzienlijk lager in CPET's waarin

zich een V'O$_2$/HR-breekpunt bevond. Verder werden verschillende pathologische V'O$_2$/HR-hellingen (V'O$_2$/HR-helling buiten het normale bereik) waargenomen ondanks normale rust- pulmonaaldrukken gemeten door DE. Of deze patiënten pulmonale hypertensie in rust ontwikkelen, vormt een interessant focus voor verder onderzoek.

Hoofdstuk 3 en 4 beschrijven het gebruik van een nieuw beschikbaar echocardiografisch instrument voor het meten van myocardiale vervorming (strain) door middel van een echo cor. Deze tweedimensionale "speckle-tracking" strainanalyse voor de evaluatie van de linkerventrikel (LV) bekijkt de regionale en globale strain in drie orthogonale richtingen (longitudinaal, circumferentieel en radiair). De rechterventrikelfunctie (RV) werd beoordeeld door de "speckle-tracking" strainanalyse van de RV vrije wand. De relatie tussen LV systolische dysfunctie, gemeten met deze techniek, en functionele capaciteit (piek-zuurstofopname tijdens CPET) en ventriculaire aritmieën werd geëvalueerd in **hoofdstuk 3**. Elke strain bleek onafhankelijk geassocieerd met de piek-zuurstofopname. Bovendien was elke strain geassocieerd met abnormale Holter-elektrocardiografie resultaten. In **hoofdstuk 4** werd de potentiële rol van longfibrose en pulmonale hypertensie (PHT) in de ontwikkeling van RV-dysfunctie geëvalueerd. Vergeleken met controles hadden SSc-patiënten zonder longfibrose en PHT een verminderde strain van de RV vrije wand. Zowel longfibrose als PHT waren onafhankelijk geassocieerd met een verminderde strain van de RV vrije wand en dus RV-dysfunctie. De bevindingen van zowel de LV- als RV-strainanalyse in SSc moeten worden onderzocht in grotere prospectieve studies om de voorspellende waarde van deze metingen te kunnen beoordelen.

In **hoofdstuk 5 en 6** worden frequent, door SSc-patiënten gemelde, klachten beschreven: kortademigheid en inspanningsintolerantie. Kortademigheid kan ontstaan in SSc door complicerende interstitiële longaandoeningen en/of pulmonale hypertensie. Een toegenomen pulmonale impedantie, die wordt beïnvloed door de weerstand van long en borstwand en respiratoire luchtstromingsweerstand, wordt erkend als de meest voorkomende oorzaak van dyspneu. Om kortademigheid te kunnen beoordelen in SSc, kunnen mondocclusiedrukken gemeten worden als een index van de respiratoire drive, wat in **hoofdstuk 5** wordt beschreven. Daarnaast kunnen deze drukken gemeten worden tijdens het inademen van CO$_2$ en gerelateerd worden aan longfunctietesten. De normale waarden van mondocclusiedrukken (V'E/P0.1>8 l/min/cm H$_2$O) zijn onafhankelijk van leeftijd en geslacht. Verder heeft de techniek een hoge reproduceerbaarheid binnen elk proefpersoon. In SSc-patiënten bleek een abnormale V'E/P0.1 een betere correlatie met de ernst van de dyspnoe te hebben dan traditionele longfunctieparameters. Verder bleek dat in deze patiënten de ΔP0.1/

$\Delta PetCO_2$, als een index van de centrale chemoreceptorrespons op hypercapnie, significant hoger (abnormaler) te zijn dan bij SSc-patiënten met normale mondocclusiedrukken. Aangezien abnormale mondocclusiedrukken (V'E/P0.1<8 l/min/cm H_2O) een sterke relatie hebben met een toegenomen pulmonale impedantie, kan deze test gemakkelijk gebruikt worden als een eerste diagnostische test voor de analyse van dyspnoe in de polikliniek. In **hoofdstuk 6** wordt de perifere chemoreflex onderzocht in relatie tot patiënt-gerapporteerde inspanningsintolerantie. De perifere chemoreflex speelt een belangrijke rol in de controle van de ademhaling in rust en tijdens inspanning. Activering van deze chemoreceptor leidt gedurende de inspanning tot een respiratoire compensatie voor metabole acidose. Deze respons wordt gereflecteerd door een sterke toename van de ventilatoire equivalent voor CO_2 aan het einde van de isocapnische bufferfase en een dalende eind-expiratoire pCO_2. Naast een inspanningstest, kan de perifere chemoreflex gemeten worden door het verschil tussen de euoxische en hyperoxische ventilatoire respons op hypercapnie (eVHR-hVHR). Aangezien de ziekte SSc vooral een microvasculaire stoornis is, kunnen SSc-gerelateerde inflammatoire en fibrotische reacties in de halsslagader (glomus caroticum, carotid body) een verminderde perifere chemoreflex veroorzaken. In ons onderzoek trad bij alle SSc-patiënten een respiratoire compensatie voor de ontstane metabole acidose op. Echter, de eVHR-hVHR verschilde significant tussen de lcSSc- en dcSSc-patiënten, wat een veranderde ademregulatie bij deze patiënten suggereert. Deze bevindingen kunnen de behandelend arts helpen om beter de gerapporteerde inspanningsintolerantie en dyspnoe bij inspanning te begrijpen.

In **hoofdstuk 7** wordt de relatie tussen longstructuur en longfunctie bestudeerd door middel van longdensitometrie en longfunctietesten. Data van een hoge resolutie CT-scan van de thorax (HRCT), een middel om kwantitatief de structuur van de hele long te analyseren, kunnen worden gekwantificeerd door middel van densitometrie. Daarom kan de kwantitatieve CT-densitometrie een gevoeliger instrument zijn om longweefsel te beoordelen dan het geoefende oog van de radioloog. Voor SSc hebben we de optimale score percentiele dichtheid in SSc geëvalueerd door kwantitatieve CT-densitometrie en vergeleken met longfunctietesten. Longvolume en de n^e percentiele dichtheid (tussen 1 en 99%) van de gehele longen werden berekend uit CT-histogrammen. De n-percentiel dichtheid wordt gedefinieerd als de drempelwaarde van dichtheden, uitgedrukt in Hounsfield eenheden. Regressieanalyse voor de relatie tussen de DLCO als % van voorspeld en de n-percentiele dichtheid bleek optimaal op 85% (Perc85). Er was een significante correlatie tussen de Perc85 en de DLCO als % van voorspeld en de FVC als % van voorspeld. We concludeerden dat de optimale longdensitometrieparameter de 85[e] percentiel is (Perc85) en een longstructuurfunctierelatie

in SSc aantoont. Deze resultaten bieden de mogelijkheid voor toekomstige studies om te bepalen of structurele veranderingen voorafgaan aan veranderingen in de longfunctie.

*
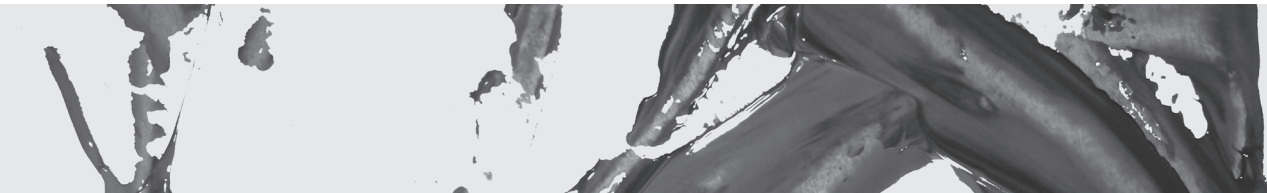
Dankwoord

Dankwoord

Promoveren doe je niet alleen. Het kost niet alleen veel tijd en energie van jezelf, maar ook van anderen. Graag wil ik *iedereen* bedanken die heeft bijgedragen aan de totstandkoming van dit proefschrift. In het bijzonder zou ik graag de volgende mensen willen bedanken. Allereerst natuurlijk alle patiënten met systemische sclerose en de gezonde proefpersonen die hebben meegedaan aan mijn onderzoek.

Ook vrienden zijn belangrijk bij het promoveren voor de nodige steun en ontspanning. Frans, Menno, leden van de BBGG en de Bonobo's: bedankt!

Christian, Tom, met jullie steun heb ik de samenwerking tussen onze afdelingen, waarvan dit werk een mooi voorbeeld is, kunnen voortzetten. Ik hoop dat we dit kunnen blijven doen!

Jan, met jouw visie, de eigenschap om altijd overal een passende oplossing voor te vinden en vooral je geduld is ons werk geworden tot wat het nu is. Gelukkig kunnen we samen verder werken aan het pad dat we ingeslagen hebben. Bedankt daarvoor!

Willem, na je komst in 2011 was ik overdonderd door je directe en praktische benadering van de vraagstukken waar we mee worstelden. Je fysiologische kennis en kunde hebben vervolgens wel geleid tot nieuwe inzichten en publicaties. Een hoogtepunt van onze samenwerking was onze trip naar Graz, Oostenrijk, om aldaar in samenwerking met Oostenrijkse longartsen inspanningsgegevens te bekijken. Ondanks de bijna-crash van hun computer, zijn we met hen een vruchtbare samenwerking gestart. Veel dank voor al je hulp en ik hoop in de toekomst nog met je van gedachten te kunnen blijven wisselen!

Joke, veel dank voor al je hulp. Susan en Wim, als ouders hebben jullie van dichtbij meegemaakt dat dit project niet makkelijk is verlopen. Altijd kon ik rekenen op jullie steun en begrip. Bedankt!

Lieve Wilma en Gijs, als laatste maar zeker niet de minste. Wat heb ik het toch getroffen met jullie in mijn leven. Lieve Wilma, je bent o zo belangrijk voor mij; als mijn lieve vrouw, maar ook als klankbord. Lieve Gijs, dat je in ons leven bent gekomen is zo ontzettend mooi; je relativeert en brengt het leven terug tot wat het hoort te zijn: bij elkaar zijn en van elkaar genieten!
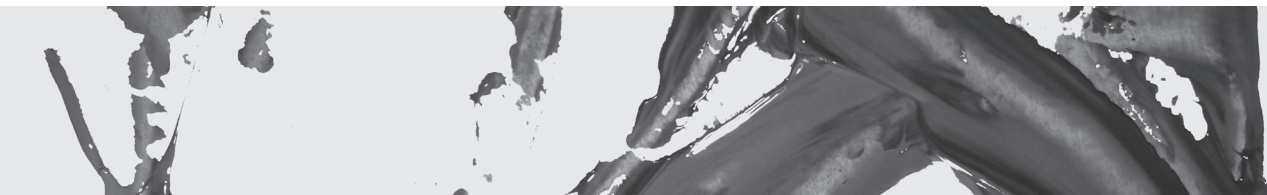
About the author

Curriculum Vitae

Maarten Klemens Ninaber was born on December 18th 1979 in Capelle aan den IJssel, the Netherlands. In 1998 he graduated from the Gymnasium at Marnix College Ede. He studied medicine at the Leiden University Medical Center / Leiden University from 1998 and received his medical degree on December 17th 2004. Afterwards he started working at the department of Pulmonary Rehabilitation of the Rijnlands Revalidatie Centrum until September 2005. He started his specialty training in Pulmonology in October 2005 under supervision of Luuk Willems and received his degree as a chest physician in October 2011. From October 2011 he works as a chest physician and staff member at the department of Pulmonology of the Leiden University Medical Center, Leiden, the Netherlands. He started his PhD project formally in 2013 at the department of Pulmonology of the Leiden University Medical Center together with Jan Stolk and Willem Hamersma, of which the results are described in this thesis.

List of publications

(1) Yiu KH, Ninaber MK, Kroft LJ, Schouffoer AA, Stolk J, Scherer HU, Meijs J, de Vries-Bouwstra J, Tse HF, Delgado V, Bax JJ, Huizinga TW, Marsan NA. Rheumatology (Oxford). 2015 Oct 15. pii: kev342. [Epub ahead of print]

(2) Ninaber MK, Stolk J, Smit J, Le Roy EJ, Kroft LJ, Bakker ME, de Vries Bouwstra JK, Schouffoer AA, Staring M, Stoel BC. Lung structure and function relation in systemic sclerosis: application of lung densitometry. Eur J Radiol 2015;84(5):975-9.

(3) Ninaber M, Dik H, Peters E. Complete pathological resolution of pulmonary Langerhans cell histiocytosis. Respirol Case Rep 2014;2(2):76-8.

(4) Joyce E, Ninaber MK, Katsanos S, Debonnaire P, Kamperidis V, Bax JJ, Taube C, Delgado V, Ajmone Marsan N. Subclinical left ventricular dysfunction by echocardiographic speckle-tracking strain analysis relates to outcome in sarcoidosis. Eur J Heart Fail 2015;17(1):51-62.

(5) Ninaber MK, Hamersma WB, Schouffoer AA, Kovacs G, Olschewski H, Holman ER, Ajmone Marsan N, Stolk J. Detection of pulmonary vasculopathy by novel analysis of oxygen uptake in patients with systemic sclerosis: association with pulmonary arterial pressures. Clin Exp Rheumatol 2014;32(6 Suppl 86):S-60-7.

(6) Ninaber MK, Hamersma WB, Schouffoer AA, van 't Wout EF, Stolk J. The global peripheral chemoreflex drive in patients with systemic sclerosis: a rebreathing and exercise study. QJM 2015;108(1):33-8.

(7) Ninaber MK, Hamersma WB, Schuerwegh AJ, Stolk J. Increased respiratory drive relates to severity of dyspnea in systemic sclerosis. BMC Pulm Med 2014;14:57.

(8) van Hulsteijn LT, van Duinen N, Ninaber MK, Romijn JA, van Dijk JG, van Kralingen KW, Havekes B, Smid L, Lammers GJ, Jansen JC, Smit JW, Thijs RD, Corssmit EP. Carotid body tumors are not associated with an increased risk for sleep-disordered breathing. Sleep Breath 2014;18(1):103-9.

(9) Joyce E, Delgado V, Ninaber MK, Marsan NA. The invisible made visible: multi-modality imaging in the evaluation of cardiac sarcoidosis. Eur Heart J 2013;34(17):1278.

(10) Hoogerwerf MA, Ninaber MK, Willems LN, Kaptein AA. "Feelings are facts": illness perceptions in patients with lung cancer. Respir Med 2012;106(8):1170-6.

(11) Yiu KH, Schouffoer AA, Marsan NA, Ninaber MK, Stolk J, Vlieland TV, Scherptong RW, Delgado V, Holman ER, Tse HF, Huizinga TW, Bax JJ, Schuerwegh AJ. Left ventricular dysfunction assessed by speckle-tracking strain analysis in patients with systemic sclerosis: relationship to functional capacity and ventricular arrhythmias. Arthritis Rheum 2011;63(12):3969-78.

(12) Schouffoer AA, Ninaber MK, Beaart-van de Voorde LJ, van der Giesen FJ, de Jong Z, Stolk J, Voskuyl AE, Scherptong RW, van Laar JM, Schuerwegh AJ, Huizinga TW, Vlieland TP. Randomized comparison of a multidisciplinary team care program with usual care in patients with systemic sclerosis. Arthritis Care Res (Hoboken) 2011;63(6):909-17.

(13) Ninaber MK, de Vaal JB, Corsmit OT, Cluitmans FH, de Leeuw JG, Smit F. Severe arterial hypoxemia in liver cirrhosis. Respir Care 2009;54(3):393-7.

(14) Ninaber MK, Schot R, Fregonese L, Stolk J. A syringe simulation of biological controls for quality assessment of prospective lung volume measurements. Respiration 2008;76(2):187-92.

(15) Steens RF, Csizmadia CG, George EK, Ninaber MK, Hira Sing RA, Mearin ML. A national prospective study on childhood celiac disease in the Netherlands 1993-2000: an increasing recognition and a changing clinical picture. J Pediatr 2005;147(2):239-43.

(16) Collin P, Kaukinen K, Vogelsang H, Korponay-Szabó I, Sommer R, Schreier E, Volta U, Granito A, Veronesi L, Mascart F, Ocmant A, Ivarsson A, Lagerqvist C, Bürgin-Wolff A, Hadziselimovic F, Furlano RI, Sidler MA, Mulder CJ, Goerres MS, Mearin ML, Ninaber MK, Gudmand-Høyer E, Fabiani E, Catassi C, Tidlund H, Alainentalo L, Mäki M. Antiendomysial and antihuman recombinant tissue transglutaminase antibodies in the diagnosis of coeliac disease: a biopsy-proven European multicentre study. Eur J Gastroenterol Hepatol 2005;17(1):85-91.